Development of new hybrid methods in density functional theory by linear separation of the electron-electron interaction

Kamal Sharkas

UPMC
SORBONNE UNIVERSITÉS

THÈSE DE DOCTORAT
DE L'UNIVERSITÉ PIERRE ET MARIE CURIE

Spécialité :

CHIMIE THÉORIQUE

ED 388 - Ecole Doctorale de Chimie Physique et Chimie Analytique de Paris Centre

présentée par

M. Kamal SHARKAS

pour obtenir le grade de

DOCTEUR DE L'UNIVERSITÉ PIERRE ET MARIE CURIE

Sujet de la thèse:

Développement de nouvelles méthodes hybrides en théorie de la fonctionnelle de la densité par séparation linéaire de l'interaction électronique.

Soutenue le 10 juillet 2013 devant le Jury composé de :

Prof.	**Esmaïl ALIKHANI**	Université P. et M. Curie - CNRS	Président
Prof.	**Gábor I. CSONKA**	Budapest University (BUTE)	Rapporteur
Prof.	**Thierry LEININGER**	Université de Toulouse - CNRS	Rapporteur
Prof.	**Carlo ADAMO**	Chimie ParisTech - CNRS	Examinateur
Dr.	**Emmanuel FROMAGER**	Université de Strasbourg - CNRS	Examinateur
Dr.	**Andreas SAVIN**	Université P. et M. Curie - CNRS	Directeur de thèse
Dr.	**Julien TOULOUSE**	Université P. et M. Curie - CNRS	Co-directeur de thèse

Développement de nouvelles méthodes hybrides en théorie de la fonctionnelle de la densité par séparation linéaire de l'interaction électronique.

Résumé

Cette thèse rassemble des contributions méthodologiques aux méthodes hybrides en théorie de la fonctionnelle de la densité (DFT). La combinaison de la DFT et de plusieurs méthodes de fonction d'onde a été réalisée par séparation linéaire de l'interaction électronique dans l'extension multidéterminantale de la méthode de Kohn-Sham. Afin d'améliorer le calcul des effets de corrélation de (quasi-)dégénérescence des systèmes moléculaires, nous avons développé les hybrides multiconfigurationnels qui combinent la DFT avec un calcul de champ autocohérent multiconfigurationnel. Le couplage de la DFT avec une théorie de perturbation Møller-Plesset du deuxième ordre (MP2) a donné la justification théorique et le développement d'approximations "double hybrides" qui ont été testées sur des systèmes moléculaires et étendus.

Mots-clés

théorie de la fonctionnelle de la densité; corrélation électronique; hybride multiconfigurationnel; approximation double hybride; molécules; cristaux moléculaires.

Development of new hybrid methods in density functional theory by linear separation of the electron-electron interaction.

Abstract

This thesis draws together methodological contributions to the hybrid methods in density functional theory (DFT). The combination of DFT and several wave function methods has been done by linear separation of the electron-electron interaction in the multideterminantal extension of the Kohn-Sham scheme. Aiming at improving the calculation of (near-)degeneracy correlation effects in molecular systems, we have developed the multiconfigurational hybrids which combine DFT with a multiconfiguration self-consistent field calculation. The coupling between DFT and second-order Møller-Plesset perturbation theory (MP2) has provided the theoretical justification and development of *double hybrid* approximations which have been tested for molecular and extended systems.

Keywords

density functional theory; electronic correlation; multiconfigurational hybrid; double hybrid approximation; molecules; molecular crystals.

Remerciements

Je remercie Olivier Parisel pour m'avoir accueilli dans de bonnes conditions au sein du laboratoire de Chimie Théorique de l'Université Pierre et Marie Curie.

Je remercie sincèrement mon directeur de thèse Andreas Savin pour m'avoir encadré et appris. J'ai apprécié ses grandes compétences scientifiques, sa disponibilité et sa gentillesse.

Je tiens à rendre hommage à Julien Toulouse, mon co-directeur de thèse, pour m'avoir encadré. J'ai apprécié sa précision, sa patience et son enthousiasme pour la recherche.

Je remercie les membres du jury, Gábor I. Csonka et Thierry Leininger pour avoir accepté le travail de rapporteurs, ainsi que Carlo Adamo, Esmaïl Alikhani, Roberto Dovesi et Emmanuel Fromager pour avoir accepté d'évaluer ma thèse. Un merci particulier à Roberto Dovesi qui m'a accueilli au sein du laboratoire de Chimie Théorique à Turin.

I am thankful to Bartolomeo Civalleri (Mimmo), Lorenzo Maschio and all the young students in the theoretical chemistry group for a very pleasant and fructuous stay in Turin.

Enfin, J'adresse ma gratitude à l'ensemble des membres, anciens et actuels, du laboratoire de Chimie Théorique; qu'ils m'excusent de ne pas tous les mentionner.

Contents

Chapter 1

Introduction générale

Ce chapitre rappelle tout d'abord les modèles principaux de la chimie quantique, puis introduit les méthodes développées au cours de cette thèse.

1.1 Apperçu de quelques méthodes de calcul de structure électronique

La chimie quantique applique les lois de la mécanique quantique pour extraire les différentes propriétés physico-chimiques de la matière à l'échelle moléculaire. Les particules considérées à ce niveau de description sont les noyaux atomiques et les électrons. Dans l'approximation non-relativiste, l'évolution dans le temps d'un ensemble d'électrons et de noyaux est régie par l'équation de Schrödinger dépendante du temps. Dans la plupart des problèmes de chimie quantique, le point crucial est la résolution de l'équation de Schrödinger stationnaire, c'est-à-dire la recherche des fonctions propres de l'hamiltonien du système. Les noyaux sont beaucoup plus lourds que les électrons. Ceci nous permet de découpler le mouvement des électrons de celui des noyaux, c'est ce que l'on appelle l'approximation de Born-Oppenheimer. Dans cette approximation, le problème standard de la chimie quantique est d'obtenir les états propres de l'hamiltonien électronique, qui n'agit que sur les variables électroniques. Parmi ces états, l'état fondamental est celui de plus basse énergie dans le spectre de l'hamiltonien électronique.

Sauf dans le cas des systèmes atomiques ou moléculaires ne comprenant qu'un seul électron (et d'autres modèles très simples), on ne peut pas résoudre exactement l'équation de Schrödinger et l'on doit utiliser des méthodes d'approximation. Face à ce défi, on peut distinguer deux familles de méthodes. La première famille cible le calcul direct de la fonction d'onde du système. Ce sont les méthodes de fonction d'onde (WFT pour *Wave Function Theory*). La deuxième famille considère que la connaissance de la densité électronique d'un système quelconque suffit pour le décrire pleinement. Ce sont les méthodes basées sur la théorie de la fonctionnelle de la densité (DFT pour *Density Functional Theory*).

1.1.1 Méthodes de fonction d'onde

Deux types de méthodes d'approximation sont principalement utilisées : les méthodes variationnelles et les méthodes de perturbation. Les méthodes variationnelles sont fondées

sur le principe variationnel, qui établit que, pour l'état fondamental, l'énergie associée à toute fonction d'onde autre que la fonction exacte est toujours supérieure à l'énergie exacte. Dans les méthodes de perturbation, on approche la fonction d'onde exacte sous la forme d'un développement en série à partir d'une solution approchée connue.

La méthode Hartree-Fock (HF) est souvent la première approche utilisée. C'est une approximation variationnelle consistant à restreindre les solutions approchées aux seules fonctions d'onde de type déterminant de Slater. Le déterminant de Slater est le produit antisymétrisé d'orbitales moléculaires (OM), développées sur une base d'orbitales atomiques (OA) selon l'approche CLOA (combinaison linéaire d'orbitales atomiques). Cette méthode suppose que chacun des électrons d'un système atomique ou moléculaire est une particule indépendante qui ne subit que le champ moyen des autres électrons. La description quantitative des propriétés chimiques ne peut se faire correctement qu'en prenant en compte la tendance des électrons à s'éviter instantanément les uns des autres. Ce phénomène est appelé corrélation électronique. L'énergie de corrélation mesure l'erreur sur l'énergie commise en utilisant le déterminant de Hartree-Fock pour calculer la valeur moyenne de l'hamiltonien électronique. C'est donc la différence entre l'énergie électronique non-relativiste exacte et celle de Hartree-Fock. Il faut donc aller au-delà de l'approximation Hartree-Fock pour calculer une partie de l'énergie de corrélation. On peut utiliser plusieurs types de méthodes, dites de fonction d'onde ou post Hartree-Fock, prenant en compte la corrélation électronique.

La corrélation peut être classée en deux catégories : la corrélation dynamique et statique (ou non-dynamique). La première est associée à la corrélation au sein de paires électroniques, et caractérisée par sa convergence lente avec la taille de la base utilisée. Pour la majorité des molécules dans leur état fondamental et proches de leur géométrie d'équilibre, la corrélation dynamique est prédominante. On inclut aussi dans la corrélation dynamique les interactions de dispersion, qui sont parfois dominantes dans les complexes faiblement liés. La seconde est associée à la présence de niveaux très proches en énergie (dégénérescence ou quasi-dégénérescence) dans le système et nécessite d'utiliser des fonctions d'onde multidéterminantales. Les effets de corrélation statique sont souvent importants pour des molécules dans des états excités ou proches de la dissociation.

En principe, la fonction d'onde exacte peut s'obtenir à partir d'un ensemble complet de déterminants construits avec une base complète d'OM. Partant du déterminant Hartree-Fock, on cherche une meilleure fonction d'onde développée en combinaison linéaire du déterminant Hartree-Fock et des déterminants construits par excitations d'électrons d'OM occupées à des OM virtuelles. Dans la méthode d'interaction de configurations (IC), les coefficients des déterminants dans la combinaison sont déterminés en appliquant le principe variationnel. Si on prend en compte toutes les configurations excitées, il s'agit de l'interaction de configurations complète (full CI). Les résultats obtenus par IC complète sont les meilleurs résultats que l'on puisse obtenir avec la base d'OA choisie, mais en pratique un calcul IC complet est souvent trop coûteux en temps de calcul. Généralement, on utilise le formalisme IC tronqué. Par exemple, un calcul CISD, dans lequel on se limite à considérer les excitations simples et doubles, reproduit typiquement 95% de l'énergie de corrélation pour les petites molécules dans la géométrie d'équilibre. Pour les molécules plus grandes ou les états excités, il devient important de prendre en compte les excitations triples ou supérieures, mais l'absence d'extensivité peut rendre ces approches peu fiables.

Ce problème d'extensivité est résolu par les méthodes de *coupled cluster* (CC). Ces méthodes consistent à exprimer la fonction d'onde du système en utilisant l'*ansatz* expo-

nentiel. Elles sont une variante des méthodes IC permettant d'optimiser les coefficients des configurations par une technique alternative à la méthode variationnelle basée sur la projection de l'équation de Schrödinger sur l'espace de référence.

La méthode de perturbation de Møller-Plesset est une autre manière de calculer la corrélation dynamique. Elle consiste à appliquer la théorie de perturbation de Rayleigh-Schrödinger standard à la recherche de l'énergie fondamentale de l'hamiltonien électronique à partir de l'hamiltonien de Hartree-Fock, dont on connait les valeurs et états propres. On peut développer l'énergie jusqu'à un ordre quelconque. En pratique, on utilise les approximations MP2, MP3 et MP4, où l'énergie est développée jusqu'à l'ordre deux, trois et quatre respectivement.

Les méthodes post Hartree-Fock décrites ci-dessus sont monoréférentielles, c'est-à-dire qu'elles s'appuient sur une seule configuration obtenue par un calcul Hartree-Fock. La validité de ces méthodes est alors mise en question en présence de quasi-dégénérescences (distribution des électrons au sein de couches partiellement occupées). Les méthodes multidéterminantales MCSCF (*MultiConfiguration Self-Consistent Field*) fournissent une bonne description de la corrélation statique. Ces méthodes consistent à minimiser l'énergie électronique avec une fonction d'onde multiconfigurationnelle qui s'écrit comme somme de plusieurs déterminants de Slater. Contrairement aux méthodes IC, on optimise simultanément les OM et les coefficients des configurations dans un calcul MCSCF. Une variante de MCSCF est CASSCF (*Complete Active Space Self-Consistent Field*) dans laquelle la fonction d'onde contient toutes les configurations électroniques qui peuvent être formées en distribuant les électrons considérés parmi les orbitales d'un espace choisi (IC complète dans l'espace considéré).

Pour tenir compte à la fois de la corrélation dynamique et statique, on peut obtenir une fonction d'onde multidéterminantale du type MCSCF puis appliquer un méthode multiréférentielle du type MRCI (*MultiReference Configuration Interaction*), MRCC (*MultiReference Coupled Cluster*) ou CASPT2 (*Complete Active Space Perturbation Theory*).

1.1.2 Méthodes DFT

Les méthodes issues de la théorie de la fonctionnelle de la densité (DFT) sont la deuxième approche usuelle de la chimie quantique. Elle repose sur la densité électronique, une fonction de 3 variables. Ainsi, la variable principale dans la résolution de l'équation de Schrödinger est réduit de $3N$ dimensions (avec N le nombre d'électrons) pour les méthodes de fonction d'onde à 3 dimensions dans les méthodes DFT.

La DFT est une méthode variationnelle, basée sur le théorème de Hohenberg et Kohn [1] qui montre que la densité de l'état fondamental détermine (à une constante additive près) le potentiel externe dans l'hamiltonien d'un système électronique. Toutes les observables du système, en particulier l'énergie de l'état fondamental, sont donc des fonctionnelles de la densité de l'état fondamental. Sauf pour quelques cas simples, la dépendance de la fonctionnelle d'énergie exacte vis-à-vis de la densité, pour l'état fondamental, est inconnue. La DFT est en réalité le plus souvent appliquée dans le cadre de la méthode de Kohn-Sham [2]. Cette méthode se fonde sur l'hypothèse de l'existence d'un système fictif d'électrons non-interagissants, qui posséde la même densité électronique que le système physique. Dans l'approche de Kohn-Sham de la DFT, toute la difficulté du problème à N électrons est concentrée dans la recherche d'une expression pour la fonctionnelle dite d'échange-corrélation se rapprochant le plus de l'expression exacte. Pour cela,

il existe plusieurs approximations qui fournissent très souvent une précision raisonnable pour un faible coût de calcul.

L'approximation de la densité locale (LDA pour *Local Density Approximation*) propose d'utiliser, en chaque point de l'espace, l'énergie d'échange-corrélation calculée pour un gaz d'électrons homogène, en supposant que, dans un petit volume entourant le point considéré, le système est localement homogène. Pour traiter les effets de polarisation de spin, il faut distinguer les densités associées aux deux composantes du spin. Cette extension de la méthode LDA, qui prend en compte les degrés de liberté de spin, porte le nom de méthode LSDA (*Local Spin Density Approximation*).

Le point faible de la méthode L(S)DA est l'hypothèse d'une densité électronique variant lentement dans l'espace. On peut raffiner cette approximation en exprimant les différents termes d'énergie non seulement en fonction de la densité mais aussi de son gradient, ce que l'on appelle les approximations GGA (*Generalized gradient approximation*) [3–20], et de son Laplacien et/ou la densité d'énergie cinétique, ce que l'on appelle les approximations meta-GGA [21–34].

1.1.3 Méthodes hybrides WFT/DFT

L'étape suivante dans la recherche de l'énergie la plus proche possible de l'énergie exacte du système est de combiner les avantages des méthodes de fonction d'onde et DFT. On parle alors de méthodes hybrides. Le développement de la DFT dans ce sens est toujours très actif et les modèles théoriques que nous avons élaborés au cours de cette thèse poursuivent cette direction de recherche.

L'approche hybride a été initiée par Becke [35]. En utilisant l'approche dite de la connexion adiabatique, Becke a proposé l'introduction partielle de l'échange exact (échange Hartree-Fock) dans la fonctionnelle d'échange-corrélation. Les fonctionnelles résultantes portent le nom d'hybrides globales (GH pour *Global Hybrid*) [20, 36–48]. La portion d'échange exact est déterminée de manière semi-empirique, comme dans la fonctionnelle d'échange-corrélation la plus populaire B3LYP [36], ou rationalisée, comme dans la fonctionnelle d'échange-corrélation PBE0 [37]. Il existe des fonctionnelles d'échange-corrélation dites hybrides locales. La portion d'échange exact dépend de la position dans l'espace [49].

Savin *et al.* [50–58] ont proposé l'extension multidéterminantale de la méthode de Kohn-Sham, qui est basée sur la décomposition longue portée/courte portée de l'interaction électron-électron. Pour effectuer une telle décomposition, on utilise souvent la fonction erreur standard et son complémentaire. La partie courte portée est traitée par les méthodes de la densité, qui sont capables de décrire correctement les interactions à courte portée grâce aux fonctionnelles d'échange-corrélation de courte portée conçues pour ce but. La partie longue portée est contenue dans un système fictif remplaçant celui de Kohn-Sham, qui peut être, en pratique, traité par un des modèles de la chimie quantique comme les méthodes Hartree-Fock [59], MCSCF [60, 61], CI [51, 55], CC [62–67], MP2 mono- et multiréférentielle [59, 62, 68–74], RPA (*Random Phase Approximation*) [75–84], CPMFT (*Constrained-Pairing Mean-Field Theory*) [85, 86] et DMFT (*Density-Matrix Functional Theory*) [87–89].

La première approximation est de restreindre ce formalisme à des fonctions d'onde à un seul déterminant, donnant une fonctionnelle hybride à séparation de portée (RSH pour *Range Separated Hybrid*) [59] qui consiste à combiner une fonctionnelle d'échange-

corrélation de courte portée avec une énergie d'échange de longue portée de type Hartree-Fock. On remarque clairement que cette approximation n'inclue pas de corrélation de longue portée. Une variante proche consiste à n'effectuer la décomposition que sur l'énergie d'échange. Il est alors possible de combiner une fonctionnelle d'échange de courte portée avec une énergie d'échange de longue portée de type Hartree-Fock (LC pour *Long-range Corrected Hybrid*) [90–98], ou d'utiliser une fonctionnelle d'échange de longue portée avec une fonctionnelle hybridée avec l'échange Hartree-Fock de courte portée (SC pour *Screened-Coulomb Hybrid*) [99–102]. On peut considérer la portée intermédiaire (*middle range*) dans la séparation du terme d'interaction électron-électron, ce qui a conduit à la création de la fonctionnelle HISS (Henderson-Izmaylov-Scuseria-Savin) [103]. Il existe aussi des modèles combinant les hybrides LC et GH comme la fonctionnelle CAM-B3LYP (*Coulomb-Attenuating Method*) [104] dans laquelle on introduit des paramètres permettant d'incorporer diverses portions d'échange Hartree-Fock à longue et à courte portée.

Le deuxième niveau d'approximation consiste à utiliser l'approche RSH comme référence sur laquelle on applique des méthodes perturbatives à longue portée. Plusieurs méthodes perturbatives ont été utilisées dans ce contexte comme la théorie de perturbation de type Møller-Plesset au deuxième ordre (MP2) de longue portée [59, 62, 68–73], la théorie de perturbation multiréférence de longue portée [74], l'approche CCSD(T) de longue portée [62–67] et différentes variantes de RPA de longue portée [75–84]. Ces approches sont prometteuses pour décrire efficacement les effets de corrélation nonlocaux, tels que ceux impliqués dans les complexes de van der Waals, faiblement liés par des forces de dispersion [105]. Ces interactions faibles ne sont pas décrites correctement par les approximations locales (LDA) ou semilocales (GGA, meta-GGA) de l'approche de Kohn-Sham de la DFT et plusieurs approches, empiriques ou non, ont par ailleurs été proposées pour remédier à ces difficultés [106–124].

Les approximations locales ou semilocales habituelles de l'approche de Kohn-Sham de la DFT ne permettent généralement pas de décrire avec précision les systèmes ayant des orbitales quasi-dégénérées partiellement remplies [53, 125, 126]. De nombreuses approches ont été proposées pour introduire explicitement le traitement de la corrélation statique dans la DFT (voir [127] pour une revue). Fromager *et al*. [60] ont utilisé l'extension multidéterminantale de la méthode de Kohn-Sham pour développer une méthode combinant la DFT et l'approche MCSCF, basée sur une séparation de portée de l'interaction électronique. L'idée est d'utiliser l'approche MCSCF sur la partie de longue portée de l'interaction pour inclure les effets de corrélation statique principaux et d'utiliser une fonctionnelle de la densité pour décrire les interactions de courte portée. La méthode est désignée par MC-srPBE dans laquelle la fonctionnelle PBE de courte portée [63] a été utilisée. Une autre manière d'introduire des effets de corrélation statique est de combiner la DFT avec une fonctionnelle de la matrice densité à une particule pour la longue portée [87–89].

1.2 Développement de nouvelles méthodes hybrides par séparation linéaire de l'interaction

Dans cette thèse, dans l'objectif de disposer de méthodes améliorant la précision de la DFT actuelle, nous avons étudié plusieurs méthodes hybrides basées sur une décomposition linéaire de l'interaction électron-électron en introduisant une constante de couplage λ dans l'extension multidéterminantale de la méthode de Kohn-Sham. Quand $\lambda = 0$, le

couplage s'identifie à la méthode de Kohn-Sham, alors que lorsque $\lambda = 1$, on retrouve une méthode de fonction d'onde. Pour les valeurs intermédiaires de λ, cette procédure entraîne l'utilisation de la fonctionnelle d'échange-corrélation dite complémentaire modélisant les interactions qui ne sont pas prises en compte par la méthode de fonction d'onde. Les fonctionnelles complémentaires peuvent être déduites directement des fonctionnelles d'échange-corrélation habituelles. Ceci représente un avantage pratique sur la procédure de la décomposition longue portée/courte portée, dans laquelle on a besoin de construire des nouvelles fonctionnelles d'échange-corrélation de courte portée. La contribution d'échange complémentaire est du premier ordre par rapport à l'interaction électron-électron et est donc donnée par une transformation d'échelle (*scaling*) linéaire de l'énergie d'échange de Kohn-Sham habituelle. Le traitement rigoureux de la contribution de corrélation complémentaire fait appel à l'utilisation des relations de transformation d'échelle (*scaling*) uniforme des coordonnées dans la densité [128–131]. Il est possible de négliger le *scaling* de la densité, ce qui conduit à des variantes des méthodes proposées.

Après un rappel méthodologique dans le chapitre 2, le chapitre 3 propose les méthodes hybrides multiconfigurationnelles à un paramètre. En utilisant la procédure ci-dessus, nous avons développé une approche [132] combinant un calcul de fonction d'onde multiconfigurationnelle complété de façon autocohérente par une fonctionnelle complémentaire de la densité pour décrire les effets de corrélation statique dans la DFT. Cette méthode porte le nom de MCDS1H (*multiconfigurational density-scaled one-parameter hybrid*). Quand on néglige le *scaling* de la densité, on obtient une méthode appelée MC1H (*multiconfigurational one-parameter hybrid*). Nous avons implémenté cette approche dans le logiciel DALTON [133], en utilisant les fonctionnelles d'échange-corrélation PBE [5] et BLYP [3, 4]. Concernant la constante de couplage λ, une étude [132] sur la réaction de cycloaddition de l'ozone avec l'éthylène et l'acétylène montre qu'une bonne valeur de ce paramètre est λ=0.25. Nous avons également testé la performance des approximations hybrides multiconfigurationnelles pour calculer les courbes d'énergie potentielle de cinq molécules diatomiques, H_2, Li_2, C_2, N_2 et F_2.

Le chapitre 4 expose les approximations doubles hybrides (DH) à un paramètre. Nous avons développé une reformulation rigoureuse de ces approximations DH qui ont été proposées par Grimme [134]. Elles consistent à combiner une fraction (a_x) d'énergie d'échange Hartree-Fock avec une fonctionnelle d'échange semilocale et une fraction (a_c) d'énergie de corrélation Møller-Plesset au deuxième ordre (MP2) avec une fonctionnelle de corrélation semilocale. Dans la première approximation double hybride à deux paramètres B2-PLYP de Grimme [134], les paramètres a_x=0.53 et a_c=0.27 ont été optimisés sur l'ensemble thermochimique G2/97 [135]. Les doubles hybrides permettent d'atteindre en moyenne une précision proche de la précision chimique pour les propriétés thermochimiques [136], et sont de plus en plus utilisées [137–151]. Cependant, et malgré des tentatives de justification à partir de la théorie de perturbation de Görling-Levy [145], ces approximations souffraient jusqu'à présent d'un manque de justification théorique.

Notre formulation [152] utilise l'extension multidéterminantale de la méthode de Kohn-Sham avec séparation linéaire de l'interaction. La première étape consiste à se limiter à des fonctions d'onde à un seul déterminant. Comme déjà signalé précédemment, la contribution de corrélation complémentaire peut être calculée soit en considérant le *scaling* de

la densité, donnant l'approximation DS1H (*density-scaled one-parameter hybrid*), soit en négligeant le *scaling* de la densité, donnant l'approximation appelée 1H (*one-parameter hybrid*). La deuxième étape consiste à ajouter l'énergie de corrélation apportée par les orbitales virtuelles, selon une théorie de perturbation de Rayleigh-Schrödinger non linéaire appliquée sur les références DS1H et 1H. On retrouve à l'ordre 1 l'énergie de DS1H et 1H. A l'ordre 2, on obtient les approximations DS1DH (*density-scaled one-parameter double-hybrid*) et 1DH (*one-parameter double-hybrid*) respectivement. Dans l'approximation double hybride à un paramètre 1DH, dans laquelle le *scaling* de la densité est négligé pour la fonctionnelle de corrélation, nous avons établi que la fraction d'énergie de corrélation Møller-Plesset (MP2) est donnée par le carré de la fraction d'énergie d'échange Hartree-Fock, $a_x=\lambda$ et $a_c=\lambda^2$. Les approximations doubles hybrides DS1DH et 1DH ont été implémentées dans le logiciel MOLPRO [153], en utilisant les fonctionnelles PBE et BLYP. Le paramètre de couplage λ a été optimisé sur des ensembles de tests représentatifs d'énergies d'atomisation AE6 et de barrières de réaction BH6 [154]. Nous avons mené une étude sur des ensembles de tests plus grands pour comparer les performances de 1DH-BLYP (la meilleure DH à un paramètre issue de l'optimisation), B2-PLYP et l'approximation double hybride à séparation de portée RSH+lrMP2 [59].

Le chapitre 5 présente une autre famille d'approximations doubles hybrides. Brémond et Adamo [155] ont proposé l'approximation double hybride PBE0-DH avec une dépendance en λ^3 pour la fraction d'énergie de corrélation MP2. En utilisant le formalisme précédent, nous avons donné une justification théorique [156] de cette forme d'approximations doubles hybrides. La fonctionnelle de corrélation avec *scaling* de la densité peut être approchée par une interpolation linéaire entre l'énergie de corrélation MP2 et l'énergie de corrélation de Kohn-Sham habituelle. En appliquant cette approximation sur le modèle DS1DH, on arrive à une nouvelle famille d'approximation LS1DH (linearly scaled one-parameter double-hybrid) où la fraction de l'énergie de corrélation MP2 est λ^3 ou bien, $a_c = a_x^3$. Ceci donne donc une base théorique plus solide pour l'approximation PBE0-DH.

Notre travail a été poursuivi par Fromager [157] qui a donné la justification théorique des approximations doubles hybrides à deux paramètres en introduisant une fraction d'échange exact multidéterminantal dans l'approximation DS1DH. Ceci demande un traitement par la procédure, dite d'optimisation du potentiel effectif (OEP pour *Optimized Effective Potential*), donnant une approximation appelée DS2-HF-OEP. La connection entre cette approximation et les doubles hybrides à deux paramètres standard se fait en négligeant le *scaling* et les corrections à l'ordre 2 de la densité.

Le chapitre 6 teste, sur un ensemble de cinq cristaux moléculaires, quelques approximations doubles hybrides, incluant celles développées au cours de cette thèse, qui ont été implémentées dans la suite logicielle CRYSTAL09 [158] et CRYSCOR09 [159] pour des calculs périodiques en base de gaussiennes localisées. Nous avons calculés les énergies réticulaires (ou énergies de cohésion, *lattice energy*) des cristaux d'urée, de formamide, d'acide formique, d'ammoniac, et de dioxyde de carbone. Cette étude montre que les doubles hybrides sont capables de reproduire de manière globalement satisfaisante les énergies réticulaires des systèmes avec liaisons hydrogènes, mais elles ont tendance à sous-estimer significativement l'énergie réticulaire du cristal de dioxyde carbone qui est lié en grande

partie par des interactions de dispersion.

Le chapitre 7 résume les conclusions et les perspectives des développements de cette thèse.

Bibliography

[1] P. Hohenberg and W. Kohn, Phys. Rev. **136**, B 864 (1964).

[2] W. Kohn and L. J. Sham, Phys. Rev. A **140**, 1133 (1965).

[3] C. Lee, W. Yang and R. G. Parr, Phys. Rev. B **37**, 785 (1988).

[4] A. D. Becke, Phys. Rev. A **38**, 3098 (1988).

[5] J. P. Perdew, K. Burke and M. Ernzerhof, Phys. Rev. Lett. **77**, 3865 (1996).

[6] D. C. Langreth and J. P. Perdew, Solid State Commun. **31**, 567 (1979).

[7] D. C. Langreth and J. P. Perdew, Phys. Rev. B **21**, 5469 (1980).

[8] J. P. Perdew, A. Ruzsinszky, G. I. Csonka, O. A. Vydrov, G. E. Scuseria, L. A. Constantin, X. L. Zhou and K. Burke, Phys. Rev. Lett. **100**, 136406 (2008).

[9] J. P. Perdew and W. Yue, Phys. Rev. B **33**, 8800 (1986).

[10] J. P. Perdew, Phys. Rev. B **33**, 8822 (1986).

[11] A. D. Becke, J. Chem. Phys. **84**, 4524 (1986).

[12] J. P. Perdew, J. A. Chevary, S. H. Vosko, K. A. Jackson, M. R. Pederson, D. J. Singh and C. Fiolhais, Phys. Rev. B **46**, 6671 (1992).

[13] F. A. Hamprecht, A. J. Cohen, D. J. Tozer and N. C.Handy, J. Chem. Phys. **109**, 6264 (1998).

[14] T. Tsuneda, T. Suzumura and K. Hirao, J. Chem. Phys. **110**, 10664 (1999).

[15] A. D. Boese, N. L. Doltsinis, N. C. Handy and M. J. Sprik, J. Chem. Phys. **112**, 1670 (2000).

[16] A. D. Boese and N. C. Handy, J. Chem. Phys. **114**, 5497 (2001).

[17] N. C. Handy and A. J. Cohen, Mol. Phys. **99**, 403 (2001).

[18] N. C. Handy and A. J. Cohen, J. Chem. Phys. **116**, 5411 (2002).

[19] T. W. Keal and D. J. Tozer, J. Chem. Phys. **121**, 5654 (2004).

[20] Y. Zhao and D. G. Truhlar, J. Chem. Phys. **128**, 184109 (2008).

[21] A. D. Becke, J. Chem. Phys. **88**, 1053 (1988).

[22] A. D. Becke, Int. J. Quantum. Chem. **52**, 625 (1994).

[23] A. D. Becke and M. R. Roussel, Phys. Rev. A **39**, 3761 (1989).

[24] J. P. Perdew, S. Kurth, A. Zupan and P. Blaha, Phys. Rev. Lett. **82**, 2544 (1999).

[25] J. P. Perdew and L. A. Constantin, Phys. Rev. B **75**, 155109 (2007).

[26] J. P. Perdew, A. Ruzsinszky, J. Tao, G. I. Csonka and G. E. Scuseria, Phys. Rev. A **76**, 042506 (2007).

[27] J. P. Perdew, A. Ruzsinszky, G. I. Csonka, L. A. Constantin and J. W. Sun, Phys. Rev. Lett. **103**, 026403 (2009).

[28] J. Tao, J. P. Perdew, V. N. Staroverov and G. E. Scuseria, Phys. Rev. Lett. **91**, 146401 (2003).

[29] C. Lee and R. G. Parr, Phys. Rev. A **35**, 2377 (1987).

[30] A. D. Becke, J. Chem. Phys. **104**, 1040 (1996).

[31] A. D. Becke, J. Chem. Phys. **109**, 2092 (1998).

[32] T. van Voorhis and G. E. Scuseria, J. Chem. Phys. **109**, 400 (1998).

[33] A. D. Boese and N. C. Handy, J. Chem. Phys. **116**, 9559 (2002).

[34] Y. Zhao and D. G. Truhlar, J. Chem. Phys. **125**, 194101 (2006).

[35] A. D. Becke, J. Chem. Phys. **98**, 1372 (1993).

[36] P. J. Stephens, F. J. Devlin, C. F. Chabalowski and M. J. Frisch, J. Phys. Chem. **98**, 11623 (1994).

[37] J. P. Perdew, M. Ernzerhof and K. Burke, J. Chem. Phys **105**, 9982 (1996).

[38] A. D. Becke, J. Chem. Phys. **107**, 8554 (1997).

[39] C. Adamo and V. Barone, J. Chem. Phys. **101**, 6158 (1999).

[40] B. J. Lynch, P. L. Fast, M. Harris and D. G. Truhlar, J. Phys. Chem. A **104**, 4811 (2000).

[41] P. J. Wilson, T. J. Bradly and D. J. Tozer, J. Chem. Phys. **115**, 9233 (2001).

[42] A. J. Cohen and N. C. Handy, Mol. Phys. **99**, 607 (2001).

[43] X. Xu and W. A. Goddard III, Proc. Natl. Acad. Sci. U.S.A. **229**, 2673 (2004).

[44] T. W. Keal and D. J. Tozer, J. Chem. Phys. **123**, 121103 (2005).

[45] Y. Zhao, N. E. Schultz and D. G. Truhlar, J. Chem. Theory Comput. **2**, 364 (2006).

[46] Y. Zhao and D. G. Truhlar, J. Chem. Theory Comput. **110**, 13126 (2006).

[47] Y. Zhao and D. G. Truhlar, J. Chem. Theory Comput. **110**, 5121 (2006).

[48] Y. Zhao and D. G. Truhlar, Theor. Chem. Acc. **120**, 215 (2008).

[49] J. Jaramillo, G. E. Scuseria and M. Ernzerhof, J. Chem. Phys. **118**, 1068 (2003).

[50] H. Stoll and A. Savin, in *Density Functional Method in Physics*, edited by R. M. Dreizler and J. da Providencia (Plenum, Amsterdam, 1985), pp. 177–207.

[51] A. Savin and H.-J. Flad, Int. J. Quantum. Chem. **56**, 327 (1995).

[52] A. Savin, in *Recent Advances in Density Functional Theory*, edited by D. P. Chong (World Scientific, 1996).

[53] A. Savin, in *Recent Developments of Modern Density Functional Theory*, edited by J. M. Seminario (Elsevier, Amsterdam, 1996), pp. 327–357.

[54] T. Leininger, H. Stoll, H.-J. Werner and A. Savin, Chem. Phys. Lett. **275**, 151 (1997).

[55] R. Pollet, A. Savin, T. Leininger and H. Stoll, J. Chem. Phys. **116**, 1250 (2002).

[56] R. Pollet, F. Colonna, T. Leininger, H. Stoll, H.-J. Werner and A. Savin, Int. J. Quantum. Chem. **91**, 84 (2003).

[57] A. Savin, F. Colonna and R. Pollet, Int. J. Quantum. Chem. **93**, 166 (2003).

[58] J. Toulouse, F. Colonna and A. Savin, Phys. Rev. A **70**, 062505 (2004).

[59] J. G. Ángyán, I. Gerber, A. Savin and J. Toulouse, Phys. Rev. A **72**, 012510 (2005).

[60] E. Fromager, J. Toulouse and H. J. A. Jensen, J. Chem. Phys. **126**, 074111 (2007).

[61] E. Fromager, F. Réal, P. Wåhlin, U. Wahlgren and H. J. A. Jensen, J. Chem. Phys. **131**, 054107 (2009).

[62] E. Goll, H.-J. Werner and H. Stoll, Phys. Chem. Chem. Phys. **7**, 3917 (2005).

[63] E. Goll, H.-J. Werner, H. Stoll, T. Leininger, P. Gori-Giorgi and A. Savin, Chem. Phys. **329**, 276 (2006).

[64] E. Goll, H. Stoll, C. Thierfelder and P. Schwerdtfeger, Phys. Rev. A **76**, 032507 (2007).

[65] E. Goll, H.-J. Werner and H. Stoll, Chem. Phys. **346**, 257 (2008).

[66] E. Goll, M. Ernst, F. Moegle-Hofacker and H. Stoll, J. Chem. Phys. **130**, 234112 (2009).

[67] E. Goll, H.-J. Werner and H. Stoll, Z. Phys. Chem. **224**, 481 (2010).

[68] I. C. Gerber and J. G. Ángyán, Chem. Phys. Lett. **416**, 370 (2005).

[69] I. C. Gerber and J. G. Ángyán, J. Chem. Phys. **126**, 044103 (2007).

[70] J. G. Ángyán, Phys. Rev. A **78**, 022510 (2008).

[71] E. Fromager and H. J. A. Jensen, Phys. Rev. A **78**, 022504 (2008).

[72] S.Chabbal, H.-J. Werner, H. Stoll and T. Leininger, Mol. Phys. **108**, 3373 (2010).

[73] S. Chabbal, D. Jacquemin, C. Adamo, H. Stoll and T. Leininger, J. Chem. Phys. **133**, 151104 (2010).

[74] E. Fromager, R. Cimiraglia and H. J. A. Jensen, Phys. Rev. A **81**, 024502 (2010).

[75] J. Toulouse, I. C. Gerber, G. Jansen, A. Savin and J. G. Ángyán, Phys. Rev. Lett. **102**, 096404 (2009).

[76] W. Zhu, J. Toulouse, A. Savin and J. G. Ángyán, J. Chem. Phys. **132**, 244108 (2010).

[77] J. Toulouse, W. Zhu, J. G. Ángyán and A. Savin, Phys. Rev. A **82**, 032502 (2010).

[78] J. Toulouse, W. Zhu, A. Savin, G. Jansen and J. G. Ángyán, J. Chem. Phys. **135**, 084119 (2011).

[79] J. G. Ángyán, R.-F. Liu, J. Toulouse and G. Jansen, J. Chem. Theory Comput. **7**, 3116 (2011).

[80] B. G. Janesko, T. M. Henderson and G. E. Scuseria, J. Chem. Phys. **130**, 081105 (2009).

[81] B. G. Janesko, T. M. Henderson and G. E. Scuseria, J. Chem. Phys. **131**, 034110 (2009).

[82] B. G. Janesko and G. E. Scuseria, J. Chem. Phys. **131**, 154106 (2009).

[83] J. Paier, B. G. Janesko, T. M. Henderson, G. E. Scuseria, A. Grüneis and G. Kresse, J. Chem. Phys. **132**, 094103 (2010).

[84] R. M. Irelan, T. M. Henderson and G. E. Scuseria, J. Chem. Phys. **135**, 094105 (2011).

[85] T. Tsuchimochi, G. E. Scuseria and A. Savin, J. Chem. Phys. **132**, 024111 (2010).

[86] T. Tsuchimochi and G. E. Scuseria, J. Chem. Phys. **134**, 064101 (2011).

[87] K. Pernal, Phys. Rev. A **81**, 052511 (2010).

[88] D. R. Rohr, J. Toulouse and K. Pernal, Phys. Rev. A **82**, 052502 (2010).

[89] D. R. Rohr and K. Pernal, J. Chem. Phys. **135**, 074104 (2011).

[90] H. Iikura, T. Tsuneda, T. Yanai and K. Hirao, J. Chem. Phys. **115**, 3540 (2001).

[91] T. T. Y. Tawada, S. Yanagisawa, T. Yanai and K. Hirao, J. Chem. Phys. **120**, 8425 (2004).

[92] R. Baer and D. Neuhauser, Phys. Rev. Lett. **94**, 043002 (2005).

[93] I. Gerber and J. G. Ángyán, Chem. Phys. Lett. **415**, 100 (2005).

[94] J.-W. Song, S. Tokura, T. Sato, M. A. Watson and K. Hirao, J. Chem. Phys. **127**, 154109 (2007).

[95] J.-D. Chai and M. Head-Gordon, J. Chem. Phys. **128**, 084106 (2008).

[96] O. A. Vydrov and G. E. Scuseria, J. Chem. Phys. **125**, 234109 (2006).

[97] M. A. Rohrdanz, K. M. Martins and J. M. Herbert, J. Chem. Phys. **130**, 054112 (2009).

[98] J.-W. Song, M. A. Watson and K. Hirao, J. Chem. Phys. **131**, 144108 (2009).

[99] J. Heyd, G. E. Scuseria and M. Ernzerhof, J. Chem. Phys. **118**, 8207 (2003).

[100] J. Heyd and G. E. Scuseria, J. Chem. Phys. **120**, 7274 (2004).

[101] J. Heyd and G. E. Scuseria, J. Chem. Phys. **121**, 1187 (2004).

[102] R. Peverati and D. G. Truhlar, Phys. Chem. Chem. Phys. **14**, 16187 (2012).

[103] T. M. Henderson, A. F. Izmaylov, G. E. Scuseria and A. Savin, J. Chem. Phys. **127**, 221103 (2007).

[104] T. Yanai, D. P. Tew and N. C. Handy, Chem. Phys. Lett. **393**, 51 (2004).

[105] J. F. Dobson, K. McLennan, A. Rubio, J. Wang, T. Gould, H. M. Le and B. P. Dinte, Aust. J. Chem. **54**, 513 (2001).

[106] M. Elstner, P. Hobza, T. Frauenheim, S. Suhai and E. Kaxiras, J. Chem. Phys. **114**, 5149 (2001).

[107] X. Wu, M. C. Vargas, S. Nayak, V. Lotrich and G. Scoles, J. Chem. Phys. **115**, 8748 (2001).

[108] Q. Wu and W. Yang, J. Chem. Phys. **116**, 515 (2002).

[109] U. Zimmerli, M. Parrinello and P. Koumoutsakos, J. Chem. Phys. **120**, 2693 (2004).

[110] S. Grimme, J. Comput. Chem. **25**, 1463 (2004).

[111] A. D. Becke and E. R. Johnson, J. Chem. Phys. **122**, 154104 (2005).

[112] J. G. Ángyán, J. Chem. Phys. **127**, 024108 (2007).

[113] T. Sato and H. Nakai, J. Chem. Phys. **131**, 224104 (2009).

[114] O. A. von Lilienfeld, I. Tavernelli and U. Rothlisberger, Phys. Rev. Lett. **93**, 153004 (2004).

[115] J.-D. Chai and M. Head-Gordon, J. Chem. Phys. **131**, 174105 (2009).

[116] Y. Lin, C. Tsai, G. Li and J.-D. Chai, J. Chem. Phys. **136**, 154109 (2012).

[117] Y. Lin, G. Li, S. Mao and J.-D. Chai, J. Chem. Theory Comput. **9**, 263 (2013).

[118] Y. Andersson, D. C. Langreth and B. I. Lundqvist, Phys. Rev. Lett. **76**, 102 (1996).

[119] J. F. Dobson and B. P. Dinte, Phys. Rev. Lett. **76**, 1780 (1996).

[120] M. Dion, H. Rydberg, E. Schröder, D. C. Langreth and B. I. Lundqvist, Phys. Rev. Lett. **92**, 246401 (2004).

[121] M. Kamiya, T. Tsuneda and K. Hirao, J. Chem. Phys. **117**, 6010 (2002).

[122] O. A. Vydrov and T. van Voorhis, J. Chem. Phys. **130**, 104105 (2009).

[123] O. A. Vydrov and T. van Voorhis, Phys. Rev. Lett. **103**, 063004 (2009).

[124] A. Heßelmann, G. Jansen and M. Schütz, J. Chem. Phys. **122**, 014103 (2005).

[125] E. J. Baerends, Phys. Rev. Lett. **87**, 133004 (2001).

[126] A. J. Cohen, P. Mori-Sánchez and W. Yang, J. Chem. Phys. **129**, 121104 (2008).

[127] J. Gräfenstein and D. Cremer, Mol. Phys. **103**, 279 (2005).

[128] M. Levy and J. P. Perdew, Phys. Rev. A **32**, 2010 (1985).

[129] M. Levy, W. Yang and R. G. Parr, J. Chem. Phys. **83**, 2334 (1985).

[130] M. Levy, Phys. Rev. A **43**, 4637 (1991).

[131] M. Levy and J. P. Perdew, Phys. Rev. B **48**, 11638 (1993).

[132] K. Sharkas, A. Savin, H. J. A. Jensen and J. Toulouse, J. Chem. Phys. **137**, 044104 (2012).

[133] C. Angeli, K. L. Bak, V. Bakken, O. Christiansen, R. Cimiraglia, S. Coriani, P. Dahle, E. K. Dalskov, T. Enevoldsen, B. Fernandez, L. Ferrighi, L. Frediani, C. Hättig, K. Hald, A. Halkier, H. Heiberg, T. Helgaker, H. Hettema, B. Jansik, H. J. A. Jensen, D. Jonsson, P. Jørgensen, S. Kirpekar, W. Klopper, S. Knecht, R. Kobayashi, J. Kongsted, H. Koch, A. Ligabue, O. B. Lutnæs, K. V. Mikkelsen, C. B. Nielsen, P. Norman, J. Olsen, A. Osted, M. J. Packer, T. B. Pedersen, Z. Rinkevicius, E. Rudberg, T. A. Ruden, K. Ruud, P. Salek, C. C. M. Samson, A. S. de Meras, T. Saue, S. P. A. Sauer, B. Schimmelpfennig, A. H. Steindal, K. O. Sylvester-Hvid, P. R. Taylor, O. Vahtras, D. J. Wilson and H.Ågren, DALTON, a molecular electronic structure program, Release DALTON2011 (2011), see http://daltonprogram.org.

[134] S. Grimme, J. Chem. Phys. **124**, 034108 (2006).

[135] L. A. Curtiss, K. Raghavachari, P. C. Redfern and J. A. Pople, J. Chem. Phys. **106**, 1063 (1997).

[136] T. Schwabe and S. Grimme, Phys. Chem. Chem. Phys. **8**, 4398 (2006).

[137] J. C. Sancho-García and A. J. Pérez-Jiménez, J. Chem. Phys. **131**, 084108 (2009).

[138] A. Tarnopolsky, A. Karton, R. Sertchook, D. Vuzman and J. M. L. Martin, J. Phys. Chem. A **112**, 3 (2008).

[139] A. Karton, A. Tarnopolsky, J.-F. Lamère, G. C. Schatz and J. M. L. Martin, J. Phys. Chem. A **112**, 12868 (2008).

[140] S. Kozuch, D. Gruzman and J. M. L. Martin, J. Phys. Chem. C **114**, 20801 (2010).

[141] S. Kozuch and J. M. L. Martin, Phys. Chem. Chem. Phys. **13**, 20104 (2011).

[142] B. Chan and L. Radom, J. Chem. Theory Comput. **7**, 2852 (2011).

[143] T. Benighaus, R. A. DiStasio Jr., R. C. Lochan, J.-D. Chai and M. Head-Gordon, J. Phys. Chem. A **112**, 2702 (2008).

[144] L. Goerigk and S. Grimme, J. Chem. Theory Comput **7**, 291 (2011).

[145] Y. Zhang, X. Xu and W. A. Goddard III, Proc. Natl. Acad. Sci. U.S.A. **106**, 4963 (2009).

[146] I. Y. Zhang, Y. Luo and X. Xu, J. Chem. Phys. **132**, 194105 (2010).

[147] I. Y. Zhang, Y. Luo and X. Xu, J. Chem. Phys. **133**, 104105 (2010).

[148] X. Xu and I. Y. Zhang, Int. Rev. Phys. Chem. **30**, 115 (2011).

[149] I. Y. Zhang, J. Wu and X. Xu, Chem. Commun. **46**, 3057 (2010).

[150] Y. Zhang, X. Xu and Y. S. Jung and W. A. Goddard III, Proc. Natl. Acad. Sci. U.S.A. **108**, 19896 (2011).

[151] I. Y. Zhang, N. Q. Su, E. Brémond and C. Adamo, J. Chem. Phys. **136**, 174103 (2011).

[152] K. Sharkas, J. Toulouse and A. Savin, J. Chem. Phys. **134**, 064113 (2011).

[153] H.-J. Werner, P. J. Knowles, G. Knizia, F. R. Manby, M. Schütz, and others, MOLPRO, version 2010.1, a package of ab initio programs, Cardiff, UK, 2010, see http://www.molpro.net.

[154] B. J. Lynch and D. G. Truhlar, J. Phys. Chem. A **107**, 8996 (2003).

[155] E. Brémond and C. Adamo, J. Chem. Phys. **135**, 024106 (2011).

[156] J. Toulouse, K. Sharkas, E. Brémond and C. Adamo, J. Chem. Phys. **135**, 101102 (2011).

[157] E. Fromager, J. Chem. Phys. **135**, 244106 (2011).

[158] R. Dovesi, V. R. Saunders, C. Roetti, R. Orlando, C. M. Zicovich-Wilson, F. Pascale, B. Civalleri, K. Doll, N. M. Harrison, I. J. Bush, P. D′Arco and M. Llunell., CRYSTAL, Release CRYSTAL09 (2009), see http://www.crystal.unito.it.

[159] C. Pisani, M. Schütz, S. Casassa, D. Usvyat, L. Maschio, M. Lorenz and A. Erba, Phys. Chem. Chem. Phys. **14**, 7615 (2012).

Chapter 2

Models and approximations

This chapter presents an introduction to and a survey of the quantum many-body problem studied in this thesis. It describes in a nutshell some aspects of zero-temperature and time-independent wave function and density functional methods, and introduces the notations used in this thesis.

2.1 N-electron problem

The term *ab initio* is Latin for *from the first principles*, implying that an *ab initio* calculation is to be done without the use of experimentally-derived inputs except for the mass of the electron, m, the magnitude of the charge of the electron, e, and Planck's constant, $\hbar$. The used units throughout this thesis are called Hartree atomic units ($\hbar = m = e^2/(4\pi\varepsilon_0) = 1$).

2.1.1 Separation of space and time

Understanding electron motion and behaviour in atoms, molecules and solids is a key part of materials science. The relevant equation is the time-dependent Schrödinger wave equation

$$\hat{\mathcal{H}}\Psi(\mathbf{r},t) = i\frac{\partial}{\partial t}\Psi(\mathbf{r},t), \tag{2.1}$$

where $\hat{\mathcal{H}}$ is the Hamiltonian operator, $\Psi(\mathbf{r},t)$ is the wave function of N interacting electrons and $\mathbf{r} \equiv \{\mathbf{r}_1, \mathbf{r}_2, ..., \mathbf{r}_N\}$ stands for the collection of all electronic spatial coordinates. We consider the stationary states that have the form

$$\Psi(\mathbf{r},t) = \Psi(\mathbf{r})e^{-iEt}, \tag{2.2}$$

which shows that the wave function can be factored into a product of a space part and a time part and that the time dependence is given by a phase factor. Inserting this wave function in Eq (2.1) leads to the time-independent Schrödinger equation

$$\hat{\mathcal{H}}\Psi(\mathbf{r}) = E\Psi(\mathbf{r}), \tag{2.3}$$

which is the central equation in molecular electronic-structure theory. The properties of a system are determined by the eigenfunction Ψ and the eigenvalue E of the Hamiltonian, which represents the energy of the system.

2.1.2 Separation of nuclear and electronic variables (Born-Oppenheimer approximation)

In the nonrelativistic approximation, for a system of N interacting electrons moving around M nuclei, with $\mathbf{r}_i$ denoting electronic and $\mathbf{R}_\alpha$ denoting nuclear spatial coordinates, considering all the terms in atomic units, the Hamiltonian looks like,

$$\hat{\mathcal{H}}(\mathbf{r},\mathbf{R}) = -\frac{1}{2}\sum_{i}^{N}\nabla_i^2 - \sum_{\alpha}^{M}\frac{1}{2M_\alpha}\nabla_\alpha^2 - \sum_{i}^{N}\sum_{\alpha}^{M}\frac{Z_\alpha}{r_{i\alpha}} + \sum_{i}^{N}\sum_{j>i}^{N}\frac{1}{r_{ij}} + \sum_{\alpha}^{M}\sum_{\beta>\alpha}^{M}\frac{Z_\beta Z_\alpha}{R_{\alpha\beta}}. \quad (2.4)$$

The Laplacian operators ∇_i^2 and ∇_α^2 involve differentiation with respect to the coordinates of the ith electron and αth nucleus. M_α is the mass of nucleus α in atomic units, and Z_α is the atomic number of the nucleus α. The distance between the ith electron and the αth nucleus is $r_{i\alpha} = |\mathbf{r}_{i\alpha}| = |\mathbf{r}_i - \mathbf{R}_\alpha|$; the distance between the ith and jth electron is $r_{ij} = |\mathbf{r}_{ij}| = |\mathbf{r}_i - \mathbf{r}_j|$; and the distance between the αth and βth nucleus is $R_{\alpha\beta} = |\mathbf{R}_{\alpha\beta}| = |\mathbf{R}_\alpha - \mathbf{R}_\beta|$.

The Hamiltonian in Eq (2.4) is composed of five terms: the two first terms are the kinetic energy of the N electrons and the M nuclei, respectively. The Coulomb attraction between the electrons and nuclei is represented by term three, and the fourth and fifth terms describe respectively the interelectron and internuclear repulsion energies.

One can simplify this Hamiltonian if one notes the difference in mass between electrons and nuclei (a factor of $10^3 - 10^5$). The nuclei are much heavier than electrons, thus they move more slowly. The electronic problem can be solved for nuclei which are momentarily clamped to fixed positions in space. Such an approximation is known as the Born-Oppenheimer (BO) approximation [1]. This approximation decouples electron motion from the motion of the nuclei then the corresponding total wave function can be written as a product of its electronic and nuclear components

$$\Psi_{total}(\mathbf{r},\mathbf{R}) = \Psi_{el}(\mathbf{r};\mathbf{R})\Psi_{nuc}(\mathbf{R}). \quad (2.5)$$

The separation of nuclear and electronic coordinates is an essential first step in simplifying a molecular Schrödinger equation to the point where actual computation can take place. The electronic wave function $\Psi_{el}(\mathbf{r};\mathbf{R})$ describes the motion of the electrons and depends explicitly on the electronic coordinate $\mathbf{r}$ but depends parametrically on the nuclear coordinates $\mathbf{R}$, and is determined by

$$\hat{H}_{el}(\mathbf{r};\mathbf{R})\Psi_{el}(\mathbf{r};\mathbf{R}) = E_{el}(\mathbf{R})\Psi_{el}(\mathbf{r};\mathbf{R}). \quad (2.6)$$

The kinetic energy of the nuclei can be neglected and the Coulomb repulsion between the nuclei can be considered constant. The remaining terms in (2.4) are called the electronic Hamiltonian

$$\hat{H}_{el} = -\frac{1}{2}\sum_{i}^{N}\nabla_i^2 - \sum_{i}^{N}\sum_{\alpha}^{M}\frac{Z_\alpha}{r_{i\alpha}} + \sum_{i}^{N}\sum_{j>i}^{N}\frac{1}{r_{ij}}. \quad (2.7)$$

The total energy is given by the sum of the electronic energy and the nuclear repulsion

$$E_{total} = E_{el} + \sum_{\alpha}^{M}\sum_{\beta>\alpha}^{M}\frac{Z_\beta Z_\alpha}{R_{\alpha\beta}}. \quad (2.8)$$

The nuclear wave function $\Psi_{nuc}(\mathbf{R})$ is a solution of the nuclear Schrödinger equation

$$\Big(-\sum_{\alpha}^{M} \frac{1}{2M_\alpha}\nabla_\alpha^2 + E_{total}(\mathbf{R})\Big)\Psi_{nuc}(\mathbf{R}) = E\Psi_{nuc}(\mathbf{R}), \tag{2.9}$$

which is the key equation in theoretical vibrational spectroscopy. Because we will only consider electronic wave functions and Hamiltonians throughout this thesis, we drop the subscript '*el*'.

2.1.3 Spin-orbitals

An orbital is a wave function describing a single electron. For an atom one has *atomic orbitals* and for a molecule one has *molecular orbitals*. A *spatial orbital* $\psi_i(\mathbf{r})$ is a function of the position vector $\mathbf{r}$ and describes the spatial distribution of the ith electron such that $|\psi_i(\mathbf{r})|^2 d\mathbf{r}$ is the probability of finding the ith electron in the volume $d\mathbf{r}$ at the position $\mathbf{r}$. It is well known that the probability of finding the ith electron in all the space is one, $\int |\psi_i(\mathbf{r})|^2 d\mathbf{r} = 1$. We also request that two different spatial orbitals to be orthogonal, $\int \psi_i(\mathbf{r})\psi_j(\mathbf{r})d\mathbf{r} = 0$. A set of spatial orbitals which has these two properties is called orthonormal. In Dirac's notation

$$\langle\psi_i|\psi_j\rangle \;=\; \delta_{ij} = \begin{cases} 1 & i = j \\ 0 & i \neq j \end{cases} \tag{2.10}$$

The elementary particles are characterized not only by their spatial coordinates but also by their intrinsic spin $\mathbf{s}$ which is a vector quantity. The electron is known to have a spin with a quantum number 1/2, whose z-component is quantized to take one of two possible eigenvalues $+1/2$ or $-1/2$ corresponding two eigenfunctions $\alpha(s)$ or $\beta(s)$ respectively. The composition of spatial $\mathbf{r} = \{x, y, z\}$ and spin s coordinates is called the space-spin coordinate, $\mathbf{x} = \{\mathbf{r}, s\}$. With this variable, we define a *spin orbital* $\phi(\mathbf{x})$ as a one-electron wave function which includes the spin of the electron. If the spin-orbit interaction is neglected, the spatial and spin coordinates are independent, and consequently the spin orbital may be written as a product of a spatial orbital and either the α or β spin function

$$\begin{aligned} \phi_i^\alpha(\mathbf{x}) &= \psi_i^\alpha(\mathbf{r})\alpha(s) \\ \phi_i^\beta(\mathbf{x}) &= \psi_i^\beta(\mathbf{r})\beta(s), \end{aligned} \tag{2.11}$$

where we have recognized the fact that the spatial part of a spin orbital may depend on whether the spin part is α or β. If the spatial orbitals are orthonormal, so are the spin orbitals

$$\langle\phi_i|\phi_j\rangle \;=\; \delta_{ij}, \tag{2.12}$$

which is a consequence of the normalization of the spin functions

$$\begin{aligned} \langle\alpha|\alpha\rangle = \langle\beta|\beta\rangle &= 1 \\ \langle\alpha|\beta\rangle &= 0. \end{aligned} \tag{2.13}$$

2.1.4 Slater determinant

In *ab-initio* methods, we seek to solve the Schrödinger equation (2.6) in which the main difficulty arises from the interaction between the electrons in the electronic Hamiltonian (2.7). The starting point is to set this term to zero, *i.e* the electrons move independently in the nuclear potential. In this approximation, the electronic Hamiltonian can be written as a sum of one-electron Hamiltonians $\hat{h}_i = \hat{h}(\mathbf{r}_i)$

$$\begin{aligned} \hat{H} &= \sum_i^N \hat{h}_i \\ \hat{h}_i &= -\frac{1}{2}\nabla_i^2 - \sum_\alpha^M \frac{Z_\alpha}{r_{i\alpha}}, \end{aligned} \tag{2.14}$$

and the wave function as a product of spin orbitals describing a single electron

$$\Psi_{HP}(\mathbf{x}_1, \mathbf{x}_2, ..., \mathbf{x}_N) = \phi_1(\mathbf{x}_1)\phi_2(\mathbf{x}_2)...\phi_N(\mathbf{x}_N). \tag{2.15}$$

This approximate wave function is called the *Hartree product* (HP) [2]. This model was used in the early days of quantum mechanics to perform calculations of the atomic structure, but it has some shortcomings. It is well known that electrons are identical particles, a fact which must be reflected by the wave function. If two electrons i and j were to be interchanged, there should be no change in any of the observable properties of the system. Especially, the probability density, as defined by the square amplitude of the wave function, should be the same after such a manipulation. A basic requirement on any reasonable trial electronic wave function should be that the latter is an eigenfunction of the permutation operators with eigenvalues of (-1), $\hat{P}_{ij}\Psi = -\Psi$ for any two electrons i and j, where $\hat{P}_{ij}$ is the permutation operator interchanging the coordinates of these two electrons. This is the *Antisymmetry Principle* which states that a many electron wave function must be antisymmetric with respect to interchange of the coordinates (including spin) of any two electrons.

The Hartree product (2.15) does not satisfy the Antisymmetry Principle, but it is possible to get an acceptable wave function from it. Let us consider the case of two electrons. The Hartree product is $\Psi_{HP}(\mathbf{x}_1, \mathbf{x}_2) = \phi_1(\mathbf{x}_1)\phi_2(\mathbf{x}_2)$. If we swap the coordinates of electron 1 with electron 2, we get $\Psi_{HP}(\mathbf{x}_2, \mathbf{x}_1) = \phi_1(\mathbf{x}_2)\phi_2(\mathbf{x}_2)$. One can construct an approximate wave function $\Phi(\mathbf{x}_1, \mathbf{x}_2)$ which satisfies the Antisymmetry Principle, $\Phi(\mathbf{x}_1, \mathbf{x}_2) = -\Phi(\mathbf{x}_2, \mathbf{x}_1)$, as the sum of two Hartree products

$$\begin{aligned} \Phi(\mathbf{x}_1, \mathbf{x}_2) &= \frac{1}{\sqrt{2}}[\phi_1(\mathbf{x}_1)\phi_2(\mathbf{x}_2) - \phi_1(\mathbf{x}_2)\phi_2(\mathbf{x}_1)] \\ &= \frac{1}{\sqrt{2}}\begin{vmatrix} \phi_1(\mathbf{x}_1) & \phi_2(\mathbf{x}_1) \\ \phi_1(\mathbf{x}_2) & \phi_2(\mathbf{x}_2) \end{vmatrix}, \end{aligned} \tag{2.16}$$

where $1/\sqrt{2}$ is a normalization constant. Therefore, for N electrons, the approximate wave function is

$$\Phi(\mathbf{x}_1, \mathbf{x}_2, ..., \mathbf{x}_N) = \frac{1}{\sqrt{N!}}\begin{vmatrix} \phi_1(\mathbf{x}_1) & \phi_2(\mathbf{x}_1) & \dots & \phi_N(\mathbf{x}_1) \\ \phi_1(\mathbf{x}_2) & \phi_2(\mathbf{x}_2) & \dots & \phi_N(\mathbf{x}_2) \\ \vdots & \vdots & \ddots & \vdots \\ \phi_1(\mathbf{x}_N) & \phi_2(\mathbf{x}_N) & \dots & \phi_N(\mathbf{x}_N) \end{vmatrix}. \tag{2.17}$$

This form of the wave function was applied to the N-electron problem by Slater [3] and is known as a Slater determinant. By writing the wave function in this form, we provide a way which automatically satisfies the *Pauli Exclusion Principle*, *i.e.* two identical fermions cannot be found in the same quantum state (having the same spin orbital), which is a corollary of the antisymmetry principle. If $\phi_i = \phi_j$, two columns are identical in (2.17), then $\Phi = 0$ according to the determinant property. Because the determinant wave function (2.17) is only a function of the N occupied spin orbitals $\phi_i(\mathbf{x})$, $\phi_j(\mathbf{x})$, ..., $\phi_k(\mathbf{x})$, we introduce the abbreviation $\Phi = |ij...k\rangle$. The antisymmetry property of Slater determinant is expressed as

$$|...i...j...\rangle \;=\; -|...j...i...\rangle. \tag{2.18}$$

2.1.5 Variational theorem

Since an exact or almost exact numerical solution of the Schrödinger equation (2.6) is not in sight and appears hopeless for $N>2$, approximations must be made. A standard tool for computing approximate solutions of (2.6) is the variation method based on the *Variational Theorem*. For any initial trial wave function, Φ, we have

$$E[\Phi] \;=\; \frac{\langle\Phi|\hat{H}|\Phi\rangle}{\langle\Phi|\Phi\rangle} \geq E_0 \tag{2.19}$$

where E_0 is the exact ground state energy. Approximate solutions for the ground state (excited states can be treated similarly) can thus be obtained by a minimization of $E[\Phi]$ for a reasonable ansatz Φ. By expressing the approximate wave function in terms of parameters and minimizing the functional (2.19) with respect to these parameters one can obtain progressively better approximations to the energy and the eigenfunctions of the Hamiltonian. The energies obtained are more accurate than the wave functions and represent rigorous upper bounds to the exact ground state energy. Quantitatively, if the accuracy of the approximate wave function assumed is of order δ, the energy is accurate to order δ^2.

2.2 Hartree-Fock and post Hartree-Fock approximations

The essence of the Hartree-Fock method is that the wave function is written as a Slater determinant [4]. We will now use this wave function representation to obtain the expectation value $\langle\Phi|\hat{H}|\Phi\rangle$ of the Hamiltonian operator.

2.2.1 Expectation values with a Slater determinant

The electronic Hamiltonian for a many electron system can be written in terms of one-, and two-electron operators

$$\hat{H} \;=\; \sum_{i}^{N} \hat{h}_i + \sum_{i}^{N}\sum_{j>i}^{N} \hat{v}_{ij}, \tag{2.20}$$

where $\hat{h}_i = \hat{h}(\mathbf{r}_i)$ is the one-electron operator introduced before (2.14); and $\hat{v}_{ij} = v(|\mathbf{r}_i - \mathbf{r}_j|)$ is the electron-electron interaction which is usually taken to be the Coulomb interaction

$$\hat{v}_{ij} = \frac{1}{|\mathbf{r}_i - \mathbf{r}_j|} = \frac{1}{r_{ij}}. \tag{2.21}$$

In evaluating the energy as an expectation value of the Hamiltonian, we need the one- and the two-electron terms which arise from $\hat{h}_i$ and $\hat{v}_{ij}$. The Hamiltonian contains sums of these operators and the total energy of a single Slater determinant is the sum of matrix elements

$$\begin{aligned} E^{HF} &= \langle \Phi | \hat{H} | \Phi \rangle \\ &= \sum_{i}^{N} h_{ii} + \sum_{i}^{N} \sum_{j>i}^{N} (J_{ij} - K_{ij}). \end{aligned} \tag{2.22}$$

The physical interpretation and mathematical expression of each three terms are given below.

The h_{ii} matrix element is the average kinetic energy and potential energy for the electrostatic attraction between the nuclei and the electron in ϕ_i, given by the one-electron integral

$$h_{ii} = \langle i | \hat{h} | i \rangle = \int \phi_i^*(\mathbf{x}_1) \Big(-\frac{1}{2}\nabla^2 - \sum_{\alpha}^{M} \frac{Z_\alpha}{r_{1\alpha}} \Big) \phi_i(\mathbf{x}_1) d\mathbf{x}_1. \tag{2.23}$$

The J_{ij} matrix element, called the *Coulomb integral*, is the potential energy for the electrostatic repulsion between two electrons, with electron density functions $\phi_i^*(\mathbf{x}_1)\phi_i(\mathbf{x}_1)$ and $\phi_j^*(\mathbf{x}_2)\phi_j(\mathbf{x}_2)$. It is given by the two-electron integral

$$J_{ij} = \langle ij | ij \rangle = \int \phi_i^*(\mathbf{x}_1)\phi_j^*(\mathbf{x}_2) \frac{1}{r_{12}} \phi_i(\mathbf{x}_1)\phi_j(\mathbf{x}_2) d\mathbf{x}_1 d\mathbf{x}_2. \tag{2.24}$$

The K_{ij} matrix element, called the *exchange integral*, is given by the two-electron integral

$$K_{ij} = \langle ij | ji \rangle = \int \phi_i^*(\mathbf{x}_1)\phi_j^*(\mathbf{x}_2) \frac{1}{r_{12}} \phi_j(\mathbf{x}_1)\phi_i(\mathbf{x}_2) d\mathbf{x}_1 d\mathbf{x}_2, \tag{2.25}$$

which is zero unless the spin orbitals ϕ_i and ϕ_j have the same spin.

2.2.2 Hartree-Fock equations

The orbitals that define the Slater determinant wave function have to be determined. We therefore apply the Variational Principle to (2.22), assuming that the orbitals leading to the lowest energy are the *best* in a general sense. According to the differential calculus, we change the orbitals by a small (infinitesimal) amount, $\phi_i \Rightarrow \phi_i + \delta\phi_i$. This leads to a change in the total wave function $\Phi \Rightarrow \Phi + \delta\Phi$, as well as in the energy expression. To apply the Variational Principle to (2.22), we define the Coulomb and the exchange operators for an orbital ϕ_i by their action on any arbitrary one-electron function ϕ_j

$$\hat{J}_i \phi_j(\mathbf{x}_2) = \Big(\int \phi_i^*(\mathbf{x}_1) \frac{1}{r_{12}} \phi_i(\mathbf{x}_1) d\mathbf{x}_1 \Big) \phi_j(\mathbf{x}_2) \tag{2.26}$$

$$\hat{K}_i \phi_j(\mathbf{x}_2) = \Big(\int \phi_i^*(\mathbf{x}_1) \frac{1}{r_{12}} \phi_j(\mathbf{x}_1) d\mathbf{x}_1 \Big) \phi_i(\mathbf{x}_2). \tag{2.27}$$

The Coulomb operator simply multiplies the test function by the electrostatic potential arising from the orbital ϕ_i, so it is just an ordinary local multiplicative operator. By contrast, the exchange operator is nonlocal, and produces a function which is the product of ϕ_i with an electrostatic potential. This potential is determined by the differential overlap of the test function with the orbital ϕ_i.

Then, we rewrite (2.22) using a symmetric double summation for the Coulomb and the exchange operators which yields a factor 1/2 in front of them (the Coulomb "self-interaction" J_{ii} is exactly canceled by the corresponding "exchange" element K_{ii})

$$E^{HF} = \sum_i^N \langle\phi_i|\hat{h}|\phi_i\rangle + \frac{1}{2}\sum_{ij}^N \langle\phi_i|\hat{J}_j - \hat{K}_j|\phi_i\rangle. \tag{2.28}$$

In the minimization of (2.28), the constraint that the spin orbitals remain orthonormal (2.12) needs to be enforced. A convenient way to do this is using the method of *Lagrange multipliers*. The Lagrangian

$$\mathcal{L}^{HF} = E^{HF} - \sum_{ij}^N \lambda_{ij}(\langle\phi_i|\phi_j\rangle - \delta_{ij}), \tag{2.29}$$

where λ_{ij} are the Lagrange multipliers, is stationary with respect to a small change in the spin orbital

$$\delta\mathcal{L}^{HF} = \delta E^{HF} - \sum_{ij}^N \lambda_{ij}(\langle\delta\phi_i|\phi_j\rangle - \langle\phi_i|\delta\phi_j\rangle) = 0. \tag{2.30}$$

After allowing the spin orbital variation $\delta\phi$ in each orbital of (2.28), we find that the energy variation is given by variation of the expectation value of a single operator

$$\delta E^{HF} = \sum_i^N (\langle\delta\phi_i|\hat{F}_i|\phi_i\rangle - \langle\phi_i|\hat{F}_i|\delta\phi_i\rangle), \tag{2.31}$$

where $\hat{F}_i \equiv \hat{F}$ is the *Fock Operator* which is identical for all electrons and so we may drop the index i

$$\hat{F} = \hat{h} + \sum_j^N (\hat{J}_j - \hat{K}_j). \tag{2.32}$$

This operator is associated with the variation of the energy, not the energy itself. The variation of the Lagrangian (2.30) reduces to

$$\delta\mathcal{L}^{HF} = \sum_i^N \langle\delta\phi_i|\Big[\hat{F}|\phi_i\rangle - \sum_j^N \lambda_{ij}|\phi_j\rangle\Big] + c.c. = 0, \tag{2.33}$$

where *c.c.* denotes the complex conjugate. The equation (2.33) is only possible if the term in the squared bracket is zero; therefore,

$$\hat{F}|\phi_i\rangle = \sum_j^N \lambda_{ij}|\phi_j\rangle, \tag{2.34}$$

where j runs over occupied spin orbitals. The λ_{ij} form a hermitian matrix since $\hat{F}$ is hermitian. This equation can be simplified under a unitary transformation which leaves the wave function Φ unchanged and makes the Lagrange multipliers diagonal, *i.e.* $\lambda_{ij} = 0$ and $\lambda_{ii} = \epsilon_i$. We then get the *canonical Hartree-Fock equations*

$$\hat{F}|\phi_i\rangle = \epsilon_i|\phi_i\rangle, \tag{2.35}$$

which are satisfied by the spin orbitals that minimize the energy. The corresponding orbitals are the canonical Hartree-Fock orbitals, and the eigenvalues ϵ_i are known as orbital energies. We note that $E^{HF} \neq \sum_i \epsilon_i$. Actually,

$$E^{HF} = \sum_i^N \epsilon_i - \frac{1}{2}\sum_{ij}^N (J_{ij} - K_{ij}), \tag{2.36}$$

$$\epsilon_i = \langle\phi_i|\hat{F}|\phi_i\rangle = h_{ii} + \sum_j^N (J_{ij} - K_{ij}). \tag{2.37}$$

In the HF theory, the molecular orbital describes the "motion" of one electron in the electric field generated by the nuclei and some average distribution of the other electrons. In a mathematical context, this method can be thought of as a procedure for obtaining the best possible one-electron orbitals of a many-electron system. Furthermore, the expectation value of single-particle operators within this approximation are correct to second order. Therefore, Hartree-Fock theory provides an accurate and meaningful first approximation to the exact wave function.

2.2.2.1 Restricted and unrestricted Hartree-Fock

Since the spin-free Hamiltonian of a system of electrons commutes with the total spin operators $\hat{S}^2$ and $\hat{S}_z$, an eigenfunction of the former should also be eigenfunction of the latter. In other words, the exact wave function for a many-electron system, which is an eigenfunction of a spin-free Hamiltonian must be a pure spin state eigenfunction satisfying the relations

$$\hat{S}^2\Psi = S(S+1)\Psi, \tag{2.38}$$

$$\hat{S}_z\Psi = M_s\Psi. \tag{2.39}$$

A Slater determinant made up from N_α orbitals of α spin and N_β orbitals of β spin will always be an eigenfunction of the $\hat{S}_z$ operator with eigenvalue $M_s = \frac{1}{2}(N_\alpha - N_\beta)$. The requirement (2.39) is therefore fulfilled whenever we use a determinant as our approximate N-electron wave function. However, the determinant is not necessarily an eigenfunction of $\hat{S}^2$, and (2.38) may not be fulfilled.

The general case (2.11), where each electron can have different spatial orbitals, is known as Unrestricted Hartree-Fock (UHF). We may now introduce the substitutions (2.11) in the expressions for the energy and Fock operator, which yields the following spatial equation

$$\hat{F}^\alpha\psi_i^\alpha(\mathbf{r}) = \epsilon_i^\alpha\psi_i^\alpha(\mathbf{r}), \tag{2.40}$$

where

$$\hat{F}^{\alpha} = \hat{h} + \sum_{j}^{N} \hat{J}_j - \sum_{j}^{N_\alpha} \hat{K}_j^{\alpha}. \tag{2.41}$$

For the Fock operator, we must make a distinction depending on whether it operates on an α orbital or a β orbital (the operator $\hat{K}_j^{\alpha}$ only acts on the N_α electrons of spin α). Equivalent equations exist for electrons of spin β. The straightforward implementation of the α equations (2.40) and the β equivalent ones is known as *Unrestricted Hartree-Fock Theory*, since there is no attempt to impose the constraint (2.38) on the wave function.

A simpler situation occurs when the electronic state under consideration is a spin singlet ($S = M_s = 0$, spin multiplicity=1), which necessarily requires an even number of electrons. The spin orbitals can be required to occur in pairs having the same spatial orbital

$$\begin{aligned} \phi_i^{\alpha}(\mathbf{x}) &= \psi_i(\mathbf{r})\alpha(s) \\ \phi_i^{\beta}(\mathbf{x}) &= \psi_i(\mathbf{r})\beta(s), \end{aligned} \tag{2.42}$$

and

$$\hat{F}\psi_i(\mathbf{r}) = \epsilon_i \psi_i(\mathbf{r}), \tag{2.43}$$

where

$$\hat{F} = \hat{h} + \sum_{j}^{\frac{N}{2}} (2\hat{J}_j - \hat{K}_j). \tag{2.44}$$

The determinant is then an eigenfunction of the operators $\hat{S}_z$ and $\hat{S}^2$. The above ansatz (2.42) therefore ensures correct spin properties for a singlet wave function. The *Restricted Hartree-Fock* equations (2.43) are simpler to solve than the corresponding UHF ones. Since the α and β orbitals have identical spatial parts, the two Fock operators must also be the same (2.44) in this closed shell theory and by only constructing one Fock operator, the work and the memory requirements are reduced.

There is a method for applying RHF equations to an open shell system known as *Restricted Open Shell Hartree*-Fock (ROHF). In ROHF, the paired electrons are restricted to have the same spatial orbital as in RHF and the unpaired electrons are treated with different spatial orbitals as in UHF. Such a determinant is an eigenfunction of $\hat{S}_z$ and $\hat{S}^2$ with $S = M_s = \frac{n_o}{2}$, where n_o is the number of the singly occupied spatial orbitals.

2.2.2.2 Solution of the restricted Hartree-Fock equations

The resulting integro-differential equations from the Hartree-Fock approximation can be solved numerically, but in general they are still too complicated to be solved exactly, and further approximations are needed. Roothann [5] made the HF approximation more practical for numerical solutions by using the basis set expansion approach, *i.e.* the technique of expanding a spatial molecular orbital (MO) $\psi_i(\mathbf{r})$ as a Linear Combination of Atomic Orbitals (LCAO) $\chi_p(\mathbf{r})$

$$\psi_i(\mathbf{r}) = \sum_{\nu}^{N_{basis}} C_{\nu i}\chi_\nu(\mathbf{r}), \tag{2.45}$$

where N_{basis} is an integer (the number of basis functions) larger, in most cases, than the number of electrons N in the system. This transforms the RHF or UHF equations, which are coupled integro-differential equations, to a set of algebraic ones. Within the LCAO scheme we have to minimize the energy with respect to the coefficients $C_{\nu i}$ which specify the MOs. Inserting this expansion into the HF equations (2.43) and multiplying by $\langle\chi_\mu|$ leads to

$$\sum_{\nu}^{N_{basis}} C_{\nu i}\langle\chi_\mu|\hat{F}|\chi_\nu\rangle \;=\; \epsilon_i \sum_{\nu}^{N_{basis}} C_{\nu i}\langle\chi_\mu|\chi_\nu\rangle. \tag{2.46}$$

Introducing the overlap matrix $\mathbf{S}$ with elements

$$S_{\mu\nu} \;=\; \langle\chi_\mu|\chi_\nu\rangle \equiv \langle\mu|\nu\rangle, \tag{2.47}$$

and the Fock matrix $\mathbf{F}$ with elements

$$F_{\mu\nu} \;=\; \langle\chi_\mu|\hat{F}|\chi_\nu\rangle \equiv \langle\mu|\hat{F}|\nu\rangle. \tag{2.48}$$

Writing (2.46) as a matrix equation yields the Roothann equations

$$\mathbf{FC} \;=\; \mathbf{SCE}, \tag{2.49}$$

where $\mathbf{E}$ is a diagonal matrix of orbital energies, $E_{ij} = \epsilon_i\delta_{ij}$, and $\mathbf{C}$ is the matrix of the LCAO expansion coefficients. In order to determine the MOs ψ_i, we need the Fock matrix element $F_{\mu\nu}$ which can be expressed as:

$$F_{\mu\nu} \;=\; H_{\mu\nu}^{core} + \sum_{\lambda\sigma} P_{\lambda\sigma}\big[\langle\mu\lambda|\nu\sigma\rangle - \frac{1}{2}\langle\mu\lambda|\sigma\nu\rangle\big], \tag{2.50}$$

where

$$H_{\mu\nu}^{core} \;=\; \langle\chi_\mu|\hat{h}|\chi_\nu\rangle \equiv \langle\mu|\hat{h}|\nu\rangle, \tag{2.51}$$

and we have introduced the density matrix

$$P_{\mu\nu} \;=\; 2\sum_{j}^{\frac{N}{2}} C_{\mu j}C_{\nu j}. \tag{2.52}$$

In (2.50), we introduced the physicists' notation of the two-electron integral

$$\langle\chi_\mu\chi_\lambda|\chi_\nu\chi_\sigma\rangle \equiv \langle\mu\lambda|\nu\sigma\rangle \;=\; \int \chi_\mu^*(\mathbf{r}_1)\chi_\lambda^*(\mathbf{r}_2)\frac{1}{r_{12}}\chi_\nu(\mathbf{r}_1)\chi_\sigma(\mathbf{r}_2)d\mathbf{r}_1 d\mathbf{r}_2. \tag{2.53}$$

The total electronic HF energy of the system, in the AO basis, is

$$E^{HF} \;=\; \sum_{\mu\nu}^{N_{basis}} P_{\mu\nu}H_{\mu\nu}^{core} + \frac{1}{2}\sum_{\mu\nu\lambda\sigma}^{N_{basis}} P_{\mu\nu}P_{\lambda\sigma}\big[\langle\mu\lambda|\nu\sigma\rangle - \frac{1}{2}\langle\mu\lambda|\sigma\nu\rangle\big]. \tag{2.54}$$

The Self-Consistent Field (SCF) is a method to solve the Roothaan equation (2.49) which is a generalized matrix eigenvalue equation. It is convenient to bring it on a conventional matrix eigenvalue form,*i.e.*, without the matrix $\mathbf{S}$. This can be achieved if we

express the orbitals in an orthonormal basis. We introduce the matrix $\mathbf{U}$ such that the AOs are orthonormal through the following transformation

$$\mathbf{U}^{\dagger}\mathbf{S}\mathbf{U} = \mathbf{I}, \tag{2.55}$$

where $\mathbf{U}^{\dagger}$ is the adjoint matrix of $\mathbf{U}$ and $\mathbf{I}$ is the identity matrix. In a SCF calculation, the matrix $\mathbf{U}$ can be taken equal to $\mathbf{S}^{-1/2}$. As long as the transformation $\mathbf{U}$ is non-singular, we can write (2.49) as

$$(\mathbf{U}^{\dagger}\mathbf{F}\mathbf{U})(\mathbf{U}^{-1}\mathbf{C}) = (\mathbf{U}^{\dagger}\mathbf{S}\mathbf{U})(\mathbf{U}^{-1}\mathbf{C})\mathbf{E}, \tag{2.56}$$

which is of the form

$$\mathbf{F}'\mathbf{C}' = \mathbf{C}'\mathbf{E}, \tag{2.57}$$

with

$$\begin{aligned} \mathbf{F}' &= \mathbf{U}^{\dagger}\mathbf{F}\mathbf{U} \\ \mathbf{C} &= \mathbf{U}\mathbf{C}', \end{aligned} \tag{2.58}$$

The solution of (2.57) is obtained by diagonalizing the matrix $\mathbf{F}'$. However, this matrix depends on the elements of the matrix $\mathbf{C}$. We can therefore make a guess of a set of orbitals in order to get the process started. With these orbitals we can now construct an approximate Fock operator which can then be diagonalized to obtain a new set of orbitals. These orbitals replace the old ones in constructing a new Fock operator, and so on. The procedure is repeated until the change in the density matrix or the total energy between one iteration and the next is below a certain given threshold. When the orbitals satisfy (2.35), they represent the *self-consistent* solution. This approach is referred to as the Self-Consistent Field method.

The purpose with the above scheme is to determine the orbitals from which to construct a molecular wave function, and we thus need as many spin orbitals as there are electrons in the system. However, the number of solutions usually does not equal the number of electrons N, but rather the number of basis functions N_{basis} used in the expansion (2.45). In most cases $N_{basis} > N$ so one has to select a subset of solutions to the Hartree-Fock equations. Normally, the *Aufbau Principle* is used, where one can construct the ground (reference) state by filling the energetically lowest-lying orbitals with N electrons and ignoring the remaining orbitals. These eigenfunctions used in the Fock operator are termed the *occupied* orbitals, the remaining, unused eigenfunctions are referred to as *virtual* orbitals. Virtual orbitals are often used to construct wave functions for excited states or for correlation.

2.2.3 Second quantized form of the Hamiltonian

After performing a SCF calculation, we get an orthonormalized basis set of N_{basis} molecular orbitals (MO), $\{\phi_p\}$, $p = 1, ..., N_{basis}$, which we reorder with increasing energy. One can then use the second quantization formalism to reexpress the Hamiltonian (2.7). The creation (annihilation) operator $\hat{c}^{\dagger}_{p\sigma}$ ($\hat{c}_{p\sigma}$) creates (annihilates) an electron with spin σ in the MO ϕ_p. Thus, the Hamiltonian in the second quantized form can be written as

$$\hat{H} = \sum_{ai\sigma}\langle a|\hat{h}|i\rangle\hat{c}^{\dagger}_{a\sigma}\hat{c}_{i\sigma} + \frac{1}{2}\sum_{abij\sigma\sigma'}\langle ab|ij\rangle\hat{c}^{\dagger}_{a\sigma}\hat{c}^{\dagger}_{b\sigma'}\hat{c}_{j\sigma'}\hat{c}_{i\sigma}. \tag{2.59}$$

The sum is over all spatial orbitals and spin σ. The matrix elements $\langle a|\hat{h}|i\rangle$ represent the core Hamiltonian containing kinetic energy and electron-nuclear attraction, while $\langle ab|ij\rangle$ are the two-electron repulsion integrals. The Hamiltonian (2.59) is not equal to the usual one (2.7). If N_{basis} is infinitely large, the set $\{\phi_p\}$, can be complete, and in this limit the eigenfunctions and eigenvalues of these two Hamiltonians are identical. If N_{basis} is finite, the orbital space is necessarily incomplete and the second quantized Hamiltonian can be interpreted as the projection of the exact one to a finite subspace spanned by the basis orbitals. It is possible to formulate the Hamiltonian (2.59) in terms of spin summed excitation operators $\hat{E}_{pq}$, defined as

$$\hat{E}_{pq} = \hat{c}^{\dagger}_{p\alpha}\hat{c}_{q\alpha} + \hat{c}^{\dagger}_{p\beta}\hat{c}_{q\beta} = \sum_{\sigma}\hat{c}^{\dagger}_{p\sigma}\hat{c}_{q\sigma}. \tag{2.60}$$

After some manipulations for the second term in (2.59), where we use the known anti-commutator relations for the creation-annihilation operators [6], we can write down the Hamiltonian in the operator basis constructed from the excitation operators :

$$\hat{H} = \sum_{ai}\langle a|\hat{h}|i\rangle\hat{E}_{ai} + \frac{1}{2}\sum_{abij}\langle ab|ij\rangle(\hat{E}_{ai}\hat{E}_{bj} - \delta_{ib}\hat{E}_{aj}). \tag{2.61}$$

The summations are now over the molecular spatial orbital basis. We note that the number of electrons does not appear in the definition of the Hamiltonian. All such information is found in the Slater determinant basis. Using the occupation number formalism, a determinant Φ can be written as a series of 1 and 0 indicating which spin orbitals are occupied in the determinant

$$|\Phi\rangle = \hat{c}^{\dagger}_{p_1\sigma_1}\hat{c}^{\dagger}_{p_2\sigma_2}...\hat{c}^{\dagger}_{p_i\sigma_i}...|0\rangle = |n_1, n_2, ..., n_i, ..., n_{2N_{basis}}\rangle, \tag{2.62}$$

where n_i is the occupation number (0 or 1) for spin orbital $p_i\sigma_i$ and $|0\rangle$ is the vacuum state where all occupations are zero.

2.2.4 Post Hartree-Fock methods

The Hartree-Fock method is one of the simplest methods to solve the Schrödinger equation, where the electrons are moving in the average field of the other electrons, which is obviously an approximation. In reality the motion of the electrons depends on the instantaneous positions of all the other electrons, and on average they are further apart than described by the Hartree-Fock wave function. Therefore, the motion of the electrons is "correlated". The phenomenon is known as *electron correlation*. In the HF approximation, the probability of finding two electrons with parallel spins at the same point in the space is zero, then the motion of electrons with the same spin is correlated in this approximation. Conventionally correlation energy E_c is defined as

$$E_c = E_{exact} - E_{HF}, \tag{2.63}$$

where E_{exact} is the exact non-relativistic ground state energy, at 0 K, of the system within the Born-Oppenheimer approximation, and E_{HF} is the restricted Hartree-Fock energy in a complete basis set.

2.2.4.1 Dynamic correlation

Dynamic correlation is dominated by the correlated motion of electrons with opposite spins, which is not correctly described by HF theory. It arises from the Coulomb repulsion given by the term r_{ij}^{-1} in the Hamiltonian operator. This term is singular in the regions close to $r_{ij} = 0$. From mathematical point of view, it is stated that the exact wave function contains a cusp in r_{ij} to cancel this singularity, while the HF wave function does not show this cusp. Dynamical correlation represents the lowering in the energy due to the reduction in probability of two electrons being close to one another.

2.2.4.2 Static correlation

Static (nondynamical) correlation is due to those configurations that are low-lying in energy and that mix strongly with the Hartree-Fock configuration. This kind of correlation can usually be dealt with by multiconfigurational SCF techniques. Static correlation is often small in closed-shell molecules near their equilibrium geometry, but it increases enormously in importance as a molecule is distorted and bonds are formed or broken. It is well known that the problem with improper molecular dissociation is corrected by the use of a few additional determinants (or configurations) of energies close to the HF energy. For this reason this error is said to be due to near-degeneracy effects. These effects can also be important in open-shell situations such as excited states or transition metals.

2.2.4.3 Configuration Interaction

All variants of the HF method lead to a wave function in which all the information about the electronic structure is contained in the occupied molecular orbitals and their occupation numbers. We use the molecular orbitals to construct more complex wave functions. Given a set of atomic orbitals of dimension N_{basis}, we can form a set of MOs of the same dimension, which gives rise to $2N_{basis}$ spin orbitals. Using these spin orbitals, we can form a set of

$$N_{det} = \binom{2N_{basis}}{N} = \frac{2N_{basis}!}{N!(2N_{basis}-N)!} \tag{2.64}$$

Slater determinants for a system with N electrons. The total wave function Ψ_{CI} can be expanded in these determinants by classifying them relative to the Hartree-Fock configuration Φ

$$\Psi_{\mathrm{CI}} = \sum_I C_I \Phi_I = C_0\Phi + \sum_{ia} C_i^a \Phi_i^a + \sum_{\substack{a>b \\ i>j}} C_{ij}^{ab} \Phi_{ij}^{ab} + \sum_{\substack{a>b>c \\ i>j>k}} C_{ijk}^{abc} \Phi_{ijk}^{abc} + ..., \tag{2.65}$$

where i, j, ... index occupied spin orbitals in Φ while a, b, ... index unoccupied spin orbitals. Φ_i^a, Φ_{ij}^{ab}, Φ_{ijk}^{abc}, ... are the singly, doubly, triply, ... excited determinants, in which one, two, three, ... of the spin orbitals occupied in Φ are replaced by virtual orbitals. For example, Φ_{ij}^{ab} denotes a configuration obtained by exciting two electrons in MOs i and j to MOs a and b. Since Ψ_{CI} depends linearly on the CI expansion coefficients C_I (C_0, C_i^a, ...), the application of the variational principle yields the eigenvalue problem

$$\sum_J (H_{IJ} - E)C_J = 0, \tag{2.66}$$

where E is the variational energy of Eq. (2.19).

If all levels of excitation up to N-tuply excited state are used in (2.65) for an N-electron system, we have a solution that is exact within the one-electron subspace spanned by the $2N_{basis}$ spin orbitals. This procedure is called full CI. This is the best (in the variational sense) wave function we can build from a given set of AOs. If this is done for a complete one-electron basis, *i.e.* N_{basis} tends to infinity, we have a complete CI expansion of the exact wave function Ψ_{exact}. The lowest Hamiltonian expectation value corresponding to this wave function is

$$E_{exact} = \langle \Psi_{exact} | \hat{H} | \Psi_{exact} \rangle, \tag{2.67}$$

which appears in the definition (2.63).

Even in a rather small basis set, the number of possible determinants, N_{det} (2.64), which can be generated is enormously large. This type of CI where all these determinants are used is therefore normally not a tractable method for treating the correlation problem. Therefore, in practice, we need to truncate the expansion (2.65) and only to consider a certain number of excited determinants. This is commonly done after the double excitation level (CI with single and double excitations, CISD). This type of wave function has been shown to yield results of very high quantitative accuracy for cases where the HF wave function is a good zeroth order approximation to the wave function. The next level of progress is inclusion of triply excited determinants, giving the CISDT method, etc.

The limitation in the truncated CI methods is that they are not *size-consistent*, nor *size-extensive*. The size-consistency indicates that the energy of two infinitely separated systems is the sum of the individual components. The size-extensivity means that the energy of a system should increase linearly with the number of independent subsystems. This implies that the accuracy of these methods will degrade as the size of the system increases, unlike the HF and full CI methods which are size-extensive.

2.2.4.4 Coupled Cluster

The CI expansion (2.65) can be written as

$$|\Psi_{\rm CI}\rangle = (\hat{1} + \hat{T}_1 + \hat{T}_2 + ... + \hat{T}_N)|\Phi\rangle = (1 + \hat{T})|\Phi\rangle, \tag{2.68}$$

where we have used intermediate normalization for which $\langle \Phi | \Psi_{\rm CI} \rangle = 1$. Eq. (2.68) has all the single excitations, grouped into the $\hat{T}_1$ term

$$\hat{T}_1 = \sum_{ia} T_a^i \hat{c}_a^\dagger \hat{c}_i, \tag{2.69}$$

including both the CI coefficients, $C_i^a \equiv T_a^i$, which are also called the amplitudes of *connected clusters*, and excitation operators that generate the singly-excited configurations from Φ. The double excitations are all grouped into the $\hat{T}_2$ term, etc. Then the sum of all the excitation operators are denoted by $\hat{T}$.

Let us consider now not the linear approach of Eq. (2.68), but the following exponential formulation

$$|\Psi_{\rm CC}\rangle = \exp(\hat{T})|\Phi\rangle, \tag{2.70}$$

which we can expand in a power series

$$\begin{aligned} |\Psi_{\mathrm{CC}}\rangle &= \big[\hat{1} + \hat{T} + \frac{1}{2}\hat{T}^2 + \frac{1}{6}\hat{T}^3 + ...\big]|\Phi\rangle \\ &= \big[\hat{1} + \hat{T}_1 + \big(\hat{T}_2 + \frac{1}{2}\hat{T}_1^2\big) + \big(\hat{T}_3 + \hat{T}_2\hat{T}_1 + \frac{1}{6}\hat{T}_1^3\big) + ...\big]|\Phi\rangle. \end{aligned} \tag{2.71}$$

If we include all levels of excitation, up to N-fold, the wave function is equivalent to a full CI wave function. However, it is more practical to truncate at some fixed excitation level. Suppose one considers only the operators $\hat{T}_1$ and $\hat{T}_2$. The exponential expansion in the exact coupled cluster wave function (2.71) becomes

$$|\Psi_{\mathrm{CCSD}}\rangle = \big[\hat{1} + \hat{T}_1 + (\hat{T}_2 + \frac{1}{2}\hat{T}_1^2) + (\hat{T}_1\hat{T}_2 + \frac{1}{6}\hat{T}_1^3) + ...\big]|\Phi\rangle, \tag{2.72}$$

giving the CCSD model (Coupled Cluster Singles and Doubles), which includes not only single and double excitations, but higher excitations termed *disconnected clusters*, to infinite order, whose amplitudes are products of the coefficients of the single and double excitations. Indeed, with the exponential ansatz, we retain all disconnected clusters arising from the truncated set of connected ones. Therefore, unlike the CISD method, the CCSD method is size-consistent thanks to the disconnected clusters. The next higher level is for $\hat{T} = \hat{T}_1 + \hat{T}_2 + \hat{T}_3$ giving the CCSDT model, where we include the triples, and so on.

Due to the nonlinear nature of the wave function (2.71), the number of disconnected cluster amplitudes grows factorially with the excitation level and obtaining these amplitudes by using an equation like (2.66) is not feasible so the variational approach can not be used as a computational method. The cluster amplitudes can be optimised by substituting Ψ_{CC} into the Schrödinger equation and then projecting onto the space of Φ, Φ_i^a, Φ_{ij}^{ab}, etc. This gives a set of nonlinear simultaneous equations for the cluster amplitudes.

2.2.4.5 Perturbation Theory

The most straightforward method to deal with the dynamical correlation is the many-body perturbation theory. In this method, the problem which needs to be solved is assumed to deviate only slightly from a solved one. For treating dynamical correlation, we use nondegenerate Rayleigh-Schrödinger perturbation theory with Møller-Plesset (MP) [7] partitioning of the Hamiltonian

$$\hat{H} = \hat{H}_0 + \hat{W} \tag{2.73}$$

where $\hat{H}_0$, the sum of the Fock operators (2.32)

$$\hat{H}_0 = \sum_{i=1}^{N} \hat{F}_i, \tag{2.74}$$

is chosen as the reference Hamiltonian. The perturbative operator $\hat{W}$ can be given as

$$\hat{W} = \hat{H} - \sum_{i=1}^{N} \hat{F}_i \tag{2.75}$$

$$= \hat{W}_{ee} - \hat{V}_{\mathrm{Hx}}[\Phi], \tag{2.76}$$

where $\hat{W}_{ee} = \sum_{i<j} r_{ij}^{-1}$, is the Coulomb interaction, and $\hat{V}_{\rm Hx}[\Phi] = \sum_j (\hat{J}_j - \hat{K}_j)$ is the nonlocal HF potential operator which involves the (average) electron-electron repulsion. By the choice (2.73), the perturbation operator $\hat{W}$ describes the electron correlation and the aim of this scheme is to improve the HF energy towards the exact solution of the Schrödinger equation $\hat{H}|\Psi\rangle = E|\Psi\rangle$ in the same basis set.

Since we know the eigenfunctions and eigenvalues of the zeroth-order Hamiltonian $\hat{H}_0$

$$\hat{H}_0|\Phi_I\rangle = E_I^{(0)}|\Phi_I\rangle, \tag{2.77}$$

where $|\Phi_{I=0}\rangle = |\Phi\rangle$ is the HF determinant and $|\Phi_{I\neq 0}\rangle$ are the excited determinants, and $E_{I=0}^{(0)} = E^{(0)}$ and $E_{I\neq 0}^{(0)}$ are the associated eigenvalues. The ground-state energy E can then be expanded as a perturbation series in $\hat{W}$. The nth-order treatment is denoted MPn to indicate the total energy up to order n, and $E^{(n)}$ indicates the energy correction at order n. The zeroth-order perturbation energy is

$$E^{\rm MP0} = \langle\Phi|\hat{H}_0|\Phi\rangle = E^{(0)} = \sum_{i=1}^{N} \epsilon_i, \tag{2.78}$$

where ϵ_i are the eigenvalues of the Fock operator. The zeroth-order approximation can be improved by taking into account the effect of $\hat{W}$, then we find the HF energy which is the sum of the zeroth and first-order energies,

$$\begin{aligned} E^{\rm MP1} &= \langle\Phi|\hat{H}_0 + \hat{W}|\Phi\rangle, \\ &= E^{(0)} + E^{(1)}, \\ &= E^{HF}. \end{aligned} \tag{2.79}$$

Equation (2.79) shows that the first order of perturbation theory with the partitioning (2.73) just corrects the sum of orbital energies to the true HF energy, *i.e.* there is no first-order correction to the HF energy and the electron correlation energy starts at order two. The simplest correlated level is MP2 requiring the knowledge of the first-order perturbation theory wave function $|\Phi^{(1)}\rangle$

$$|\Phi^{(1)}\rangle = \sum_{i<j}^{occ} \sum_{a<b}^{vir} T_{ab}^{ij} |\Phi_{ij}^{ab}\rangle, \tag{2.80}$$

where the amplitudes T_{ab}^{ij} are given by

$$T_{ab}^{ij} = -\frac{\langle\Phi|\hat{W}|\Phi_{ij}^{ab}\rangle}{\langle\Phi_{ij}^{ab}|\hat{H}_0 - E^{(0)}|\Phi_{ij}^{ab}\rangle} = \frac{\langle\Phi|\hat{W}_{ee}|\Phi_{ij}^{ab}\rangle}{\epsilon_i + \epsilon_j - \epsilon_a - \epsilon_b}. \tag{2.81}$$

We notice that $|\Phi^{(1)}\rangle$ (2.80) involves only double excitations. Singly exited configurations will not contribute because of the Brillouin's theorem, $\langle\Phi|\hat{H}|\Phi_i^a\rangle = 0$. Triply and higher order excited states have also matrix elements zero, $\langle\Phi|\hat{H}|\Phi_{ijk\ldots}^{abc\cdots}\rangle = 0$, since the Hamiltonian $\mathcal{H}$ contains only one- and two-electron operators. Then the second order energy is

given by

$$\begin{aligned} E_c \approx E^{(2)} &= \langle\Phi|\hat{W}|\Phi^{(1)}\rangle = \langle\Phi|\hat{H}-\hat{H}_0|\Phi^{(1)}\rangle = \langle\Phi|\hat{H}|\Phi^{(1)}\rangle, \\ &= \sum_{i<j}^{occ}\sum_{a<b}^{vir}\frac{\left|\langle\Phi|\hat{W}_{ee}|\Phi_{ij}^{ab}\rangle\right|^2}{\epsilon_i+\epsilon_j-\epsilon_a-\epsilon_b}, \\ &= \sum_{i<j}^{occ}\sum_{a<b}^{vir}\frac{\Big(\langle ij|ab\rangle-\langle ij|ba\rangle\Big)^2}{\epsilon_i+\epsilon_j-\epsilon_a-\epsilon_b}. \end{aligned} \tag{2.82}$$

The MP2 method is probably the most economical available approach for treating dynamical correlation and typically accounts for 80-95% of the correlation energy [8]. MP4 is more expensive than CISD but often gives better results. MP5 and higher orders are, in general, impractically expensive. The perturbation theory gives size-extensive results.

2.2.4.6 Multiconfiguration Self-Consistent Field

The one-determinant Hartree-Fock wave function used in standard single-reference methods is not a good description in many cases, in particular for the degeneracies that occur along a potential energy surface. In restricted Hartree-Fock, the restriction that two electrons are placed in each spatial orbital is responsible for the lack of flexibility to account for the static correlation. This leads, for example, to the large error obtained at the asymptotic limit when a diatomic molecule is dissociated. In unrestricted Hartree-Fock as a single configuration method, we ignore the spin symmetry of the wave function, and the diatomic molecule dissociates correctly, but the behavior in the intermediate bond breaking region is generally incorrect and the wave function suffers form massive spin contamination.

A simple way to provide this flexibility is to include more than one reference determinant. A more appropriate zeroth-order wave function for cases of degeneracies or near-degeneracies is a Multi-Configuration Self-Consistent Field (MCSCF) [9] wave function

$$|\Psi_{\rm MC}\rangle = \sum_m c_m|\Phi_m\rangle. \tag{2.83}$$

This method can be seen as a CI where the coefficients c_m in front of each determinant and the molecular orbitals in the determinants $|\Phi_m\rangle$ are simultaneously optimized by the Variational Principle. The total MCSCF wave function is usually expanded in terms of a spin-adapted configurational basis called the Configuration State Functions (CSFs). Assuming that the Hamiltonian does not contain any spin-dependent terms, we can use the Hamiltonian (2.61) introduced before for giving the MCSCF energy expression as the expectation value of $\hat{H}$

$$E = \langle\Psi_{\rm MC}|\hat{H}|\Psi_{\rm MC}\rangle = \sum_{ai}\langle a|\hat{h}|i\rangle D_{ai} + \sum_{abij}\langle ab|ij\rangle P_{abij}, \tag{2.84}$$

where

$$D_{ai} = \langle\Psi_{\rm MC}|\hat{E}_{ai}|\Psi_{\rm MC}\rangle = \sum_{mn} c_m^* c_n \langle\Phi_m|\hat{E}_{ai}|\Phi_n\rangle, \tag{2.85}$$

and

$$P_{abij} = \frac{1}{2}\langle\Psi_{\rm MC}|(\hat{E}_{ai}\hat{E}_{bj} - \delta_{ib}\hat{E}_{aj})|\Psi_{\rm MC}\rangle = \frac{1}{2}\sum_{mn} c_m^* c_n \langle\Phi_m|(\hat{E}_{ai}\hat{E}_{bj} - \delta_{ib}\hat{E}_{aj})|\Phi_n\rangle, \tag{2.86}$$

are the one-particle reduced density matrix and the two-particle reduced density matrix, respectively. The energy expression (2.84) contains the variational parameters of the wave function (2.83). The one- and two-electron integrals depend on the molecular orbitals, while the density matrices **D** and **P** depend on the CI expansion coefficients and the molecular orbitals. The MCSCF optimization is based on the consideration that the electronic energy (2.84) is a function of the variational parameters, then we can expand it as a Taylor series in these parameters giving the energy hypersurface. Usually the expansion is truncated at second order (second order methods). The optimization is achieved when we reach the stationary point on the energy hypersurface where the gradient of the energy with respect to the variational parameters is zero.

Two particularly important MCSCF methods are the Complete Active Space SCF method (CASSCF) and the Restricted Active Space SCF method (RASSCF). The CAS [10] wave function is made by partitioning orbital space for each symmetry block into three sets: inactive, active and virtual. The inactive orbitals remain doubly occupied in all configurations of the MCSCF wave function. The virtual (also called secondary or external) orbitals remain unoccupied in all configurations. The active space, CAS(n,m), contains a fixed number, n, of electrons which are distributed over the m active orbitals in all possible ways, restricted by the given space and spin symmetry requirements, giving all possible CSFs to be used in (2.83). In this sense the CASSCF approach is a full CI within the active space. The number of CSFs grows factorially with n and m and the method rapidly becomes expensive. The RAS [11] model has been considered as an extension of the CAS model. The inactive and virtual spaces have the same properties as for the CAS wave function, but the active space is divided into three subspaces RAS1, RAS2 and RAS3. The RAS1 and RAS3 spaces consist of orbitals in which the number of created holes and electrons, respectively, is restricted up to a given maximum. The RAS2 space is like the active orbital space in CAS where all possible configurations, resulting from the distribution of the active electrons over the RAS2 orbitals, are included.

2.3 Density Functional Theory (DFT)

As assumed by the Thomas-Fermi model [12, 13], all properties of a system can be expressed in terms of the electron density $n(\mathbf{r})$, the number of electrons per unit volume at $\mathbf{r}$. This model fails to yield an accurate description of electronic systems of chemical interest. But in 1964, Hohenberg and Kohn [14] derived a theorem supporting from a mathematical point of view the ideas of Thomas and Fermi.

2.3.1 Hohenberg-Kohn variational theorem

We consider N electrons moving in an external potential $\hat{V}_{\rm ext}$. The Hamiltonian is

$$\hat{H} = \hat{T} + \hat{W}_{ee} + \hat{V}_{\rm ext}, \tag{2.87}$$

where $\hat{T}$ and $\hat{W}_{ee}$ are the kinetic and electron-electron interaction operators, respectively. $\hat{V}_{\rm ext} = \int v_{\rm ext}(\mathbf{r})\hat{n}(\mathbf{r})d\mathbf{r}$, where $v_{\rm ext}(\mathbf{r})$ is the scalar (usually electron-nuclear) multiplicative potential, and $\hat{n}(\mathbf{r})$ is the density operator. For all densities such that $\int n(\mathbf{r})d\mathbf{r} = N$, which arise from some antisymmetric wave function Ψ, Levy [15, 16] defined the functional

$$F[n] \;=\; \min_{\Psi\Rightarrow n}\langle\Psi|\hat{T}+\hat{W}_{ee}|\Psi\rangle, \tag{2.88}$$

where the search is constrained to the subspace of all the antisymmetric Ψ that give the density n. We denote $\Psi[n]$ to be the minimizing wave function.

$$F[n] \;=\; \langle\Psi[n]|\hat{T}|\Psi[n]\rangle + \langle\Psi[n]|\hat{W}_{ee}|\Psi[n]\rangle = T[n] + W_{ee}[n]. \tag{2.89}$$

Let E_0, Ψ_0, and n_0 be the ground-state energy, wave function, and density, respectively. Then if we insert $\Psi[n]$ in expression of the total energy

$$\begin{aligned} E[n] \equiv \int v_{\rm ext}(\mathbf{r})n(\mathbf{r})d\mathbf{r} + F[n] \;&=\; \langle\Psi[n]|\hat{T}+\hat{W}_{ee}+\hat{V}_{\rm ext}|\Psi[n]\rangle, \\ &\geq\; E_0 = E[n_0], \end{aligned} \tag{2.90}$$

we must get a higher number according to the minimum property of the ground state. The ground-state energy can be given as

$$E_0 \;=\; \min_{n}\Big\{\int v_{\rm ext}(\mathbf{r})n(\mathbf{r})d\mathbf{r} + F[n]\Big\}, \tag{2.91}$$

where the minimum is taken over all N-representable densities. The minimization (2.91) implies that,

$$v_{\rm ext}(\mathbf{r}) \;=\; \Big(-\frac{\delta F[n]}{\delta n(\mathbf{r})}\Big)_{n=n_0}, \tag{2.92}$$

which means that, within an additive constant, the ground-state density n_0 determines the potential $v_{\rm ext}(\mathbf{r})$, so it determines the ground-state wave function $\Psi_0 = \Psi[n_0]$, from which all the ground-state properties can be calculated.

2.3.2 Kohn-Sham formulation

The equations (2.90) and (2.91) in the previous subsection provide a method for calculating ground-state properties such that if a form of $F[n]$ can be found, we have to minimize $E[n]$ in (2.90) for the potential $v_{\rm ext}(\mathbf{r})$ of interest. But the task of finding good approximations to $F[n]$ is not easy. There is a problem with the expression of the kinetic part $T[n]$ in terms of the density, which represents the main drawback of the Thomas-Fermi approach, the old practical application of DFT.

In 1965, Kohn and Sham (KS) [17] introduced a method for evaluating $T[n]$ by replacing the kinetic energy of the interacting electrons with that of an equivalent non-interacting reference (Kohn-Sham) system whose ground-state density is that of the interacting one n_0. Assume that n_0 is the ground-state density of the non-interacting Hamiltonian

$$\hat{H}_{\rm KS} \;=\; \hat{T} + \hat{V}_{\rm KS}, \tag{2.93}$$

where $\hat{V}_{\rm KS}$ is the external local Kohn-Sham potential $\hat{V}_{\rm KS} = \int v_{\rm KS}(\mathbf{r})\hat{n}(\mathbf{r})d\mathbf{r}$, and the potential $v_{\rm KS}(\mathbf{r})$ is such that its wave function, a single Slater determinant $\Phi[n]$, will give the ground-state density $n_0 = \langle\Phi[n]|\hat{n}(\mathbf{r})|\Phi[n]\rangle$ and simultaneously minimize the expectation value of $\hat{T}$. It then follows from (2.91) that

$$E_{\rm KS} = \min_n\Big\{\int v_{\rm KS}(\mathbf{r})n(\mathbf{r})d\mathbf{r} + T_s[n]\Big\} = \int v_{\rm KS}(\mathbf{r})n_0(\mathbf{r})d\mathbf{r} + T_s[n_0], \qquad (2.94)$$

where $T_s[n] = \langle\Phi[n]|\hat{T}|\Phi[n]\rangle$ is non-interacting kinetic energy functional. Although $T_s[n]$ is different from the true $T[n]$, it is a major part and can be exactly calculated in this approach. The Euler equation corresponding to (2.94) is

$$v_{\rm KS}(\mathbf{r}) = \Big(-\frac{\delta T_s[n]}{\delta n(\mathbf{r})}\Big)_{n=n_0}. \qquad (2.95)$$

Now, one may write $F[n]$ as

$$F[n] = T_s[n] + E_{\rm H}[n] + E_{xc}[n], \qquad (2.96)$$

where

$$E_{\rm H}[n] = \frac{1}{2}\int\int \frac{n(\mathbf{r})n(\mathbf{r}')}{|\mathbf{r}-\mathbf{r}'|}\,d\mathbf{r}\,d\mathbf{r}', \qquad (2.97)$$

is the classical electrostatic Hartree energy functional and $E_{xc}[n]$ is the unknown exchange-correlation functional. Combining (2.96) with (2.92) and (2.95) gives

$$v_{\rm KS}(\mathbf{r}) = v_{\rm ext}(\mathbf{r}) + v_{\rm H}(\mathbf{r}) + v_{xc}(\mathbf{r}), \qquad (2.98)$$

where

$$v_{\rm H}(\mathbf{r}) = \frac{\delta E_{\rm H}[n]}{\delta n(\mathbf{r})} = \int \frac{n(\mathbf{r}')}{|\mathbf{r}-\mathbf{r}'|}\,d\mathbf{r}', \qquad (2.99)$$

is the Hartree potential due to the whole electron distribution. $v_{xc}(\mathbf{r})$ is the exchange-correlation potential

$$v_{xc}(\mathbf{r}) = \frac{\delta E_{xc}[n]}{\delta n(\mathbf{r})}. \qquad (2.100)$$

The minimization (2.94) leads to the Kohn-Sham equations for determining the lowest N eigenfunctions of $\hat{H}_{\rm KS}$, which form the minimizing determinant $\Phi[n]$

$$\hat{H}_{\rm KS}|\phi_i\rangle = \varepsilon_i|\phi_i\rangle, \qquad (2.101)$$

where ε_i is the eigenvalue. These equations must be solved self-consistently, since $\hat{H}_{\rm KS}$ depends on $n(\mathbf{r})$, and when the self-consistency is achieved $n(\mathbf{r}) = n_0(\mathbf{r})$. The Kohn-Sham method is in principle exact, though in practice we must find approximations for $E_{xc}[n]$. It is convenient to partition $E_{xc}[n]$ into its exchange and correlation contributions

$$E_{xc}[n] = E_x[n] + E_c[n], \qquad (2.102)$$

where $E_x[n]$ is the exchange functional

$$E_x[n] = \langle\Phi[n]|\hat{W}_{ee}|\Phi[n]\rangle - E_{\rm H}[n], \tag{2.103}$$

and $E_c[n]$ is the correlation functional

$$E_c[n] = \langle\Psi[n]|\hat{T}+\hat{W}_{ee}|\Psi[n]\rangle - \langle\Phi[n]|\hat{T}+\hat{W}_{ee}|\Phi[n]\rangle. \tag{2.104}$$

The correlation energy has kinetic and potential components: $E_c[n] = T_c[n] + U_c[n]$, the definitions of these contributions are $T_c[n] = T[n] - T_s[n]$ and $U_c[n] = W_{ee}[n] - (E_{\rm H}[n] + E_x[n])$, respectively.

2.3.3 Exchange-Correlation energy $E_{xc}[n]$

A commonly used scheme to find approximations for $E_{xc}[n]$ is the adiabatic connection [18]. The relationship between the real system and the KS reference system can be studied by a continuum of fictitious systems. These systems with a relative strength of the electron-electron interaction $\lambda\hat{W}_{ee}$ have the same electron density. For $\lambda = 1$, one gets the real system, for $\lambda = 0$, the KS reference system. The Hamiltonian of the fictitious systems reads

$$\hat{H}^\lambda = \hat{T} + \hat{V}_{\rm ext} + \lambda\hat{W}_{ee} + \hat{V}^\lambda_{{\rm H}xc}[n], \tag{2.105}$$

where $\hat{V}^\lambda_{{\rm H}xc}[n]$ is the Hartree-exchange-correlation potential operator that keeps the density constant with variations of λ.

The exchange-correlation energy of the real system can be given exactly in terms of an integral over the coupling constant λ [18–20]

$$E_{xc}[n] = \frac{1}{2}\int\int \frac{n(\mathbf{r})h_{xc}(\mathbf{r},\mathbf{r}')}{|\mathbf{r}-\mathbf{r}'|}\,d\mathbf{r}\,d\mathbf{r}', \tag{2.106}$$

where $h_{xc}(\mathbf{r},\mathbf{r}')$ is the exchange-correlation hole averaged over all coupling constants, which takes into account kinetic correlations

$$h_{xc}(\mathbf{r},\mathbf{r}') = n(\mathbf{r}')\int_0^1 d\lambda[g^\lambda(\mathbf{r},\mathbf{r}')-1], \tag{2.107}$$

with $g^\lambda(\mathbf{r},\mathbf{r}')$ the pair correlation function of the system with density $n(\mathbf{r})$ and electron-electron interaction $\lambda\hat{W}_{ee}$. The function $g(\mathbf{r},\mathbf{r}')$ takes into account the fact that the presence of an electron at $\mathbf{r}$ reduces the probability of finding a second electron at a position $\mathbf{r}'$, in the vicinity of $\mathbf{r}$.

One can define an exchange-correlation energy density per particle,

$$\varepsilon_{xc}[n] = \frac{1}{2}\int \frac{h_{xc}(\mathbf{r},\mathbf{r}')}{|\mathbf{r}-\mathbf{r}'|}\,d\mathbf{r}', \tag{2.108}$$

so that the exchange-correlation energy (2.106) can be expressed as

$$E_{xc}[n] = \int n(\mathbf{r})\varepsilon_{xc}[n(\mathbf{r})]\,d\mathbf{r}. \tag{2.109}$$

Finding approximations of $\varepsilon_{xc}[n]$ that allow for a better description of chemical systems, is one of the most important aspects of research in DFT. Although there exists a large variety of exchange-correlation functionals, we can recast most of the current approximations into 3 different categories: the Local, the Gradient Corrected and the Hybrid ones.

2.3.3.1 Local Density Approximation

The essence of the local density approximation (LDA) [17] is to treat real inhomogeneous electronic systems as locally homogeneous, and then to replace the exchange-correlation hole (2.107) by the one for an homogeneous electron gas (HEG), which is characterized by only one density

$$h_{xc}^{LDA}(\mathbf{r},\mathbf{r}') \;=\; n(\mathbf{r})\Big[g^{HEG}(|\mathbf{r}-\mathbf{r}'|,n(\mathbf{r}))-1\Big], \tag{2.110}$$

where $g^{HEG}(|\mathbf{r}-\mathbf{r}'|,n(\mathbf{r}))$ is the pair correlation function of HEG, which depends only on the distance between $\mathbf{r}$ and $\mathbf{r}'$, evaluated at $n(\mathbf{r})$. The exchange-correlation energy becomes

$$E_{xc}^{LDA}[n] \;=\; \int n(\mathbf{r})\varepsilon_{xc}^{HEG}\Big(n(\mathbf{r})\Big)\,d\mathbf{r}. \tag{2.111}$$

The exchange energy density ε_x^{HEG} can be given by the Slater-Dirac [21, 22] form

$$\varepsilon_x^{HEG}\big(n\big) \;=\; -\frac{3}{4}\Big(\frac{3}{\pi}\Big)^{\frac{1}{3}}n^{\frac{1}{3}}. \tag{2.112}$$

For spin-polarized systems, the local spin density approximation (LSDA) can be obtained by using the two spin densities, $n_\uparrow(\mathbf{r})$ and $n_\downarrow(\mathbf{r})$, such that $n(\mathbf{r})=n_\uparrow(\mathbf{r})+n_\downarrow(\mathbf{r})$, and $\zeta(\mathbf{r})=(n_\uparrow(\mathbf{r})-n_\downarrow(\mathbf{r}))/n(\mathbf{r})$ is the spin polarization. The exchange-correlation energy becomes

$$E_{xc}^{LSDA}[n_\uparrow(\mathbf{r}),n_\downarrow(\mathbf{r})] \;=\; \int[n_\uparrow(\mathbf{r})+n_\downarrow(\mathbf{r})]\varepsilon_{xc}^{HEG}\Big(n_\uparrow(\mathbf{r}),n_\downarrow(\mathbf{r})\Big)\,d\mathbf{r}, \tag{2.113}$$

where the exchange energy (as the Kohn-Sham kinetic energy $T_s[n_\uparrow,n_\downarrow]$) obeys the exact spin scaling relation [23]

$$E_x[n_\uparrow,n_\downarrow] \;=\; \frac{1}{2}E_x[2n_\uparrow]+\frac{1}{2}E_x[2n_\downarrow]. \tag{2.114}$$

However, the correlation energy has no simple spin scaling relation. The correlation energy density ε_c^{HEG}, as a function of spin-polarization, can be obtained by using expressions based on either the Random-Phase Approximation [24] or on Quantum-Monte-Carlo simulations [25] and there are popular parametrizations for both methods [26–28].

The LDA works well for the systems where the electronic density is quite uniform such as bulk metals, however, it is a very crude approximation for the systems where the density varies rapidly in dependence of position $\mathbf{r}$ (e.g., atoms and molecules). It gives, in general, reasonable geometries for covalent, ionic, and metallic bonds while it yields too short bond lengths for weakly bound systems. The incorrect asymptotic behavior of the exchange-correlation potential (it decays exponentially, not as -1/r) affects the dissociation limit, ionization energies and metallic surfaces. LDA fails to cancel exactly the electronic self-interaction included in the Hartree term of the energy.

2.3.3.2 Generalized Gradient and Meta-Generalized Gradient Approximations

The exchange-correlation energy in the Generalized Gradient Approximation (GGA), has the following form:

$$E_{xc}^{GGA}[n] = \int n(\mathbf{r})\varepsilon_{xc}^{HEG}\Big(n(\mathbf{r})\Big)\,d\mathbf{r} + \int F_{xc}\Big(n(\mathbf{r}), \nabla n(\mathbf{r})\Big)\,d\mathbf{r} \tag{2.115}$$

where the function F_{xc} is constructed to satisfy a number of known conditions for the exchange-correlation hole (e.g., sum rules, long-range decay, etc.). There are many different prescriptions for choosing F_{xc}, each one leads to distinct GGA. Among the numerous GGA functionals [29–46] here are some of the commonly used ones. The Becke 88 exchange functional (B88) [30] which takes the form of an additional correction to the LDA exchange. It contains one adjustable parameter which was optimized so that the sum of the LDA and Becke exchange terms reproduces the exchange energy of six noble gas atoms. The introduction of Becke's gradient exchange correction in 1988 was an important step for the acceptance of DFT as a valuable tool for computational chemistry. However, B88 exchange functional is responsible for repulsive potential energy curves for many rare gas diatomic molecules [47]. The Lee-Yang-Parr (LYP) [29, 48] correlation functional which has been derived as a reformulation of the Colle-Salvetti [49] expression for the correlation energy of Helium, in term of n and ∇n. This correlation functional is one-electron self-interaction error free, but can not reproduce the correct uniform electron gas like the functionals based on (2.115). A popular recipe is to use B88 exchange complemented with LYP correlation. The Perdew-Burke-Ernzerhof (PBE) exchange-correlation functional [31] verifies many of the exact properties for the exchange-correlation hole and does not contain any fitting parameters. It retains the correct features of LDA and combines them with the inhomogeneity aspects that are supposed to be important for describing real systems. GGA sometimes overcorrects LDA for bond lengths, binding energies and also atomic energies. It cannot describe long-range effects. However, hydrogen bonds are usually well accounted for. GGA functionals still do not eliminate the spurious electron self-interaction completely.

The Meta-Generalized Gradient Approximations (meta-GGA) that go beyond GGA, have been suggested to overcome the shortcomings of LDA and GGA methods. These functionals employ, in addition to the density and its gradient, either the Laplacian of the density ($\nabla^2 n(\mathbf{r})$) or the kinetic energy density

$$\tau(\mathbf{r}) = \frac{1}{2}\sum_{\alpha}^{occ} |\nabla\phi_\alpha(\mathbf{r})|^2. \tag{2.116}$$

Different meta-GGA functionals have been developed [50–63], for example, the Perdew-Kurth-Zupan-Blaha (PKZB) [53] exchange-correlation functional which depends on two fitted parameters, the nonempirical Tao-Perdew-Staroverov-Scuseria (TPSS) [57] exchange-correlation functional. The TPSS exchange functional can be combined with the Krieger-Chen-Iafrate-Savin (KCIS) [64] correlation functional. These meta-GGA correlation functionals are one-electron self-interaction error free. The results obtained using meta-GGA are quite improved with respect to PBE, especially when atomisation energy and metal surface energy are considered.

2.3.3.3 Hybrids

Becke [65] employed the adiabatic connection to suggest that the functional should contain some of the exact HF exchange[1]

$$E_x^{\rm HF} = -\frac{1}{2}\sum_{ij\sigma}\int\int \frac{\phi^*_{i\sigma}(\mathbf{r})\phi_{j\sigma}(\mathbf{r})\phi^*_{j\sigma}(\mathbf{r}')\phi_{i\sigma}(\mathbf{r}')}{|\mathbf{r}-\mathbf{r}'|}\,d\mathbf{r}\,d\mathbf{r}'. \tag{2.117}$$

Letting $\Psi^\lambda[n]$ be the unique antisymmetric ground state wave function of $\hat{H}^\lambda$ (2.105), the exchange-correlation energy can be expressed in terms of the coupling constant integration [66]

$$E_{xc}[n] \;=\; \int_0^1 U_{xc,\lambda}[n]\,d\lambda = \int_0^1 \langle\Psi^\lambda[n]|\hat{W}_{ee}|\Psi^\lambda[n]\rangle\,d\lambda - E_{\rm H}[n]. \tag{2.118}$$

A possible scheme to construct functionals from the adiabatic connection is to approximate the integrand $U_{xc,\lambda}$ by a model function of λ [65, 67–69]. Integrating (2.118) using the linear model [65], $U_{xc,\lambda}[n] = a[n] + b[n]\lambda$, gives rise to

$$E_{xc}[n] \;=\; a + \frac{1}{2}b = U_{xc,0} + \frac{1}{2}(U_{xc,1} - U_{xc,0}), \tag{2.119}$$

where $U_{xc,0} = E_x^{\rm HF}$ is the exchange energy of the KS determinant. The potential energy contribution to the exchange-correlation energy of the fully interacting system was approximated by Becke as $U_{xc,1} \approx U_{xc}^{LDA}$, leading to the half-and-half functional

$$E_{xc}[n] \;=\; \frac{1}{2}(E_x^{\rm HF} + E_x^{LDA}) + \frac{1}{2}U_c^{LDA}. \tag{2.120}$$

The last term in (2.120) is often approximated as $U_c^{LDA} \approx E_c^{LDA}$ in other versions of the half-and-half functional. Successively, Becke [67] proposed to parametrize the functional form to chosen sets of experimental data, leading to the family of the three-parameter hybrid functionals

$$E_{xc}^{\rm B3PW91}[n] \;=\; aE_x^{\rm HF} + (1-a)E_x^{LDA} + b\Delta E_x^{B88} + E_c^{VWN} + c\Delta E_c^{PW91}. \tag{2.121}$$

Alternatively, the most widely used B3LYP [70] reads as

$$E_{xc}^{\rm B3LYP}[n] \;=\; aE_x^{\rm HF} + (1-a)E_x^{LDA} + b\Delta E_x^{B88} + cE_c^{LYP} + (1-c)E_c^{VWN}, \tag{2.122}$$

where the parameters ($a = 0.2$, $b = 0.72$, $c = 0.81$) in (2.121) and (2.122) were determined by a least square fit to atomization energies, electron and proton affinities, and the ionization potentials of the atomic species and molecules in the G2 [71] test set of experimental data. B3LYP is successful as a result of some cancellation of errors, despite its known shortcomings [72]. Many single hybrid functionals have been suggested [46, 73–83]. Single hybrid functionals are known to improve significantly the accuracy of DFT results in particular for geometries and thermochemistry. They are supposed to compensate partially the many-electron self-interaction error by using the exact exchange [72]. So for kinetics, good hybrid functionals tend to have a larger percentage of exact exchange.

[1] Computed with the Kohn-Sham orbitals and eigenvalues.

Range-separated single-hybrid functionals [84, 85] are characterized by the separation of the electron-electron interaction into two parts which may be treated separately

$$\frac{1}{r_{12}} = \frac{\mathrm{erf}(\mu r_{12})}{r_{12}} + \frac{\mathrm{erfc}(\mu r_{12})}{r_{12}}, \tag{2.123}$$

where the parameter μ controls the separation between the long-range ($\mathrm{erf}(\mu r_{12})/r_{12}$) and the short-range ($\mathrm{erfc}(\mu r_{12})/r_{12}$) interactions. The long-range corrected functionals [86–95] in which we mix long-range HF with short-range DFT, are known to improve properties such as charge-transfer and Rydberg excitations in TDDFT. The screened functionals [96–99] are obtained when we use short-range HF and long-range DFT, and these hybrids are more commonly used in solid-state calculations (band gaps, lattice constants, etc).

Besides the HF exchange, unoccupied orbitals and eigenvalues are also used through the perturbative double-excitation correlation in the double hybrid functionals. These functionals are the subject of two articles [100, 101] presented in this thesis, where the theoretical foundation of types of double hybrid functionals has been provided.

Another class of hybrids, where we combine MCSCF and DFT, was explored through an article [102] exposed in this thesis. This method is called multiconfigurational hybrid functional.

2.4 Models and approximations for solids

For molecules in the gas phase, *ab initio* and DFT methods have become an alternative to experiments for determining accurately structural and energetic properties. It would be most valuable if predictions of such properties for solids could be made with similar accuracy. The serious complication in introducing the quantum chemistry techniques into solid state modeling is, on the molecular scale, the infinite dimension of solids. One way to overcome this difficulty is to adopt the perfect crystal model in which an ideally crystalline bulk material is translation-invariant. This can be exploited to define a unit cell. Then one has to enforce periodic boundary conditions (PBC) and solve the corresponding Schrödinger equation accordingly [103–105].

2.4.1 Periodicity

Bloch [106] showed that for a perfect periodic solid, at the same point $\mathbf{r}$ in different repeating unit cells, the orbitals differ only by a complex phase factor $e^{i\mathbf{k}.\mathbf{g}}$:

$$\phi(\mathbf{r}+\mathbf{g};\mathbf{k}) = e^{i\mathbf{k}.\mathbf{g}}\phi(\mathbf{r};\mathbf{k}), \tag{2.124}$$

where $\mathbf{g} = n_1\mathbf{a}_1 + n_2\mathbf{a}_2 + n_3\mathbf{a}_3$ (n_1, n_2, n_3 are integers) is a lattice vector describing translations in real space and the parallelepiped constructed by the basis vectors $\mathbf{a}_1$, $\mathbf{a}_2$ and $\mathbf{a}_3$ is the primitive unit cell. The wave vector $\mathbf{k} = k_1\mathbf{b}_1 + k_2\mathbf{b}_2 + k_3\mathbf{b}_3$ ($\mathbf{a}_i.\mathbf{b}_j = 2\pi\delta_{ij}$) is defined in the reciprocal space such that each wave vector may be written as $\mathbf{k} = \mathbf{k}' + n\mathbf{K}$ (n is an integer), where $\mathbf{K}$ is a reciprocal lattice vector defined by $\mathbf{g}.\mathbf{K} = 2\pi n$ and $\mathbf{k}'$ is within the first Brillouin zone (BZ) of reciprocal space.

The function $\phi(\mathbf{r};\mathbf{k})$ should not be vanished at infinity and at the same time we have to normalize it. We can consider a finite crystal of $N = N_1.N_2.N_3$ cells, having N_j primitive

cells along the j-th direction (j =1,2,3). Periodic boundary conditions require that

$$\phi(\mathbf{r} + mN_j\mathbf{a}_j; \mathbf{k}) = \phi(\mathbf{r}; \mathbf{k}), \tag{2.125}$$

for any integer m and every j. By using (2.124), we find that

$$e^{imN_jk_j\mathbf{b}_j.\mathbf{a}_j} = 1, \tag{2.126}$$

which implies that $k_j = n_j/N_j$ (n_j is an integer in the domain $0 \leq n_j < N_j$). Therefore, the number of wave vectors

$$\mathbf{k} = \frac{n_1}{N_1}\mathbf{b}_1 + \frac{n_2}{N_2}\mathbf{b}_2 + \frac{n_3}{N_3}\mathbf{b}_3, \tag{2.127}$$

in the first BZ is finite. When N_1, N_2, N_3 grow to infinity, the wave vector $\mathbf{k}$ can be considered as a continuous variable such that the summation over $\mathbf{k}$ vectors is replaced by three dimensional integration and the number of $\mathbf{k}$ points within the first BZ plays a role in the accuracy of the calculations.

2.4.2 Mean-field crystalline orbital theory

If we use the Fockian (2.32) in the Schrödinger equation, the Hartree-Fock level of the theory is retained. For the molecular case, we should solve the Roothann equations (2.46, 2.49). The difficulty in dealing with solids is that the equations (2.46) will have infinite dimension and the expansion (2.45) extends not only over functions centered on atoms within one primitive unit cell but also over all primitive cells labeled by $\mathbf{g}$

$$\psi_i(\mathbf{r}) = \sum_{\mathbf{g}} \sum_{\mu}^{N_{basis}} C_{\mu i}^{\mathbf{g}} \chi_\mu(\mathbf{r} - \mathbf{r}_\mu - \mathbf{g}). \tag{2.128}$$

As N grows to infinity, the direct solution of the equations

$$\sum_{\mathbf{g}'} \sum_{\nu}^{N_{basis}} (F_{\mu\nu}^{\mathbf{g}\mathbf{g}'} - \epsilon_i S_{\mu\nu}^{\mathbf{g}\mathbf{g}'}) C_{\nu i}^{\mathbf{g}'} = 0, \tag{2.129}$$

is practically impossible, where $F_{\mu\nu}^{\mathbf{g}\mathbf{g}'}$ is the Fock matrix element in direct space in the local basis set, which is invariant to translation :

$$\begin{aligned} F_{\mu\nu}^{\mathbf{g}\mathbf{g}'} &= \langle \chi_\mu(\mathbf{r} - \mathbf{r}_\mu - \mathbf{g}) | \hat{F} | \chi_\nu(\mathbf{r} - \mathbf{r}_\nu - \mathbf{g}') \rangle = \langle \chi_\mu(\mathbf{r} - \mathbf{r}_\mu) | \hat{F} | \chi_\nu(\mathbf{r} - \mathbf{r}_\nu - \mathbf{g}' + \mathbf{g}) \rangle \\ &= \langle \chi_\mu(\mathbf{r} - \mathbf{r}_\mu) | \hat{F} | \chi_\nu(\mathbf{r} - \mathbf{r}_\nu - \mathbf{l}) \rangle, \end{aligned} \tag{2.130}$$

where the linear combination between two lattice vectors, $\mathbf{g}' - \mathbf{g} = \mathbf{l}$, is a lattice vector. The same can be said of the overlap matrix element $S_{\mu\nu}^{\mathbf{g}\mathbf{g}'}$. The function $\chi_\mu(\mathbf{r} - \mathbf{r}_\mu)$ is the μ-th atomic orbital centered at $\mathbf{r}_\mu$ in the (origin or reference) 0-cell and $\chi_\nu(\mathbf{r} - \mathbf{r}_\nu - \mathbf{l})$ is that one in the $\mathbf{l}$-cell. These local functions are in turn defined by a contraction, *i.e.*, a fixed linear combination of Gaussian-type functions.

Taking advantage of translation symmetry, we can define $\mathbf{k}$-dependent Bloch functions

$$\phi_\mu(\mathbf{r}; \mathbf{k}) = \frac{1}{\sqrt{N}} \sum_{\mathbf{g}} e^{i\mathbf{k}.\mathbf{g}} \chi_\mu(\mathbf{r} - \mathbf{r}_\mu - \mathbf{g}), \tag{2.131}$$

where the wave vector $\mathbf{k}$ is indicative of different irreducible representations. Consequently, the Bloch functions belonging to different $\mathbf{k}$ vectors are mutually orthogonal and the matrix elements between them vanish

$$F_{\mu\nu}(\mathbf{k},\mathbf{k}') = \delta(\mathbf{k}-\mathbf{k}')F_{\mu\nu}(\mathbf{k},\mathbf{k}) \;=\; \delta(\mathbf{k}-\mathbf{k}')F_{\mu\nu}(\mathbf{k}). \tag{2.132}$$

where $\mathbf{k}$ is one of the sampling set points in the first BZ at which the Fock matrix, $F_{\mu\nu}(\mathbf{k})$, is diagonalized. As result, the secular problem reduces to secular problems, one for each $\mathbf{k}$ vector, resembling that of molecules:

$$\sum_{\nu}^{N_{basis}} \big(F_{\mu\nu}(\mathbf{k}) - \epsilon_i(\mathbf{k})S_{\mu\nu}(\mathbf{k})\big)C_{\nu i}(\mathbf{k}) \;=\; 0. \tag{2.133}$$

Their solutions are the single-particle crystalline orbitals (CO) which are linear combinations of Bloch functions (2.131)

$$\psi_i(\mathbf{r};\mathbf{k}) \;=\; \sum_{\mu} C_{\mu i}(\mathbf{k})\phi_\mu(\mathbf{r};\mathbf{k}). \tag{2.134}$$

The coefficients $C_{\mu i}(\mathbf{k})$, which determine the crystalline orbitals $\psi_i(\mathbf{r};\mathbf{k})$, are obtained when solving (2.133) (with the orthonormality condition) for a particular $\mathbf{k}$ vector. These coefficients are used to form the density matrix in order to calculate the total energy per unit cell.

While accurate structure predictions for solids are given by the HF-CO theory, the cohesive energies are severely underestimated and the energy-band gaps are too large compared to experiment [107] in this model which does not account for correlation effects. As another mean field method, periodic density functional theory (DFT) has quickly become the main computational tool for the electronic structure of solids. The Hartree-Fock and the Kohn-Sham equations can be solved by expanding the orbitals in one of two major kinds of basis set: atom-centered Gaussian-type orbitals (GTO) and plane waves (PW). Both choices yield very similar results if convergence is carefully checked and reached [108, 109]. Transferability of molecular GTO basis functions to periodic systems should be done with care, particularly in the case of diffuse functions, to avoid linear dependence in the definition of the wave function. Plane wave basis sets are used along with pseudopotentials or projector augmented wave method to account for core electrons. They have many advantages : the basis functions are orthonormal by definition, unbiased by the atomic positions so that they describe any point in the crystalline cell with the same quality, thereby having the ability to accurately treat different kinds of structure. The convergence of the calculation with respect to the size of the truncated PW basis set can be checked by increasing the electronic kinetic energy cutoff.

DFT calculations within the LDA are known to exhibit a significant overbinding, whereas the GGA cohesive energies of solids are generally improved. The underestimation of the band gap has been a long-standing problem for density functionals. The reason for this is the self-interaction error in LDA and GGA. Hybrid functionals combine gradient-corrected approximations with a fraction of exact exchange, which allows improvement of the performance of GGA functionals for systems where the self-interaction error may become important. However, calculating the nonlocal exchange energy can be very expensive in extended systems. This has motivated the development of screened

hybrids [96–98, 110] which are based on that the long-range contribution of the nonlocal exchange interaction is canceled by long-range correlation effects that are not accounted for in standard semilocal functionals. These functionals use a finite amount of exact exchange at short-range, but none in the long-range limit, in order to cut the computational cost of nonlocal exchange integrals for extended systems. Compared to the semilocal density functionals, the screened hybrids yield an improved description of semiconductor band gaps and lattice constants, but still underestimate the gap in insulators.

One of the failures of the one-electron levels of theory, including DFT with standard functionals, was observed in the description of long-range dispersion interactions [111, 112]. In molecular crystals, this deficiency often leads to severe errors. DFT calculations can be improved by including an empirical correction to account for van de Waals interactions. This empirical correction consists of damped pairwise interatomic potentials of the form $-C_n/r^n$ $(n \geq 6)$ to describe the attraction that decays at long range as r^{-6}, while the attractive terms of order r^{-8} and r^{-10} become important at medium range. These methods are called empirical dispersion-corrected density functionals [113–116] and can predict very reasonable molecular crystal lattice parameters and lattice energies [117–126]. However, the damped pairwise correction terms depend on the choice of functional form and the system being treated, which prevents to systematically improve the predictions. Several non-empirical methods for treating dispersion have also been used in molecular crystals [127–131]. They perform well for predicting crystal lattice energy but they are significantly more expensive than conventional DFT methods.

2.4.3 Wave Function Based Electron Correlation Methods for Solids

Attempts have been made to extend the higher correlated methods based on the wave function expansion to solid state treatment. The infinite extension of solids implies that only size-extensive methods can be applied to study these systems. Periodic second-order Møller-Plesset perturbation theory (MP2) provides an electron-correlation method with accuracy unachievable by DFT with the standard LDA, GGA and meta-GGA functionals for many systems. Efficient periodic MP2 algorithms have been developed [132–137]. Generalized from the molecular formulation, atomic-orbital Laplace-transformed MP2 method (AO-LT-MP2) [138] permits calculating the MP2 correlation energy for extended systems using occupied and virtual space spanned by Bloch functions. Another choice is to use canonical orbitals expanded in plane waves. This periodic approach is called plane wave based canonical MP2 [139, 140] which has led to the periodic canonical coupled cluster singles and doubles (CCSD) [141]. As a local correlation method [142–146], periodic local MP2 [147, 148] exploits the local character of dynamical electron correlation hole and gives the total electron correlation energy as a sum of contributions from a truncated list of orbital pairs. In this method, the occupied space is spanned by orthonormal localized crystalline orbitals (Wannier functions) generated from the occupied canonical orbitals by unitary transformation. For the virtual space, LMP2 employs mutually nonorthogonal orbitals obtained from the atomic orbital basis by projecting out the occupied space (projected AOs). Truncation of the virtual space is important to reduce the computational costs, where the excitations from an orbital pair are restricted to the PAOs centered in the vicinity of either of the two occupied orbitals. This approximation is known to reduce the basis set superposition error (BSSE) [149]. To improve the performance further, LMP2

can be combined with density fitting techniques [150].

Periodic MP2 methods are, in general, very expensive when applied to systems with medium-sized unit cell. But the recent development of parallel implementations [151, 152] opens the possibility of applications dealing with molecular crystals of chemical interest. These methods are limited to the treatment of non-conducting crystals (limitation of the MP2 method itself). For Gaussian orbital based periodic MP2, large and especially diffuse basis sets frequently cause linear dependence problems in the periodic Hartree-Fock calculations that precede the MP2 calculations. But the use of diffuse basis sets is mandatory in many cases for the convergence of MP2 energies. Dual-basis set scheme is one way to overcome this difficulty, where a smaller basis set is used for the HF calculations and then additional basis functions can be allocated in the MP2 correlation calculations.

Bibliography

[1] M. Born and J. Oppenheimer, Ann. Phys. **84**, 457 (1927).

[2] D. R. Hartree, Proc. Camb. Phil. Soc. **24**, 111 (1928).

[3] J. C. Slater, Phys. Rev. **34**, 1293 (1929).

[4] V. Fock, Physik **61**, 126 (1930).

[5] C. C. J. Roothann, Rev. Mod. Phys. **23**, 69 (1951).

[6] T. Helgaker, P. Jorgensen and J. Olsen, *Molecular Electronic-Structure Theory* (Wiley, Chichester, 2002).

[7] C. Møller and M. S. Plesset, Phys. Rev. **46**, 618 (1934).

[8] R. J. Bartlett, Ann. Rev. Phys. Chem. **32**, 359 (1981).

[9] M. W. Schmidt and M. S. Gordon, Ann. Rev. Phys. Chem. **49**, 233 (1998).

[10] P. R. T. B. O. Roos and P. E. M. Siegbahn, Chem. Phys. **48**, 157 (1980).

[11] P. J. J. Olsen, B. O. Roos and H. J. A. Jensen, J. Chem. Phys. **89**, 2185 (1988).

[12] L. H. Thomas, Proc. Camb. Phil. Soc. **23**, 542 (1927).

[13] E. Fermi, Z. Phys. **48**, 73 (1928).

[14] P. Hohenberg and W. Kohn, Phys. Rev. **136**, B 864 (1964).

[15] M. Levy, Proc. Natl. Acad. Sci. U.S.A. **76**, 6062 (1979).

[16] M. Levy, Phys. Rev. A **26**, 1200 (1982).

[17] W. Kohn and L. J. Sham, Phys. Rev. A **140**, 1133 (1965).

[18] J. Harris, Phys. Rev. A **29**, 1648 (1984).

[19] D. C. Langreth and J. P. Perdew, Solid State Commun. **17**, 1425 (1975).

[20] O. Gunnarsson and B. I. Lundqvist, Phys. Rev. B **13**, 4274 (1976).

[21] J. C. Slater, Phys. Rev. **81**, 385 (1951).

[22] P. A. M. Dirac, Proc. Camb. Phil. Soc. **26**, 376 (1930).

[23] J. P. Perdew and S. Kurth, in *A Primer in Density Functional Theory*, edited by C. Fiolhais, F. Nogueira and M. A. L. Marques (Springer, Berlin, 2003), Vol. 620 of Lecture Notes in Physics, pp. 1–55.

[24] M. Gell-Mann and K. A. Brueckner, Phys. Rev. **106**, 364 (1957).

[25] D. M. Ceperley and B. J. Alder, Phys. Rev. Lett. **45**, 566 (1980).

[26] J. P. Perdew and Y. Wang, Phys. Rev. B **45**, 13244 (1992).

[27] J. P. Perdew and A. Zunger, Phys. Rev. B **23**, 5048 (1981).

[28] S. J. Vosko, L. Wilk and M. Nusair, Can. J. Phys. **58**, 1200 (1980).

[29] C. Lee, W. Yang and R. G. Parr, Phys. Rev. B **37**, 785 (1988).

[30] A. D. Becke, Phys. Rev. A **38**, 3098 (1988).

[31] J. P. Perdew, K. Burke and M. Ernzerhof, Phys. Rev. Lett. **77**, 3865 (1996).

[32] D. C. Langreth and J. P. Perdew, Solid State Commun. **31**, 567 (1979).

[33] D. C. Langreth and J. P. Perdew, Phys. Rev. B **21**, 5469 (1980).

[34] J. P. Perdew, A. Ruzsinszky, G. I. Csonka, O. A. Vydrov, G. E. Scuseria, L. A. Constantin, X. L. Zhou and K. Burke, Phys. Rev. Lett. **100**, 136406 (2008).

[35] J. P. Perdew and W. Yue, Phys. Rev. B **33**, 8800 (1986).

[36] J. P. Perdew, Phys. Rev. B **33**, 8822 (1986).

[37] A. D. Becke, J. Chem. Phys. **84**, 4524 (1986).

[38] J. P. Perdew, J. A. Chevary, S. H. Vosko, K. A. Jackson, M. R. Pederson, D. J. Singh and C. Fiolhais, Phys. Rev. B **46**, 6671 (1992).

[39] F. A. Hamprecht, A. J. Cohen, D. J. Tozer and N. C.Handy, J. Chem. Phys. **109**, 6264 (1998).

[40] T. Tsuneda, T. Suzumura and K. Hirao, J. Chem. Phys. **110**, 10664 (1999).

[41] A. D. Boese, N. L. Doltsinis, N. C. Handy and M. J. Sprik, J. Chem. Phys. **112**, 1670 (2000).

[42] A. D. Boese and N. C. Handy, J. Chem. Phys. **114**, 5497 (2001).

[43] N. C. Handy and A. J. Cohen, Mol. Phys. **99**, 403 (2001).

[44] N. C. Handy and A. J. Cohen, J. Chem. Phys. **116**, 5411 (2002).

[45] T. W. Keal and D. J. Tozer, J. Chem. Phys. **121**, 5654 (2004).

[46] Y. Zhao and D. G. Truhlar, J. Chem. Phys. **128**, 184109 (2008).

[47] Y. Zhang, W. Pan and W. Yang, J. Chem. Phys. **107**, 7921 (1997).

[48] B. Miehlich, A. Savin, H. Stoll and H. Preuss, Chem. Phys. Lett. **157**, 200 (1989).

[49] R. Colle and O. Salvetti, Theor. Chim. Acta **37**, 329 (1975).

[50] A. D. Becke, J. Chem. Phys. **88**, 1053 (1988).

[51] A. D. Becke, Int. J. Quantum. Chem. **52**, 625 (1994).

[52] A. D. Becke and M. R. Roussel, Phys. Rev. A **39**, 3761 (1989).

[53] J. P. Perdew, S. Kurth, A. Zupan and P. Blaha, Phys. Rev. Lett. **82**, 2544 (1999).

[54] J. P. Perdew and L. A. Constantin, Phys. Rev. B **75**, 155109 (2007).

[55] J. P. Perdew, A. Ruzsinszky, J. Tao, G. I. Csonka and G. E. Scuseria, Phys. Rev. A **76**, 042506 (2007).

[56] J. P. Perdew, A. Ruzsinszky, G. I. Csonka, L. A. Constantin and J. W. Sun, Phys. Rev. Lett. **103**, 026403 (2009).

[57] J. Tao, J. P. Perdew, V. N. Staroverov and G. E. Scuseria, Phys. Rev. Lett. **91**, 146401 (2003).

[58] C. Lee and R. G. Parr, Phys. Rev. A **35**, 2377 (1987).

[59] A. D. Becke, J. Chem. Phys. **104**, 1040 (1996).

[60] A. D. Becke, J. Chem. Phys. **109**, 2092 (1998).

[61] T. van Voorhis and G. E. Scuseria, J. Chem. Phys. **109**, 400 (1998).

[62] A. D. Boese and N. C. Handy, J. Chem. Phys. **116**, 9559 (2002).

[63] Y. Zhao and D. G. Truhlar, J. Chem. Phys. **125**, 194101 (2006).

[64] J. B. Krieger, J. Chen, G. J. Iafrate and A. Savin, in *Electron Correlation and Materials Properties*, edited by A. Gonis and N. Kioussis (Plenum, New York, 1999).

[65] A. D. Becke, J. Chem. Phys. **98**, 1372 (1993).

[66] M. Levy and J. P. Perdew, Phys. Rev. A **32**, 2010 (1985).

[67] A. D. Becke, J. Chem. Phys. **98**, 5648 (1993).

[68] J. P. Perdew, M. Ernzerhof and K. Burke, J. Chem. Phys **105**, 9982 (1996).

[69] P. Mori-Sánchez, A. J. Cohen and W. Yang, J. Chem. Phys. **124**, 091102 (2006).

[70] P. J. Stephens, F. J. Devlin, C. F. Chabalowski and M. J. Frisch, J. Phys. Chem. **98**, 11623 (1994).

[71] L. A. Curtiss, K. Raghavachari, G. W. Trucks and J. A. Pople, J. Chem. Phys. **94**, 7221 (1991).

[72] G. I. Csonka, J. P. Perdew and A. Ruzsinszky, J. Chem. Theory Comput **6**, 3688 (2010).

[73] A. D. Becke, J. Chem. Phys. **107**, 8554 (1997).

[74] C. Adamo and V. Barone, J. Chem. Phys. **101**, 6158 (1999).

[75] B. J. Lynch, P. L. Fast, M. Harris and D. G. Truhlar, J. Phys. Chem. A **104**, 4811 (2000).

[76] P. J. Wilson, T. J. Bradly and D. J. Tozer, J. Chem. Phys. **115**, 9233 (2001).

[77] A. J. Cohen and N. C. Handy, Mol. Phys. **99**, 607 (2001).

[78] X. Xu and W. A. Goddard III, Proc. Natl. Acad. Sci. U.S.A. **229**, 2673 (2004).

[79] T. W. Keal and D. J. Tozer, J. Chem. Phys. **123**, 121103 (2005).

[80] Y. Zhao, N. E. Schultz and D. G. Truhlar, J. Chem. Theory Comput. **2**, 364 (2006).

[81] Y. Zhao and D. G. Truhlar, J. Chem. Theory Comput. **110**, 13126 (2006).

[82] Y. Zhao and D. G. Truhlar, J. Chem. Theory Comput. **110**, 5121 (2006).

[83] Y. Zhao and D. G. Truhlar, Theor. Chem. Acc. **120**, 215 (2008).

[84] A. Savin and H.-J. Flad, Int. J. Quantum. Chem. **56**, 327 (1995).

[85] T. Leininger, H. Stoll, H.-J. Werner and A. Savin, Chem. Phys. Lett. **275**, 151 (1997).

[86] H. Iikura, T. Tsuneda, T. Yanai and K. Hirao, J. Chem. Phys. **115**, 3540 (2001).

[87] J. Toulouse, F. Colonna and A. Savin, Phys. Rev. A **70**, 062505 (2004).

[88] J.-W. Song, S. Tokura, T. Sato, M. A. Watson and K. Hirao, J. Chem. Phys. **127**, 154109 (2007).

[89] J.-W. Song, M. A. Watson, A. Nakata and K. Hirao, J. Chem. Phys. **129**, 184113 (2008).

[90] J.-W. Song, M. A. Watson and K. Hirao, J. Chem. Phys. **131**, 144108 (2009).

[91] T. Yanai, D. P. Tew and N. C. Handy, Chem. Phys. Lett. **393**, 51 (2004).

[92] R. Baer and D. Neuhauser, Phys. Rev. Lett. **94**, 043002 (2005).

[93] J. Toulouse, F. Colonna and A. Savin, J. Chem. Phys. **122**, 014110 (2005).

[94] O. A. Vydrov and G. E. Scuseria, J. Chem. Phys. **125**, 234109 (2006).

[95] J.-D. Chai and M. Head-Gordon, J. Chem. Phys. **128**, 084106 (2008).

[96] J. Heyd, G. E. Scuseria and M. Ernzerhof, J. Chem. Phys. **118**, 8207 (2003).

[97] J. Heyd and G. E. Scuseria, J. Chem. Phys. **121**, 1187 (2004).

[98] J. Heyd and G. E. Scuseria, J. Chem. Phys. **120**, 7274 (2004).

[99] A. V. Krukau, O. A. Vydrov, A. F. Izmaylov and G. E. Scuseria, J. Chem. Phys. **125**, 224106 (2006).

[100] K. Sharkas, J. Toulouse and A. Savin, J. Chem. Phys. **134**, 064113 (2011).

[101] J. Toulouse, K. Sharkas, E. Brémond and C. Adamo, J. Chem. Phys. **135**, 101102 (2011).

[102] K. Sharkas, A. Savin, H. J. A. Jensen and J. Toulouse, J. Chem. Phys. **137**, 044104 (2012).

[103] R. Dovesi, in *Quantum-Mechanical Ab-initio Calculation of the Properties of Crystalline Materials*, edited by C. Pisani (Springer-Verlag, Berlin, 1996), vol. 67, p. 31.

[104] C. Pisani, in *Quantum-Mechanical Ab-initio Calculation of the Properties of Crystalline Materials*, edited by C. Pisani (Springer-Verlag, Berlin, 1996), vol. 67, p. 47.

[105] C. Pisani, R. Dovesi and C. Roetti, in *Lecture Notes in Chemistry* (Springer-Verlag, Berlin, 1988), vol. 48, p. 193.

[106] F. Bloch, Z. Phys. **52**, 555 (1928).

[107] B. Civalleri, D. Presti, R. Dovesi and A. Savin (Royal Society of Chemistry: Chem. Modell., 2012), vol. 9, pp. 168–185.

[108] J. Paier, R. Hirschl, M. Marsman and G. Kresse, J. Chem. Phys. **122**, 234102 (2005).

[109] S. Tosoni, C. Tuma, J. Sauer, B. Civalleri and P. Ugliengo, J. Chem. Phys. **127**, 154102 (2007).

[110] R. Peverati and D. G. Truhlar, Phys. Chem. Chem. Phys. **14**, 16187 (2012).

[111] S. Kristyan and P. Pulay, Chem. Phys. Lett. **229**, 175 (1994).

[112] P. Hobza, J. Sponer and T. Reschel, J. Comput. Chem. **16**, 1315 (1995).

[113] M. Elstner, P. Hobza, T. Frauenheim, S. Suhai and E. Kaxiras, J. Chem. Phys. **114**, 5149 (2001).

[114] S. Grimme, J. Comput. Chem. **25**, 1463 (2004).

[115] S. Grimme, J. Comput. Chem. **27**, 1787 (2006).

[116] S. Grimme, J. Antony, S. Ehrlich and H. Krieg, J. Chem. Phys. **132**, 154104 (2010).

[117] M. A. Neumann and M.-A. Perrin, J. Phys. Chem. B **109**, 15531 (2005).

[118] T. Li and S. Feng, Pharm. Res. **23**, 2326 (2006).

[119] B. Civalleri, C. Zicovich-Wilson, L. Valenzano and P. Ugliengo, Cryst. Eng. Comm **10**, 405 (2008).

[120] P. G. Karamertzanis, G. M. Day, G. W. A. Welch, J. Kendrick, F. J. J. Leusen, M. A. Neumann and S. L. Price, J. Phys. Chem. **128**, 244708 (2008).

[121] P. Ugliengo, C. Zicovich-Wilson, S. Tosoni and B. Civalleri, J. Mater. Chem. **19**, 2564 (2009).

[122] C. M. Zicovich-Wilson, B. Kirtman, B. Civalleri and A. Ramírez-Solís, Phys. Chem. Chem. Phys. **12**, 3289 (2010).

[123] K. Hongo, M. A. Watson, R. S. Sánchez-Carrera, T. Iitaka and A. Aspuru-Guzik, J. Phys. Chem. Lett. **1**, 1789 (2010).

[124] D. C. Sorescu and B. M. Rice, J. Phys. Chem. C **114**, 6734 (2010).

[125] R. Balu, E. F. C. Byrd and B. M. Rice, J. Phys. Chem. B **115**, 803 (2011).

[126] W. Reckien, F. Janetzko, M. F. Peintinger and T. Bredow, J. Comput. Chem. **33**, 2023 (2012).

[127] M. Dion, H. Rydberg, E. Schröder, D. C. Langreth and B. I. Lundqvist, Phys. Rev. Lett. **92**, 246401 (2004).

[128] T. Thonhauser, V. R. Cooper, S. Li, A. Puzder, P. Hyldgaard and D. C. Langreth, Phys. Rev. B. **76**, 125112 (2007).

[129] F. Shimojo, Z. Wu, A. Nakano, R. K. Kalia and P. Vashishta, J. Chem. Phys. **132**, 094106 (2010).

[130] D. Lu, Y. Li, D. Rocca and G. Galli, Phys. Rev. Lett. **102**, 206411 (2009).

[131] Y. Li, D. Lu, H.-V. Nguyen and G. Galli, J. Phys. Chem. **114**, 1944 (2010).

[132] S. Suhai, Phys. Rev. B **27**, 3506 (1983).

[133] J.-Q. Sun and R. J. Bartlett, J. Chem. Phys. **104**, 8553 (1996).

[134] S. Hirata and S. Iwata, J. Chem. Phys. **109**, 4147 (1998).

[135] S. Hirata and T. Shimazaki, Phys. Rev. B **80**, 1 (2009).

[136] Y.-Y. Ohnishi and S. Hirata, J. Chem. Phys. **133**, 034106 (2010).

[137] T. Shiozaki and S. Hirata, J. Chem. Phys. **132**, 151101 (2010).

[138] P. Y. Ayala, K. N. Kudin and G. E. Scuseria, J. Chem. Phys. **115**, 9698 (2001).

[139] M. Marsman, A. Grüneis, J. Paier and G. Kresse, J. Chem. Phys. **130**, 184103 (2009).

[140] A. Grüneis, M. Marsman and G. Kresse, J. Chem. Phys. **133**, 074107 (2010).

[141] A. Grüneis, G. H. Booth, M. Marsman, J. Spencer, A. Alavi and G. Kresse, J. Chem. Theory Comput. **7**, 2780 (2011).

[142] S. Saebø and P. Pulay, J. Phys. Chem. **88**, 1884 (1988).

[143] M. S. Lee, P. E. Maslen and M. Head-Gordon, J. Phys. Chem. **112**, 3592 (2000).

[144] G. E. Scuseria and P. Y. Ayala, J. Phys. Chem. **111**, 8330 (1999).

[145] M. Schütz, J. Phys. Chem. **116**, 8772 (2002).

[146] H.-J. Werner, F. R. Manby and P. J. Knowles, J. Phys. Chem. **118**, 8149 (2003).

[147] C. Pisani, M. Busso, G. Capecchi, S. Casassa, R. Dovesi, L. Maschio, C. Zicovich-Wilson and M. Schütz, J. Phys. Chem. **122**, 094113 (2005).

[148] D. Usvyat, L. Maschio, C. Pisani and M. Schütz, Z. Phys. Chem. **224**, 441 (2010).

[149] M. Schütz, G. Rauhut and H.-J. Werner, J. Phys. Chem. A **102**, 599 (1998).

[150] L. Maschio and D. Usvyat, Phys. Rev. B **78**, 073102 (2008).

[151] L. Maschio, J. Chem. Theory Comput. **7**, 2818 (2011).

[152] M. D. Ben, J. Hutter and J. VandeVondele, J. Chem. Theory Comput. **8**, 4177 (2012).

Chapter 3

A multiconfigurational hybrid density-functional theory

This chapter, written in collaboration with A. Savin, H. J. Aa. Jensen and J. Toulouse, has been published in Journal of Chemical Physics [J. Chem. Phys. **137**, 044104 (2012)].

3.1 Abstract

We propose a multiconfigurational hybrid density-functional theory which rigorously combines a multiconfiguration self-consistent-field calculation with a density-functional approximation based on a linear decomposition of the electron-electron interaction. This gives a straightforward extension of the usual hybrid approximations by essentially adding a fraction λ of exact static correlation in addition to the fraction λ of exact exchange. Test calculations on the cycloaddition reactions of ozone with ethylene or acetylene and the dissociation of diatomic molecules with the Perdew-Burke-Ernzerhof (PBE) and Becke-Lee-Yang-Parr (BLYP) density functionals show that a good value of λ is 0.25, as in the usual hybrid approximations. The results suggest that the proposed multiconfigurational hybrid approximations can improve over usual density-functional calculations for situations with strong static correlation effects.

3.2 Introduction

Density-functional theory (DFT) [1] within the Kohn-Sham (KS) scheme [2] is the most widely used method for electronic-structure calculations in atomic, molecular and solid-state systems. With the usual approximate density functionals, such as generalized-gradient approximations (GGA) and hybrid approximations mixing in a fraction of Hartree-Fock (HF) exchange, DFT KS generally gives good results for situations in which the so-called dynamic electron correlation dominates the total correlation energy, but it can yield severe errors for systems with strong static correlation, i.e. with partially filled near-degenerate orbitals (see, e.g., Ref. [3]). It has been argued that the GGA exchange density functionals actually mimic some static correlation through their self-interaction error, though in an imperfect manner (see, e.g., Refs. [4, 5]). There is often indeed a partial cancellation of errors between the self-interaction error which tends to give too low an energy and the neglect of static correlation which gives too high an energy (see,

e.g., Ref. [6]). Hybrid approximations have a smaller self-interaction error and are thus often worse than pure density functionals for describing systems with static correlation (see, e.g., Ref. [7]).

Several approaches have been proposed to include explicit static correlation in density-functional theory. Artificially breaking (space and spin) symmetry by unrestricted KS calculations is the simplest approach to simulate static correlation (see, e.g., Ref. [8]), and it often leads to reasonable potential energy surfaces but wrong spin densities. Another possible approach consists in replacing the single KS determinant by an ensemble of determinants or, equivalently, using fractional occupation numbers for the orbitals [9–22], but a successful and general method based on this idea is still lacking. Configuration-interaction schemes have also been proposed in which modified Hamiltonian matrix elements include information from DFT [23–26]. A lot of approaches consist in adding to the energy of a partially correlated wave function calculation, including near-degenerate configuration state functions coupled by the full Coulombic electron-electron interaction, an energy density functional describing the missing correlation effects [27–62]. In these last approaches, one must use a density functional which depends on the size of the multiconfigurational expansion, in order to avoid double counting of correlation between the wave function part of the calculation and the density functional. Finally, to avoid any double counting of correlation from the beginning, it has been proposed to decompose the Coulombic electron-electron interaction into long-range and short-range components, the long-range part being treated by a method capable of describing static correlation and the short-range part being described by a density functional approximation. The methods that have been used for the long-range part are: configuration interaction [63–69], multiconfigurational self-consistent field (MCSCF) [70–72], multireference perturbation theory [73], constrained-pairing mean-field theory [74, 75], and density-matrix functional theory [76–78].

In this work, we explore the possibility to combine MCSCF and DFT based on a simple linear decomposition of the Coulombic electron-electron interaction, in the spirit of the usual hybrid approximations, and similarly to what was recently done for constructing theoretically justified double-hybrid approximations [79]. This approach gives a straightforward multiconfigurational extension of the standard hybrid approximations, and aims at improving their description of static correlation. After deriving this multiconfigurational hybrid density-functional theory, we test this approach on situations with strong static correlation effects, namely the cycloaddition reactions of ozone with ethylene or acetylene and the dissociation of diatomic molecules, and we compare with other methods, in particular the range-separated multiconfigurational hybrid method of Refs. [70–72].

3.3 Theory

Using the formalism of the multideterminant extension of the KS scheme (see, e.g., Refs. [69, 71, 79, 80]), for any coupling constant λ, the *exact* energy can be expressed as the following minimization over multideterminant wave functions Ψ:

$$E = \min_{\Psi}\Big\{\langle\Psi|\hat{T}+\hat{V}_{\rm ext}+\lambda\hat{W}_{ee}|\Psi\rangle+\bar{E}^{\lambda}_{{\rm H}xc}[n_\Psi]\Big\}, \tag{3.1}$$

where $\hat{T}$ is the kinetic energy operator, $\hat{V}_{\text{ext}}$ is a scalar external potential operator (e.g., nuclei-electron), $\hat{W}_{ee}$ is the electron-electron interaction operator, and $\bar{E}^{\lambda}_{\text{H}xc}[n_\Psi]$ is the *complement* λ-dependent Hartree-exchange-correlation density functional evaluated at the density coming from Ψ. The complement density functional, $\bar{E}^{\lambda}_{\text{H}xc}[n] = E_{\text{H}xc}[n] - E^{\lambda}_{\text{H}xc}[n]$, is the difference between the usual KS density functional $E_{\text{H}xc}[n]$ and the λ-dependent density functional $E^{\lambda}_{\text{H}xc}[n]$ corresponding to the interaction $\lambda\hat{W}_{ee}$. The Hartree-exchange contribution is of first order in the electron-electron interaction and is thus linear in λ,

$$\bar{E}^{\lambda}_{\text{H}x}[n] = (1-\lambda)E_{\text{H}x}[n], \tag{3.2}$$

where $E_{\text{H}x}[n]$ is the usual KS Hartree-exchange density functional. The correlation contribution is obtained by uniform coordinate scaling of the density [81–84],

$$\bar{E}^{\lambda}_{c}[n] \;=\; E_c[n] - E^{\lambda}_{c}[n] = E_c[n] - \lambda^2 E_c[n_{1/\lambda}] \tag{3.3}$$

where $E_c[n]$ is the usual KS correlation functional, $E^{\lambda}_{c}[n]$ is the correlation functional corresponding to the interaction $\lambda\hat{W}_{ee}$, and $n_{1/\lambda}(\mathbf{r}) = (1/\lambda)^3 n(\mathbf{r}/\lambda)$ is the scaled density.

The theory is so far exact but in practice approximations must be used for the multideterminant wave function and the density functionals. In Ref. [79], by restricting the search in Eq. (4.3) to single-determinant wave functions Φ, we defined the *density-scaled one-parameter hybrid* (DS1H) approximation

$$E^{\text{DS1H}} = \min_{\Phi}\Big\{\langle\Phi|\hat{T} + \hat{V}_{\text{ext}} + \lambda\hat{W}_{ee}|\Phi\rangle + (1-\lambda)E_{\text{H}x}[n_\Phi] + E_c[n_\Phi] - \lambda^2 E_c[n_{\Phi,1/\lambda}]\Big\}, \tag{3.4}$$

and, by additionally neglecting density scaling in the correlation functional, $E_c[n_{1/\lambda}] \approx E_c[n]$, we obtained the *one-parameter hybrid* (1H) approximation,

$$E^{\text{1H}} = \min_{\Phi}\Big\{\langle\Phi|\hat{T} + \hat{V}_{\text{ext}} + \lambda\hat{W}_{ee}|\Phi\rangle + (1-\lambda)E_{\text{H}x}[n_\Phi] + (1-\lambda^2)E_c[n_\Phi]\Big\}, \tag{3.5}$$

which is similar to the usual one-parameter hybrid approximations [85, 86], except that the correlation functional is weighted by a factor of $(1-\lambda^2)$. Starting from these references and applying a second-order Møller-Plesset (MP2) perturbation theory [80, 87, 88], we also defined the *density-scaled one-parameter double-hybrid* (DS1DH) and *one-parameter double-hybrid* (1DH) approximations [79], which are one-parameter versions of the original double-hybrid approximations [89]. These latter also combine HF exchange and MP2 correlation with a semilocal exchange-correlation density functional but with two empirical parameters.

Here, we follow a different route and use an MCSCF wave function in Eq. (4.3), expanded as a linear combination of configuration state functions Φ_I,

$$|\Psi\rangle = \sum_I c_I|\Phi_I\rangle, \tag{3.6}$$

where the coefficients c_I and the orbitals are to be simultaneously optimized. With this form of wave function, we obtain a *multiconfigurational density-scaled one-parameter hybrid* (MCDS1H) approximation,

$$E^{\text{MCDS1H}} = \min_{\Psi}\Big\{\langle\Psi|\hat{T} + \hat{V}_{\text{ext}} + \lambda\hat{W}_{ee}|\Psi\rangle + (1-\lambda)E_{\text{H}x}[n_\Psi] + E_c[n_\Psi] - \lambda^2 E_c[n_{\Psi,1/\lambda}]\Big\}, \tag{3.7}$$

and, if density scaling, which is not considered in usual hybrid approximations, is neglected, we obtain a *multiconfigurational one-parameter hybrid* (MC1H) approximation,

$$E^{\mathrm{MC1H}} = \min_{\Psi}\Big\{ \langle\Psi|\hat{T} + \hat{V}_{\mathrm{ext}} + \lambda\hat{W}_{ee}|\Psi\rangle + (1-\lambda)E_{\mathrm{H}x}[n_\Psi] + (1-\lambda^2)E_c[n_\Psi]\Big\}. \qquad (3.8)$$

Equation (3.7) is the equivalent of the range-separated multiconfigurational hybrid method of Refs. [70–72], that we will refer to as MC-srDFT, but for a linear separation of the electron-electron interaction. Notice that, if we were to use no approximations for the wave function Ψ and the exchange-correlation density functional, then Eq. (3.7) would give the exact energy, *independently* of λ. In practice, of course, we must use approximations, and the energy does depend on λ, which can then be considered as an empirical parameter to be optimized.

The present scheme has two advantages over the range-separated scheme: (a) Only one list of two-electron Coulomb integrals is needed and it is just multiplied by λ in the MCSCF part and by $(1-\lambda)$ in the complement Hartree energy, whereas two lists of two-electron integrals are needed in the range-separated scheme for the long-range MCSCF part and for the short-range complement Hartree energy; (b) No new exchange and correlation density functionals need in principle to be developed since all the existing approximations developed for the KS scheme can be reused with a simple scaling, whereas new short-range density-functional approximations must be developed in the range-separated scheme.

Equations (3.7) and (3.8) can be seen as straightforward multiconfigurational extensions of the usual hybrid approximations. Indeed, the expectation value of $\lambda\hat{W}_{ee}$ over the MCSCF wave function Ψ not only introduces a fraction λ of exact exchange but also a fraction of exact static correlation. Defined in the ideal limit of reference energy levels that are degenerate, the static correlation energy is linear with respect to the electron-electron interaction, and thus we can consider that the expectation value of $\lambda\hat{W}_{ee}$ introduces a linear fraction λ of static correlation. By contrast, the dynamic correlation energy starts at quadratic order in the electron-electron interaction, so that, for sufficiently small λ, it is justified to neglect it in the wave function expectation value. Moreover, for sufficiently small λ, the weight $(1-\lambda^2)$ is close to 1 and thus Eq. (3.8) includes a nearly complete approximate correlation energy functional, that is often thought of as correctly describing dynamic correlation. Of course, if the multiconfigurational hybrid approximations of Eq. (3.7) or (3.8) are to be accurate, the fraction $(1-\lambda)$ of static correlation energy not treated by MCSCF must be accounted for by the density functional, possibly through a compensation with the self-interaction error of the scaled exchange functional $(1-\lambda)E_x[n]$.

3.4 Computational details

The calculations have been performed with a development version of the DALTON 2011 program [90], in which the MCDS1H and MC1H approximations have been implemented in the same way than for the MC-srDFT method [70, 71, 91], using the direct restricted-step second-order MCSCF algorithm of Jensen and coworkers [92–97]. For $E_x[n]$ and $E_c[n]$, we use two GGA exchange-correlation density functionals, Perdew-Burke-Ernzerhof (PBE) [98] and Becke/Lee-Yang-Parr (BLYP) [99, 100], without spin-density dependence. For implementing the density-scaled correlation functionals in the MCSCF algorithm, we need the scaling relations for the energy density, and its first- and second-order derivatives that we give in Appendix 3.7.1. The computational cost of the method is essentially the

same as for a standard MCSCF calculation, with a small extra cost due to the DFT contribution.

A good value for the empirical parameter λ in Eqs. (3.7) and (3.8) is determined on the O3ADD6 benchmark set [101, 102] for the 1,3-dipolar cycloaddition reactions of ozone (O_3) with ethylene (C_2H_4) or acetylene (C_2H_2) [103–105]. For these two reactions, there are three stationary points along the reaction coordinate: the van der Waals complex, the transition state, and the cycloadduct (primary ozonide), all in a closed-shell spin-singlet state. The O3ADD6 set consists of the six energies of these stationary points of the two reactions, calculated relative to the energy of the separated reactants, and without zero-point vibrational energy correction. Accurate calculations of these energies are difficult and require to handle the subtle balance between static and dynamic correlation effects along the reaction coordinate. The ozone reactant, the van der Waals complex, and the transition state have a strong multiconfigurational character corresponding to the HOMO $\rightarrow$ LUMO double excitation in ozone. In the cycloadduct, and to a less extent in the transition state, the stabilization of the ozone HOMO and the destabilization of the ozone LUMO greatly reduce this multiconfigurational character. In addition, there are small near-degeneracy correlation effects due to the π and π^* orbitals of the reactive π bond of ethylene and acetylene. For each separate reactant, a complete active space wave function with 2 electrons in 2 orbitals [CAS(2,2)] is chosen, the active space corresponding to the HOMO and LUMO orbitals for ozone, and to the HOMO (π) and LUMO (π^*) orbitals of the reactive π bond for ethylene and acetylene. For the van der Waals complex, the transition state, and the cycloadduct, a CAS(4,4) wave function is consistently chosen, the active space corresponding to the orbitals that connect to the ones chosen for the reactants in the dissociation limit. We use the aug-cc-pVTZ basis set [106, 107] and the fixed geometries of Ref. [104] optimized using the hybrid meta-GGA exchange-correlation functional M05 [108] with the 6-311+G(2df,2p) basis set [109, 110]. The reference values for the energies are from Ref. [104] and were obtained from extensive coupled-cluster calculations extrapolated to the complete basis set limit [103, 104]. We calculate the mean absolute error (MAE) over the six values as a function of the parameter λ. We compare the MCDS1H and MC1H approximations with (a) some non-hybrid methods: HF, MCSCF, MP2 [111], multireference MP2 (MRMP2) [104, 112], PBE [98], and BLYP [99, 100]; (b) some single-hybrid approximations: PBE0 [113, 114], B1LYP [115], and B3LYP [116, 117]; (c) some double-hybrid approximations: DS1DH-PBE [79], 1DH-BLYP [79], and B2-PLYP [89], all applied in a spin-restricted formalism. We also compare with the range-separated MC-srPBE multiconfigurational hybrid approximation [70–72] using the short-range PBE exchange-correlation functional of Ref. [118] and the value of the range-separation parameter $\mu = 0.40$ bohr^{-1} which was previously determined in Ref. [71].

We also test the MCDS1H and MC1H approximations by computing the potential energy curves the five diatomic molecules H_2, Li_2, C_2, N_2, and F_2, using in each case a full-valence CAS wave function and the cc-pVTZ basis set [106].

3.5 Results

3.5.1 O3ADD6 database

Figure 3.1 shows the MAEs for the O3ADD6 set as functions of the parameter λ for the MCDS1H and MC1H approximations with the BLYP and PBE exchange-correlation density functionals. For $\lambda = 0$, the MCDS1H and MC1H approximation reduce to a standard KS calculation with the corresponding approximate density functional. For $\lambda = 1$, they reduce to a standard MCSCF calculation. Contrary to what was found for the calculation of atomization energies using double-hybrid approximations [79], here neglecting density scaling in the correlation functional makes little difference. Toward the $\lambda = 1$ end of the curves, the MCDS1H and MC1H approximations inherit the inaccuracy of MCSCF which neglects dynamic correlation. The MAE curves of the MCDS1H-BLYP and MC1H-BLYP approximations display a marked minimum at an intermediate value of λ, thus improving upon both the standard BLYP and MCSCF calculations. The minimum is reached at $\lambda = 0.25$ for MCDS1H-BLYP and at $\lambda = 0.30$ for MC1H-BLYP, with MAEs below 2 kcal/mol. For the MCDS1H-PBE and MC1H-PBE approximations, the MAE curves have a plateau around $\lambda = 0.25$ with a MAE of about 3 kcal/mol, which is again smaller than both the standard PBE and MCSCF calculations. In view of these results, we choose the value $\lambda = 0.25$ in all MCDS1H and MC1H approximations. It is a conservative choice since it gives the same fraction of exact exchange as the one usually advocated in the usual single-hybrid approximations [119].

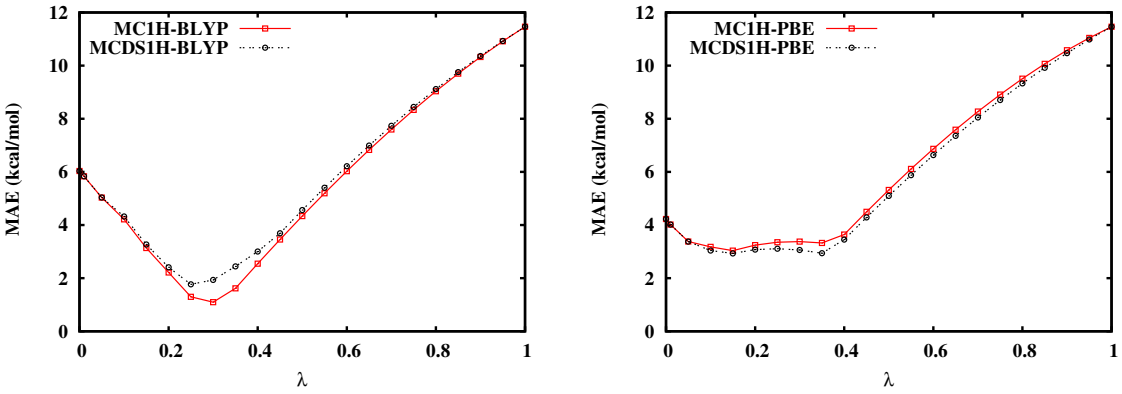

Figure 3.1: MAEs of O3ADD6 set as functions of the parameter λ for the MC1H and MCDS1H approximations with the BLYP (left) and PBE (right) exchange-correlation density functionals. All calculations were carried out with the aug-cc-pVTZ basis set.

Table 3.1 reports the energies of the van der Waals complex, the transition state, and the cycloadduct of the two reactions of the O3ADD6 set, relative to the separated reactants, calculated with the MCDS1H and MC1H approximations at $\lambda = 0.25$. For comparison, we also report results for various non-hybrid and other hybrid methods.

During the early stages of the two reactions, a weakly bound van der Waals complex is formed which lies in a shallow minimum (-1.90 kcal/mol for C_2H_2 and -1.94 kcal/mol for C_2H_4) below the reactants. The MCDS1H and MC1H approximations give significantly underestimated well depths, which are still in improvement over standard MCSCF but not over standard KS calculations with the corresponding functionals. The range-separated MC-srPBE method does also not perform better than KS PBE for these van der Waals

Table 3.1: Energies of the van der Waals (vdW) complex, the transition state (TS), and the cycloadduct (primary ozonide), relative to the separated reactants, and the corresponding MAEs (in kcal/mol) for the addition of ozone with acetylene or ethylene (O3ADD6 set), calculated by several methods. For the DS1DH-PBE and 1DH-BLYP double-hybrid approximations, we use the value $\lambda = 0.65$ which was previously optimized in Ref. [79]. For the MCDS1H and MC1H multiconfigurational hybrid approximations, we use a value of $\lambda = 0.25$ which roughly minimizes the MAE according to Fig. 3.1. For the range-separated MC-srPBE multiconfigurational hybrid approximation, we use the value of the range-separation parameter $\mu = 0.40$ bohr^{-1} which was previously determined in Ref. [71]. For the multiconfigurational methods, a CAS(4,4) wave function is chosen for the van der Waals complex, the transition state, and the cycloadduct, and a CAS(2,2) wave function for each separate reactant. All calculations were carried out with the aug-cc-pVTZ basis set. All calculations were done for M05/6-311+G(2df,2p) geometries, except for the MRMP2 results which are for CCSD(T)/cc-pVTZ geometries.

	$O_3 + C_2H_2 \rightarrow$			$O_3 + C_2H_4 \rightarrow$			
Method	vdW	TS	cycloadduct	vdW	TS	cycloadduct	MAE
HF	0.68	23.08	-87.12	1.90	17.91	-82.58	14.18
MCSCF	0.69	27.54	-77.25	1.32	22.13	-68.06	11.46
MP2	-3.18	1.13	-54.81	-4.01	-5.74	-51.18	5.67
MRMP2[a]	-2.16	8.77	-48.19	-2.09	3.43	-43.32	5.16
PBE	-1.71	-1.66	-62.44	-2.50	-4.77	-51.45	4.23
BLYP	-0.57	2.21	-53.98	-1.29	-1.55	-43.19	6.03
Single-hybrid approximations							
PBE0	-1.26	1.65	-74.00	-1.55	-1.74	-64.74	5.00
B1LYP	-0.60	4.78	-66.56	-0.83	0.71	-57.47	1.85
B3LYP	-0.67	3.81	-65.10	-1.01	-0.12	-55.64	2.06
Double-hybrid approximations							
DS1DH-PBE	-2.08	3.47	-61.21	-2.54	-1.81	-54.90	2.51
1DH-BLYP	-1.92	4.42	-58.37	-2.37	-1.14	-52.12	3.12
B2-PLYP[b]	-1.47	5.00	-60.18	-1.81	-0.13	-53.05	2.42
Multiconfigurational hybrids							
MC-srPBE	-0.93	4.12	-72.73	-0.87	0.71	-65.53	4.27
MCDS1H-PBE	-1.06	3.88	-70.41	-1.22	0.30	-60.71	3.11
MC1H-PBE	-1.08	3.66	-70.97	-1.25	0.13	-61.26	3.35
MCDS1H-BLYP	0.28	7.94	-62.47	0.26	3.78	-52.86	1.77
MC1H-BLYP	-0.36	6.74	-63.76	-0.47	2.57	-54.21	1.30
Best estimate[a]	-1.90	7.74	-63.80	-1.94	3.37	-57.15	

[a]From Ref. [104].
[b]Performed with Gaussian09 [120].

systems. A better description of the long-range dispersion correlation would indeed require inclusion of perturbation corrections on top of the active space [73]. As expected, the double-hybrid approximations, which include second-order perturbation corrections, tend to perform better for these van der Waals complexes. The best performance is achieved with MRMP2 which is able to correctly describe both multiconfigurational effects and dispersion correlations. However, one should keep in mind than the methods MP2, MRMP2, and the double hybrids are most likely less converged with respect to the basis size than the other methods.

The activation barriers of the transition states are underestimated (or not present at all) in KS PBE and BLYP calculations, and to a less extent with the single-hybrid and double-hybrid approximations, while they are largely overestimated in MCSCF. Note that here, contrary to the common case, MCSCF gives higher activation barriers than HF because the ozone reactant has more static correlation than the transition state. The MCDS1H and MC1H approximations give an improvement of about 5 kcal/mol over the KS calculations with the corresponding functionals. The range-separated MC-srPBE method gives activation barriers which are slightly better than the ones given by MCDS1H-PBE and MC1H-PBE, but largely worse than the ones given by MCDS1H-BLYP and MC1H-BLYP. The values obtained with MCDS1H-BLYP and MC1H-BLYP, as well as with MRMP2, are all within 1 kcal/mol of the best estimates.

The reaction energies of the formation of the cycloadducts are overestimated in MCSCF and underestimated in MRMP2 (by about 15 kcal/mol). Zhao *et al.* observed that even using a large (14,14) active space does not improve the MRMP2 reaction energy [104]. All the hybrid methods give more reasonable reaction energies. In particular, MC1H-BLYP gives reaction energies within less than 3 kcal/mol of the best estimates.

If we accept to look more closely to the MAE values in spite of the limited statistics, we see that MC1H-BLYP gives overall the smallest MAE with 1.30 kcal/mol. The multiconfigurational hybrid MCDS1H-PBE involving the PBE exchange-correlation functional gives a larger MAE of 3.11 kcal/mol, but turns out to perform better on average than the range-separated MC-srPBE method which gives a MAE of 4.27 kcal/mol. Neglecting density scaling in the correlation functional of multiconfigurational hybrids seems slightly favorable for BLYP and slightly unfavorable for PBE. This is in line with what was found for double-hybrid approximations [79], although the MP2 correlation part made it much more sensitive to the neglect of the density scaling. Even if the effect of neglecting density scaling is systematic in giving more negative complement correlation energies $\bar{E}_c^{\lambda}[n]$ for all density functionals, its effect on the MAE depends more on fortuitous compensation of errors for the approximate functional used.

3.5.2 Dissociation of diatomic molecules

We now turn to the calculation of potential energy curves of diatomic molecules. This is a harder problem since static correlation effects are dominant at dissociation. For the multiconfigurational hybrids, we report here only the curves of MCDS1H for PBE and of MC1H for BLYP according to the results of Section 3.5.1, but the differences between the curves of MCDS1H and MC1H for both BLYP and PBE are in fact very small for these diatomic molecules.

Figure 3.2 shows the potential energy curve of H_2 calculated by hybrid approximations using the PBE and BLYP density functionals. Around the equilibrium internuclear

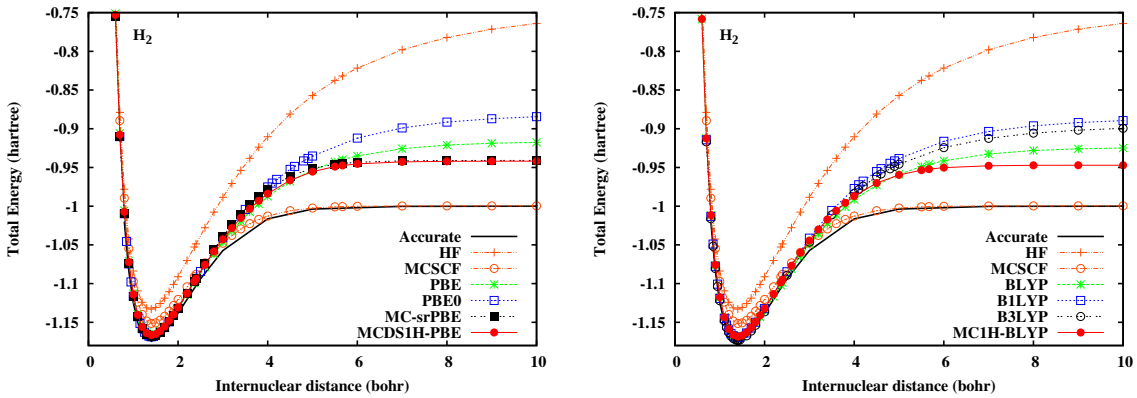

Figure 3.2: Potential energy curves of H_2 calculated by HF, MCSCF, and several methods based on the PBE (left) or BLYP (right) exchange-correlation density functionals. For the MCDS1H and MC1H multiconfigurational hybrid approximations, we use a value of $\lambda = 0.25$. For the range-separated MC-srPBE multiconfigurational hybrid approximation, we use a value of the range-separation parameter of $\mu = 0.40$ bohr^{-1}. For all multiconfigurational methods, we use a full-valence CAS wave function. The basis set is cc-pVTZ basis. The accurate curve is from Ref. [28].

distance, all DFT-based method, including MCDS1H-PBE and MC1H-BLYP, are accurate, which means that they properly describe dynamic correlation. At large distances, the single-hybrid approximations (PBE0, B1LYP, and B3LYP), which include a fraction of HF exchange energy, give less accurate potential energy curves than non-hybrid KS calculations (PBE and BLYP). By inclusion of a fraction of exact static correlation energy, the multiconfigurational hybrids (MCDS1H-PBE, MC-srPBE, and MC1H-BLYP) correct this behavior and give potential energy curves that correctly saturate beyond a distance of about 5 bohr, as the MCSCF curve does. This point is explained by a detailed analysis of the asymptotic expansion of the potential energy curves in a minimal basis in Appendix 3.7.2. However, the MCDS1H-PBE, MC-srPBE, and MC1H-BLYP methods still display significant errors on the energy of the separated atoms due to the density-functional approximations. Indeed, as in restricted KS calculations, the density functionals used in the multiconfigurational hybrids depend only of the total density and do not give accurate energies in the limit of separated atoms of open-shell character. In an unrestricted KS calculation, the energy at dissociation can be improved by breaking the spin symmetry and therefore introducing a fictitious spin density which helps to describe the separated atoms. In our present implementation of the multiconfigurational hybrids, the spin symmetry is imposed on the MCSCF wave function so that there is no fictitious spin density to be used in the density functionals.

Figure 3.5.2 shows the potential energy curves of Li_2, C_2, N_2, and F_2. The results are similar than for H_2. Around the equilibrium distance, the MCDS1H-PBE and MC1H-BLYP curves are similar to the standard hybrid or non-hybrid KS calculations. At large distances, the single-hybrid approximations give a spurious increase of the energy, whereas the MCDS1H-PBE and MC1H-BLYP curves correctly saturate. The MC1H-BLYP approximation gives good total energies, but again a significant error remains at dissociation, especially for N_2. The DS1DH-PBE and MC-srPBE approximation gives curves of very similar shape.

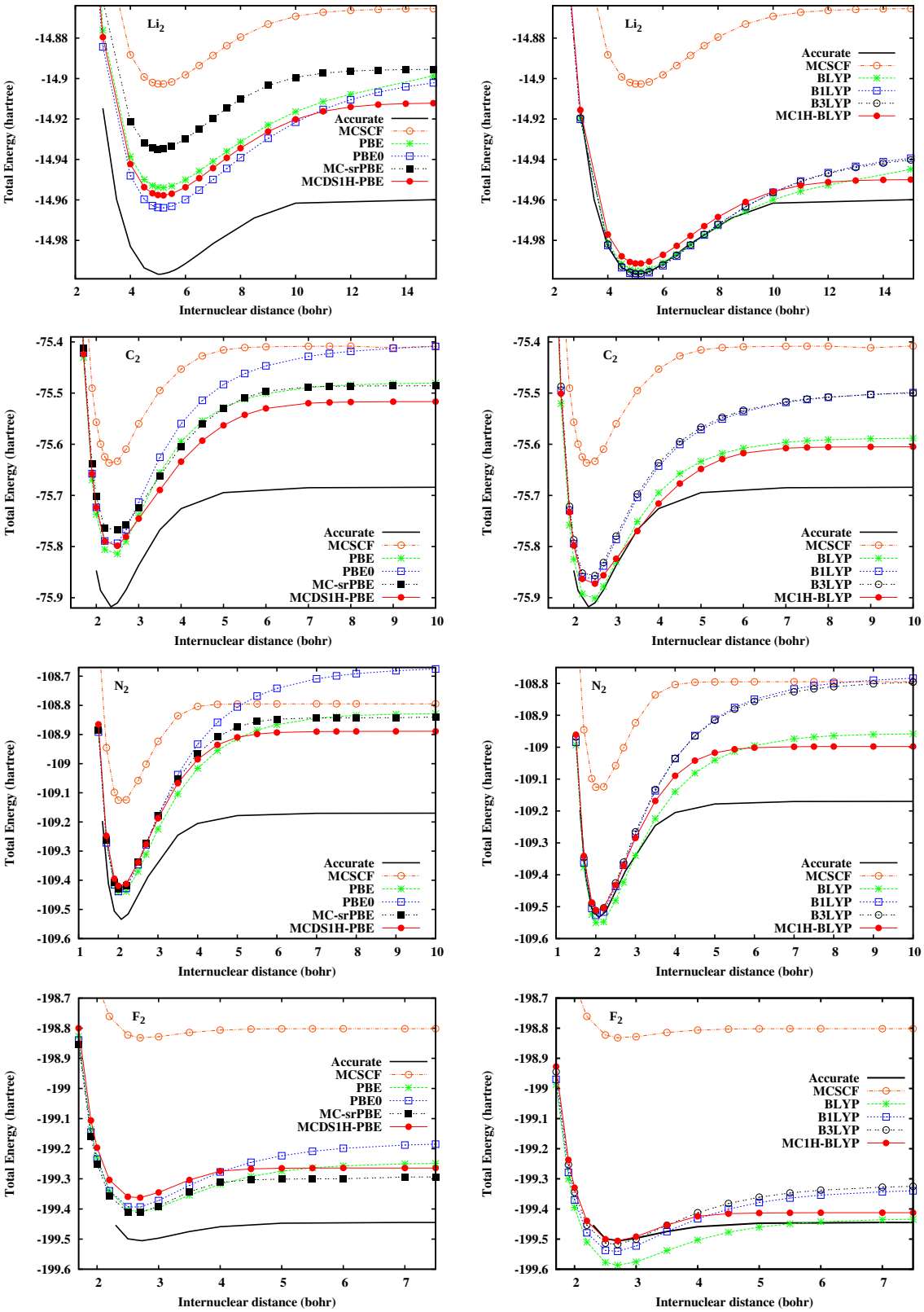

Figure 3.3: Potential energy curves of Li_2, C_2, N_2, and F_2 calculated with MCSCF and several methods based on the PBE (left) or BLYP (right) exchange-correlation density functionals. For the MCDS1H and MC1H multiconfigurational hybrid approximations, we use a value of $\lambda = 0.25$. For the range-separated MC-srPBE multiconfigurational hybrid approximation, we use a value of the range-separation parameter of $\mu = 0.40$ bohr^{-1}. For all multiconfigurational methods, we use a full-valence CAS wave function. The basis set is cc-pVTZ basis. The accurate curves are from Ref. [28].

3.6 Conclusions

We have presented a multiconfigurational hybrid density-functional theory which rigorously combines MCSCF and DFT based on a linear decomposition of the electron-electron interaction. It is straightforward extension of the usual hybrid approximations by essentially adding a fraction λ of exact static correlation in addition to the fraction λ of exact exchange. Any existing approximate exchange-correlation density functional can be used in this scheme by using a simple scaling relation with λ. Test calculations on the cycloaddition reactions of ozone with ethylene or acetylene and the dissociation of diatomic molecules with the PBE and BLYP density functionals show that a good value of λ is 0.25, as in the usual hybrid approximations.

Interestingly, the results seem to indicate that the present approach based on a simple linear decomposition of the electron-electron interaction is at least as good as the range-separated multiconfigurational hybrid method of Ref. [70–72] for including static correlation in DFT, at least with the approximate density functionals used here. Of course, with better short-range density-functional approximations (in particular, we do not have a short-range version of the LYP correlation functional for comparison), the conclusion could be different. Also, one should note that hybrid approaches combining perturbation theory with DFT based on a linear decomposition of the interaction [79] do not have the advantages of the range-separated hybrid approaches for fast basis-size convergence and explicit inclusion of long-range van der Waals interactions. For MCSCF, however, basis set convergence is not so much an issue.

The present results suggest that the proposed multiconfigurational hybrid approximations can improve over usual DFT approximations for situations with strong static correlation effects. It remains however to assess the performance of this multiconfigurational hybrid method on a larger variety of systems. Future work includes adding the dependence on the spin density in the functionals to be able to properly handle open-shell systems, and possibly other additional variables such as the on-top pair density as an alternative to the spin density for improving the accuracy of closed-shell systems [121].

Acknowledgments

We thank E. Fromager (Strasbourg, France) for discussions. K.S. thanks Professors I. Othman and M. K. Sabra (Atomic Energy Commission of Syria) for their support. This work was part of the French-Danish collaboration project “WADEMECOM.dk” supported by the French government.

3.7 Appendix

3.7.1 Scaling relations for the derivatives of the density-scaled correlation functional

We give the scaling relations for the density-scaled correlation functional $E_c^\lambda[n] = \lambda^2 E_c[n_{1/\lambda}]$ and its derivatives in the case of generalized-gradient approximations (GGA). Starting

from a standard GGA density functional written as

$$E_{c,\mathrm{GGA}}[n] = \int e_c\left(n(\mathbf{r}), |\nabla n(\mathbf{r})|\right) d\mathbf{r}, \tag{3.9}$$

where $|\nabla n(\mathbf{r})|$ is the norm of the density gradient, the corresponding scaled functional is

$$E^{\lambda}_{c,\mathrm{GGA}}[n] = \int e^{\lambda}_c\left(n(\mathbf{r}), |\nabla n(\mathbf{r})|\right) d\mathbf{r}, \tag{3.10}$$

where the energy density is obtained by scaling relation (see Ref. [79])

$$e^{\lambda}_c\left(n(\mathbf{r}), |\nabla n(\mathbf{r})|\right) = \lambda^5 e_c\left(\frac{n(\mathbf{r})}{\lambda^3}, \frac{|\nabla n(\mathbf{r})|}{\lambda^4}\right). \tag{3.11}$$

The first-order derivatives of the energy density are

$$\frac{\partial e^{\lambda}_c}{\partial n}\left(n(\mathbf{r}), |\nabla n(\mathbf{r})|\right) = \lambda^2 \frac{\partial e_c}{\partial n}\left(\frac{n(\mathbf{r})}{\lambda^3}, \frac{|\nabla n(\mathbf{r})|}{\lambda^4}\right), \tag{3.12}$$

and

$$\frac{\partial e^{\lambda}_c}{\partial |\nabla n|}\left(n(\mathbf{r}), |\nabla n(\mathbf{r})|\right) = \lambda \frac{\partial e_c}{\partial |\nabla n|}\left(\frac{n(\mathbf{r})}{\lambda^3}, \frac{|\nabla n(\mathbf{r})|}{\lambda^4}\right). \tag{3.13}$$

The second-order derivatives are

$$\frac{\partial^2 e^{\lambda}_c}{\partial n^2}\left(n(\mathbf{r}), |\nabla n(\mathbf{r})|\right) = \frac{1}{\lambda}\frac{\partial^2 e_c}{\partial n^2}\left(\frac{n(\mathbf{r})}{\lambda^3}, \frac{|\nabla n(\mathbf{r})|}{\lambda^4}\right), \tag{3.14}$$

$$\frac{\partial^2 e^{\lambda}_c}{\partial |\nabla n|^2}\left(n(\mathbf{r}), |\nabla n(\mathbf{r})|\right) = \frac{1}{\lambda^3}\frac{\partial^2 e_c}{\partial |\nabla n|^2}\left(\frac{n(\mathbf{r})}{\lambda^3}, \frac{|\nabla n(\mathbf{r})|}{\lambda^4}\right), \tag{3.15}$$

and

$$\frac{\partial^2 e^{\lambda}_c}{\partial n \partial |\nabla n|}\left(n(\mathbf{r}), |\nabla n(\mathbf{r})|\right) = \frac{1}{\lambda^2}\frac{\partial^2 e_c}{\partial n \partial |\nabla n|}\left(\frac{n(\mathbf{r})}{\lambda^3}, \frac{|\nabla n(\mathbf{r})|}{\lambda^4}\right). \tag{3.16}$$

3.7.2 Asymptotic expansion of the potential energy curve of H_2

We consider the H_2 molecule in a Slater minimal basis, with a basis function a localized on the left atom and a basis function b localized on the right atom, both basis functions being identical with exponent $\zeta = 1$. In the large internuclear distance R limit, the two molecular orbitals are $1 = (a+b)/\sqrt{2}$ and $2 = (a-b)/\sqrt{2}$. The total restricted Hartree-Fock (RHF) energy writes

$$E^{\mathrm{RHF}} = 2h_{11} + J_{11} + \frac{1}{R}, \tag{3.17}$$

where $h_{11} = t_{11} + v_{11}$ is the sum of the kinetic integral $t_{11} = (1|\hat{t}|1)$ and the nuclei-electron integral $v_{11} = (1|\hat{v}_{ne}|1)$, and $J_{11} = (11|11)$ is the Coulomb two-electron integral, and $1/R$ is the nuclear repulsion energy. By expanding the molecular orbital 1 into the localized functions a and b, and using the symmetry between a and b, it is easy to find the large R behavior of all these terms:

$$t_{11} = (a|\hat{t}|a) + (a|\hat{t}|b) = \frac{1}{2} + O(e^{-R}), \tag{3.18}$$

and

$$v_{11} = (a|\hat{v}_{ne}|a) + (a|\hat{v}_{ne}|b) = -1 - \frac{1}{R} + O(e^{-R}), \tag{3.19}$$

and

$$J_{11} = \frac{(aa|aa)}{2} + \frac{(aa|bb)}{2} + 2(aa|ab) + (ab|ab) = \frac{5}{16} + \frac{1}{2R} + O(e^{-R}), \tag{3.20}$$

where $O(e^{-R})$ stands for exponentially decaying terms in R. For the values of the integrals, see Ref. [122]. Adding all the pieces together, it leads to the following asymptotic expansion of the total RHF energy

$$E^{\mathrm{RHF}} = -\frac{11}{16} - \frac{1}{2R} + O(e^{-R}). \tag{3.21}$$

At dissociation, the RHF wave function contains 50% of the incorrect ionic contribution $H^+...H^-$, which is responsible for too high an energy and for the spurious electrostatic attraction term $-1/2R$.

The full configuration interaction (FCI) correlation energy in this basis is found by diagonalizing the 2×2 Hamiltonian matrix, leading to

$$E_c^{\mathrm{FCI}} = \frac{1}{2}\left(E_2 - E^{\mathrm{RHF}} - \sqrt{(E_2 - E^{\mathrm{RHF}})^2 + 4K_{12}^2}\right), \tag{3.22}$$

where $E_2 = 2h_{22} + J_{22} + 1/R$ is the energy of the double-excited determinant, and $K_{12} = (12|12)$ is the exchange two-electron integral. The asymptotic behavior of E_2 is exactly the same as the one of E^{RHF}, so that $E_2 - E^{\mathrm{RHF}}$ vanishes exponentially when $R \to \infty$ and the asymptotic behavior of E_c^{FCI} is determined by K_{12} only: $E_c^{\mathrm{FCI}} = -K_{12} + O(e^{-R})$. The asymptotic behavior of K_{12} is

$$K_{12} = \frac{(aa|aa)}{2} - \frac{(aa|bb)}{2} = \frac{5}{16} - \frac{1}{2R} + O(e^{-R}), \tag{3.23}$$

giving for the correlation energy

$$E_c^{\mathrm{FCI}} = -\frac{5}{16} + \frac{1}{2R} + O(e^{-R}). \tag{3.24}$$

Adding the asymptotic expansions of Eqs. (3.21) and (3.24) gives the asymptotic expansion of the total FCI energy in this basis

$$E^{\mathrm{FCI}} = -1 + O(e^{-R}), \tag{3.25}$$

which implies that the FCI potential energy curve saturates quickly at large internuclear distance.

In restricted Kohn-Sham (RKS) density-functional theory, the total energy writes

$$E^{\mathrm{RKS}} = 2h_{11} + 2J_{11} + E_x + E_c + \frac{1}{R}, \tag{3.26}$$

where E_x and E_c are the exchange and correlation energies. At large R, it behaves as

$$E^{\mathrm{RKS}} = -\frac{3}{8} + E_x + E_c + O(e^{-R}). \tag{3.27}$$

With local or semilocal density-functional approximations, E_x and E_c go exponentially to constants when $R \to \infty$, so that the asymptotic expansion of E^{RKS} does not contain a spurious term in $1/R$.

Single-hybrid approximations introduces a fraction λ of RHF exchange which have the following asymptotic expansion

$$E_x^{\mathrm{RHF}} = -J_{11} = -\frac{5}{16} - \frac{1}{2R} + O(e^{-R}), \tag{3.28}$$

and therefore introduce a wrong $-\lambda/2R$ term in the total energy,

$$E^{\mathrm{hybrid}} = -\frac{3}{8} - \frac{5\lambda}{16} + (1-\lambda)E_x + E_c - \frac{\lambda}{2R} + O(e^{-R}). \tag{3.29}$$

Single-hybrid approximations thus deteriorate the large R behavior of local or semilocal density-functional approximations (see Fig. 3.2). The multiconfigurational hybrid approximations introduced in this work correct this behavior by adding a fraction of the FCI correlation energy which, in the limit of large R, is just $\lambda E_c^{\mathrm{FCI}}$, the linearity in λ being a signature of static correlation. For example, the MC1H approximation has the following asymptotic expansion

$$E^{\mathrm{MC1H}} = -\frac{3}{8} - \frac{5\lambda}{8} + (1-\lambda)E_x + (1-\lambda^2)E_c + O(e^{-R}), \tag{3.30}$$

with no longer any spurious $1/R$ term, and thus improves the large R behavior (see Fig. 3.2). It is a typical example where exact exchange and static correlation must be considered together.

For range-separated density-functional theory, the situation is similar. Range-separated single-hybrid approximations [80, 123–126] include some long-range RHF exchange and their asymptotic expansions display a wrong $-1/2R$ term, just as RHF. Their behavior for large R is in fact worse than that of usual single-hybrid approximations since the $-1/2R$ term is not weighted by λ. However, the range-separated CI-srDFT [66, 67] or MC-srDFT [70–72] methods add some exact long-range correlation energy which removes this wrong $-1/2R$ term.

Note that other forms of single-hybrid approximations which do not use RHF exchange at long range [127, 128] allow one to avoid a wrong $-1/2R$ term in the large R limit. Symmetry breaking is another way to avoid a wrong asymptotic $-1/2R$ term since the unrestricted Hartree-Fock exchange energy does not contain such a term.

The fact that local or semilocal approximations for E_x and E_c do not introduce $1/R$ terms is in agreement with the usual conviction that approximate GGA exchange functionals not only represent exchange but also static correlation, while approximate GGA correlation functionals represent dynamic correlation only [4].

Bibliography

[1] P. Hohenberg and W. Kohn, Phys. Rev. **136**, B 864 (1964).

[2] W. Kohn and L. J. Sham, Phys. Rev. **140**, A1133 (1965).

[3] W. Koch and M. C. Holthausen, *A Chemist's Guide To Density Functional Theory* (Wiley-VCH, New York, 2001).

[4] O. V. Gritsenko, P. R. T. Schipper and E. J. Baerends, J. Chem. Phys. **107**, 5007 (1997).

[5] A. D. Becke, J. Chem. Phys. **119**, 2972 (2003).

[6] A. J. Cohen, P. Mori-Sánchez and W. Yang, Science **321**, 792 (2008).

[7] N. E. Schultz, Y. Zhao and D. G. Truhlar, J. Phys. Chem. A **109**, 11127 (2005).

[8] D. Cremer, Mol. Phys. **99**, 1899 (2001).

[9] J. Slater, J. Mann, T. Wilson and J. Wood, Phys. Rev. **184**, 672 (1969).

[10] M. Levy, Phys. Rev. A **26**, 1200 (1982).

[11] E. H. Lieb, Int. J. Quantum. Chem. **24**, 24 (1983).

[12] B. I. Dunlap and W. N. Mei, J. Chem. Phys. **78**, 4997 (1983).

[13] S. G. Wang and W. H. E. Schwarz, J. Chem. Phys. **105**, 4641 (1996).

[14] P. R. T. Schipper, O. V. Gritsenko and E. J. Baerends, Theor. Chem. Acc. **99**, 329 (1998).

[15] J. D. Goddard and G. Orlova, J. Chem. Phys. **111**, 7705 (1999).

[16] M. Filatov and S. Shaik, Chem. Phys. Lett. **304**, 429 (1999).

[17] M. Filatov and S. Shaik, J. Phys. Chem. A **103**, 8885 (1999).

[18] M. Filatov and S. Shaik, Chem. Phys. Lett. **332**, 409 (1999).

[19] M. Filatov, S. Shaik, M. Woeller, S. Grimme and S. Peyerimhoff, Chem. Phys. Lett. **316**, 135 (2000).

[20] M. Filatov and S. Shaik, J. Phys. Chem. A **104**, 6628 (2000).

[21] C. A. Ullrich and W. Kohn, Phys. Rev. Lett. **87**, 093001 (2001).

[22] K. Y. R. Takeda, S. Yamanaka, Int. J. Quantum. Chem. **93**, 317 (2003).

[23] S. Grimme and M. Waletzke, J. Chem. Phys. **111**, 5645 (1999).

[24] E. V. Beck, E. A. Stahlberg, L. W. Burggraf and J.-P. Blaudeau, Chem. Phys. **349**, 158 (2008).

[25] Q. Wu, C.-L. Cheng, and T. Van Voorhis, J. Chem. Phys. **127**, 164119 (2007).

[26] Q. Wu, B. Kaduk, and T. Van Voorhis, J. Chem. Phys. **130**, 034109 (2009).

[27] G. C. Lie and E. Clementi, J. Chem. Phys. **60**, 1275 (1974).

[28] G. C. Lie and E. Clementi, J. Chem. Phys. **60**, 1288 (1974).

[29] R. Colle and O. Salvetti, Theor. Chim. Acta **37**, 329 (1975).

[30] R. Colle and O. Salvetti, Theor. Chim. Acta **53**, 55 (1979).

[31] R. Colle and O. Salvetti, J. Chem. Phys. **79**, 1404 (1983).

[32] R. Colle and O. Salvetti, J. Chem. Phys. **93** (1990).

[33] A. Savin, Int. J. Quantum. Chem. **22**, 59 (1988).

[34] A. Savin, J. chim. phys. **86**, 757 (1989).

[35] A. Savin, in *Density functional methods in chemistry*, edited by J. Labanowski and J. Andzelm (Springer-Verlag, New York, 1991), p. 213.

[36] B. Miehlich, H. Stoll and A. Savin, Mol. Phys. **91**, 527 (1997).

[37] C. Gutlé and A. Savin, Phys. Rev. A **75**, 032519 (2007).

[38] F. Moscardo and E. San-Fabian, Int. J. Quantum. Chem. **40**, 23 (1991).

[39] E. Kraka, Chem. Phys. **161**, 141 (1992).

[40] E. Kraka, D. Cremer and S. Nordholm, in *Molecules in Natural Science and Biomedicine*, edited by Z. Maksic and M. Eckert-Maksic (Ellis Horwood, Chichester, 1992), p. 351.

[41] W. Wu and S. Shaik, Chem. Phys. Lett. **301**, 37 (1999).

[42] H. Stoll, Chem. Phys. Lett. **376**, 141 (2003).

[43] F. Ying, P. Su, Z. Chen, S. Shaik and W. Wu, J. Chem. Theory Comput. **8**, 1608 (2012).

[44] N. O. J. Malcolm and J. J. W. McDouall, J. Phys. Chem. **98**, 12579 (1994).

[45] N. O. J. Malcolm and J. J. W. McDouall, J. Phys. Chem. **100**, 10131 (1996).

[46] N. O. J. Malcolm and J. J. W. McDouall, J. Phys. Chem. A **101**, 8119 (1997).

[47] N. O. J. Malcolm and J. J. W. McDouall, Chem. Phys. Lett. **282**, 121 (1998).

[48] J. J. W. McDouall, Mol. Phys. **101**, 361 (2003).

[49] P. Borowski, K. D. Jordan, J. Nichols and P. Nachtigall, Theor. Chem. Acc. **99**, 135 (1998).

[50] J. Grafenstein and D. Cremer, Chem. Phys. Lett. **316**, 569 (2000).

[51] J. Gräfenstein and D. Cremer, Phys. Chem. Chem. Phys. **2**, 2091 (2000).

[52] J. Gräfenstein and D. Cremer, Mol. Phys. **103**, 279 (2005).

[53] R. Takeda, S. Yamanaka and K. Yamaguchi, Chem. Phys. Lett. **366**, 321 (2002).

[54] K. Nakata, T. Ukai, S. Yamanaka, T. Takada and K. Yamaguchi, Int. J. Quantum. Chem. **106**, 3325 (2006).

[55] S. Yamanaka, K. Nakata, T. Ukai, T. Takada and K. Yamaguchi, Int. J. Quantum. Chem. **106**, 3312 (2006).

[56] T. Ukai, K. Nakata, S. Yamanaka, T. Takada and K. Yamaguchi, Mol. Phys. **105**, 2667 (2007).

[57] S. Gusarov, P.-A. Malmqvist, R. Lindh and B. O. Roos, Theor. Chim. Acc. **112**, 84 (2004).

[58] A. J. Pérez-Jiménez and J. M. Pérez-Jordá, Phys. Rev. A **75**, 012503 (2007).

[59] A. J. Pérez-Jiménez, J. M. Pérez-Jordá, I. de P. R. Moreira and F. Illas, J. Comput. Chem. **28**, 2559 (2007).

[60] A. J. Pérez-Jiménez, J. M. Pérez-Jordá and J. C. Sancho-García, J. Chem. Phys. **127**, 104102 (2007).

[61] M. Weimer, F. D. Sala and A. Görling, J. Chem. Phys. **128**, 144109 (2008).

[62] Y. Kurzweil, K. V. Lawler and M. Head-Gordon, Mol. Phys. **107**, 2103 (2009).

[63] A. Savin and H.-J. Flad, Int. J. Quantum. Chem. **56**, 327 (1995).

[64] A. Savin, in *Recent Advances in Density Functional Theory*, edited by D. P. Chong (World Scientific, 1996).

[65] A. Savin, in *Recent Developments of Modern Density Functional Theory*, edited by J. M. Seminario (Elsevier, Amsterdam, 1996), pp. 327–357.

[66] T. Leininger, H. Stoll, H.-J. Werner and A. Savin, Chem. Phys. Lett. **275**, 151 (1997).

[67] R. Pollet, A. Savin, T. Leininger and H. Stoll, J. Chem. Phys. **116**, 1250 (2002).

[68] A. Savin, F. Colonna and R. Pollet, Int. J. Quantum. Chem. **93**, 166 (2003).

[69] J. Toulouse, F. Colonna and A. Savin, Phys. Rev. A **70**, 062505 (2004).

[70] J. K. Pedersen and H. J. A. Jensen, unpublished.

[71] E. Fromager, J. Toulouse and H. J. A. Jensen, J. Chem. Phys. **126**, 074111 (2007).

[72] E. Fromager, F. Réal, P. Wåhlin, U. Wahlgren and H. J. A. Jensen, J. Chem. Phys. **131**, 054107 (2009).

[73] E. Fromager, R. Cimiraglia and H. J. A. Jensen, Phys. Rev. A **81**, 024502 (2010).

[74] T. Tsuchimochi, G. E. Scuseria and A. Savin, J. Chem. Phys. **132**, 024111 (2010).

[75] T. Tsuchimochi and G. E. Scuseria, J. Chem. Phys. **134**, 064101 (2011).

[76] K. Pernal, Phys. Rev. A **81**, 052511 (2010).

[77] D. R. Rohr, J. Toulouse and K. Pernal, Phys. Rev. A **82**, 052502 (2010).

[78] D. R. Rohr and K. Pernal, J. Chem. Phys. **135**, 074104 (2011).

[79] K. Sharkas, J. Toulouse and A. Savin, J. Chem. Phys. **134**, 064113 (2011).

[80] J. G. Ángyán, I. C. Gerber, A. Savin and J. Toulouse, Phys. Rev. A **72**, 012510 (2005).

[81] M. Levy and J. P. Perdew, Phys. Rev. A **32**, 2010 (1985).

[82] M. Levy, W. Yang and R. G. Parr, J. Chem. Phys. **83**, 2334 (1985).

[83] M. Levy, Phys. Rev. A **43**, 4637 (1991).

[84] M. Levy and J. P. Perdew, Phys. Rev. B **48**, 11638 (1993).

[85] A. D. Becke, J. Chem. Phys. **104**, 1040 (1996).

[86] M. Ernzerhof, J. P. Perdew and K. Burke, in *Density Functional Theory*, edited by R. Nalewajski (Springer-Verlag, Berlin, 1996).

[87] E. Fromager and H. J. A. Jensen, Phys. Rev. A **78**, 022504 (2008).

[88] J. G. Ángyán, Phys. Rev. A **78**, 022510 (2008).

[89] S. Grimme, J. Chem. Phys. **124**, 034108 (2006).

[90] C. Angeli, K. L. Bak, V. Bakken, O. Christiansen, R. Cimiraglia, S. Coriani, P. Dahle, E. K. Dalskov, T. Enevoldsen, B. Fernandez, L. Ferrighi, L. Frediani, C. Hättig, K. Hald, A. Halkier, H. Heiberg, T. Helgaker, H. Hettema, B. Jansik, H. J. A. Jensen, D. Jonsson, P. Jørgensen, S. Kirpekar, W. Klopper, S. Knecht, R. Kobayashi, J. Kongsted, H. Koch, A. Ligabue, O. B. Lutnæs, K. V. Mikkelsen, C. B. Nielsen, P. Norman, J. Olsen, A. Osted, M. J. Packer, T. B. Pedersen, Z. Rinkevicius, E. Rudberg, T. A. Ruden, K. Ruud, P. Salek, C. C. M. Samson,

A. S. de Meras, T. Saue, S. P. A. Sauer, B. Schimmelpfennig, A. H. Steindal, K. O. Sylvester-Hvid, P. R. Taylor, O. Vahtras, D. J. Wilson and H.Ågren, DALTON, a molecular electronic structure program, Release DALTON2011 (2011), see http://daltonprogram.org.

[91] J. K. Pedersen, *Description of correlation and relativistic effects in calculations of molecular properties*, PhD thesis, University of Southern Denmark, Odense (2004).

[92] H. J. A. Jensen and P. Jørgensen, J. Chem. Phys. **80**, 1204 (1984).

[93] H. J. A. Jensen and H. Agren, Chem. Phys. Lett. **110**, 140 (1984).

[94] H. J. A. Jensen and H. Agren, Chem. Phys. **104**, 229 (1986).

[95] H. J. A. Jensen, P. Jorgensen and H. Agren, J. Chem. Phys. **87**, 451 (1987).

[96] H. J. A. Jensen, P. Jørgensen, H. Agren and J. Olsen, J. Chem. Phys. **88**, 3834 (1988).

[97] H. J. A. Jensen, in *Relativistic and Electron Correlation Effects in Molecules and Solids*, edited by G. L. Malli (Plenum, New York, 1994), p. 179.

[98] J. P. Perdew, K. Burke and M. Ernzerhof, Phys. Rev. Lett. **77**, 3865 (1996).

[99] A. D. Becke, Phys. Rev. A **38**, 3098 (1988).

[100] C. Lee, W. Yang and R. G. Parr, Phys. Rev. B **37**, 785 (1988).

[101] L. Goerigk and S. Grimme, J. Chem. Theory Comput **6**, 107 (2010).

[102] L. Goerigk and S. Grimme, J. Chem. Theory Comput **7**, 291 (2011).

[103] S. E. Wheeler, D. H. Ess and K. N. Houk, J. Phys. Chem. A **112**, 1798 (2007).

[104] Y. Zhao, O. Tishchenko, J. R. Gour, W. Li, J. J. Lutz, P. Piecuch and D. G. Truhlar, J. Phys. Chem. A **113**, 5786 (2009).

[105] T. Saito, S. Nishihara, Y. Kataoka, Y. Nakanishi, Y. Kitagawa, T. Kawakami, S.Yamanaka, M. Okumura and K. Yamaguchi, J. Phys. Chem. A **114**, 12116 (2010).

[106] T. H. Dunning, J. Chem. Phys. **90**, 1007 (1989).

[107] R. A. Kendall, T. H. Dunning and R. J. Harrison, J. Chem. Phys. **96**, 6796 (1992).

[108] Y. Zhao, N. E. Schultz and D. G. Truhlar, J. Chem. Phys. **123**, 161103 (2005).

[109] R. Krishnan, J. S. Binkley, R. Seeger and J. A. Pople, J. Chem. Phys. **72**, 650 (1980).

[110] A. D. McLean and G. S. Chandler, J. Chem. Phys. **72**, 5639 (1980).

[111] C. Møller and M. S. Plesset, Phys. Rev. **46**, 618 (1934).

[112] K. Hirao, Chem. Phys. Lett. **190**, 374 (1992).

[113] C. Adamo and V. Barone, J. Chem. Phys. **110**, 6158 (1999).

[114] C. Adamo and V. Barone, Chem. Phys. Lett. **298**, 113 (1998).

[115] C. Adamo and V. Barone, Chem. Phys. Lett. **274**, 242 (1997).

[116] A. D. Becke, J. Chem. Phys. **98**, 5648 (1993).

[117] V. Barone and C. Adamo, Chem. Phys. Lett. **224**, 432 (1994).

[118] E. Goll, H.-J. Werner, H. Stoll, T. Leininger, P. Gori-Giorgi and A. Savin, Chem. Phys. **329**, 276 (2006).

[119] J. P. Perdew, M. Ernzerhof and K. Burke, J. Chem. Phys **105**, 9982 (1996).

[120] M. J. Frisch, G. W. Trucks, H. B. Schlegel, G. E. Scuseria, M. A. Robb, J. R. Cheeseman, G. Scalmani, V. Barone, B. Mennucci, G. A. Petersson, H. Nakatsuji, M. Caricato, X. Li, H. P. Hratchian, A. F. Izmaylov, J. Bloino, G. Zheng, J. L. Sonnenberg, M. Hada, M. Ehara, K. Toyota, R. Fukuda, J. Hasegawa, M. Ishida, T. Nakajima, Y. Honda, O. Kitao, H. Nakai, T. Vreven, J. A. Montgomery, Jr., J. E. Peralta, F. Ogliaro, M. Bearpark, J. J. Heyd, E. Brothers, K. N. Kudin, V. N. Staroverov, R. Kobayashi, J. Normand, K. Raghavachari, A. Rendell, J. C. Burant, S. S. Iyengar, J. Tomasi, M. Cossi, N. Rega, J. M. Millam, M. Klene, J. E. Knox, J. B. Cross, V. Bakken, C. Adamo, J. Jaramillo, R. Gomperts, R. E. Stratmann, O. Yazyev, A. J. Austin, R. Cammi, C. Pomelli, J. W. Ochterski, R. L. Martin, K. Morokuma, V. G. Zakrzewski, G. A. Voth, P. Salvador, J. J. Dannenberg, S. Dapprich, A. D. Daniels, Ã. Farkas, J. B. Foresman, J. V. Ortiz, J. Cioslowski and D. J. Fox, Gaussian 09 Revision A.1, Gaussian Inc. Wallingford CT 2009.

[121] J. P. Perdew, A. Savin and K. Burke, Phys. Rev. A **51**, 4531 (1995).

[122] M. J. S. Dewar and J. Kelemen, J. Chem. Educ. **48**, 494 (1971).

[123] H. Iikura, T. Tsuneda, T. Yanai and K. Hirao, J. Chem. Phys. **115**, 3540 (2001).

[124] T. Yanai, D. P. Tew and N. C. Handy, Chem. Phys. Lett. **393**, 51 (2004).

[125] I. C. Gerber and J. G. Ángyán, Chem. Phys. Lett. **415**, 100 (2005).

[126] O. A. Vydrov and G. E. Scuseria, J. Chem. Phys. **125**, 234109 (2006).

[127] J. Heyd, G. E. Scuseria and M. Ernzerhof, J. Chem. Phys. **118**, 8207 (2003).

[128] T. M. Henderson, A. F. Izmaylov, G. E. Scuseria and A. Savin, J. Chem. Phys. **127**, 221103 (2007).

Chapter 4

Double-hybrid density-functional theory made rigorous

This chapter, written in collaboration with J. Toulouse and A. Savin, has been published in Journal of Chemical Physics [J. Chem. Phys. **134**, 064113 (2011)].

4.1 Abstract

We provide a rigorous derivation of a class of double-hybrid approximations, combining Hartree-Fock exchange and second-order Møller-Plesset correlation with a semilocal exchange-correlation density functional. These double-hybrid approximations contain only one empirical parameter and use a density-scaled correlation energy functional. Neglecting density scaling leads to an one-parameter version of the standard double-hybrid approximations. We assess the performance of these double-hybrid schemes on representative test sets of atomization energies and reaction barrier heights, and we compare to other hybrid approximations, including range-separated hybrids. Our best one-parameter double-hybrid approximation, called 1DH-BLYP, roughly reproduces the two parameters of the standard B2-PLYP or B2GP-PLYP double-hybrid approximations, which shows that these models are not only empirically close to an optimum for general chemical applications but are also theoretically supported.

4.2 Introduction

Density-functional theory (DFT) [1–3] is a powerful approach for electronic-structure calculations of atoms, molecules and solids. In its Kohn-Sham (KS) formulation, a series of approximations for the exchange-correlation energy have been developed for an ever-increasing accuracy: local density approximation (LDA), semilocal approximations (generalized-gradient approximations (GGA) and meta-GGA), hybrid approximations introducing Hartree-Fock (HF) exchange, and nonlocal correlation approximations using virtual KS orbitals [4].

In this context, Grimme [5] recently introduced the family of so-called *double-hybrid* (DH) density-functional approximations which mix HF exchange with a semilocal exchange density functional and second-order Møller-Plesset (MP2) correlation with a semilo-

cal correlation density functional:

$$E_{xc}^{\rm DH} = a_x E_x^{\rm HF} + (1-a_x)E_x[n] + (1-a_c)E_c[n] + a_c E_c^{\rm MP2}, \quad (4.1)$$

where the first three terms are calculated in an usual self-consistent hybrid KS calculation, and the last perturbative term evaluated with the previously obtained orbitals is added *a posteriori*. The B2-PLYP double-hybrid approximation [5] is obtained by choosing the Becke 88 (B) exchange functional [6] for $E_x[n]$ and the Lee-Yang-Parr (LYP) correlation functional [7] for $E_c[n]$, and the empirical parameters $a_x = 0.53$ and $a_c = 0.27$ optimized for the G2/97 subset of heats of formation. The mPW2-PLYP double-hybrid approximation [8] uses the modified Perdew-Wang (mPW) exchange functional [9], and has very similar optimized parameters $a_x = 0.55$ and $a_c = 0.25$. These two double-hybrid approximations reach on average near-chemical accuracy for the thermodynamical data of the G3/05 set [8]. Similar double-hybrid approximations have also been obtained by reoptimizing the parameters a_x and a_c for a spin-restricted open-shell version of the method [10] or for different test sets [11, 12]. In particular, targeting both thermochemistry and kinetics applications has given the reoptimized parameters $a_x = 0.65$ and $a_c = 0.36$ which defines the general-purpose B2GP-PLYP double-hybrid approximation [12]. The so-called multicoefficient correlation methods combining HF, DFT and MP2 energies can also be considered to be a form of double-hybrid approximation [13–15], and the connection was made explicit in Ref. [16]. Three- or four-parameter double-hybrid approximations have also been proposed [17–19], scaling differently the LDA and GGA components of the density functionals, in the style of the first hybrid DFT approximations [20]. For systems with van der Waals interactions, good accuracy can be obtained by further adding an empirical dispersion term [21] or by increasing the amount of MP2 correlation at long interelectronic distances [22].

Although the above-mentioned double-hybrid approximations yield very promising results and are already largely used, they suffer from a lack of theoretical justification. It has been tried [17] to motivate these approaches by invoking the adiabatic connection formalism [23] and second-order Görling-Levy perturbation theory (GL2) [24], but several unjustified empirical steps remain (e.g., dropping the single-excitation term in the GL2 expression). On the contrary, the range-separated double-hybrid RSH+lrMP2 method of Ref. [25], which combines long-range HF exchange and long-range MP2 correlation with a short-range exchange-correlation density functional, has been rigorously derived using the formally exact multideterminant extension of the Kohn-Sham scheme based on range separation. In this work, we apply an analogous formalism without range separation which leads to a rigorous derivation of a form of double-hybrid approximation. In this double-hybrid scheme, only one empirical parameter appears, the appropriate correlation energy functional is obtained by uniform coordinate scaling of the density, and the MP2 correlation energy expression appears naturally without the need to neglect single-excitation contributions. We test the proposed double-hybrid scheme on representative sets of atomization energies and reaction barrier heights, and compare with other hybrid approximations.

4.3 Theory

We consider the usual adiabatic connection of DFT linking the non-interacting Kohn-Sham Hamiltonian ($\lambda = 0$) to the exact Hamiltonian ($\lambda = 1$) by linearly switching on the

Coulombic electron-electron interaction $\lambda\hat{W}_{ee}$ [23],

$$\hat{H}^{\lambda} = \hat{T} + \hat{V}_{\rm ext} + \lambda\hat{W}_{ee} + \hat{V}^{\lambda}_{{\rm H}xc}[n], \tag{4.2}$$

where $\hat{T}$ is the kinetic energy operator, $\hat{V}_{\rm ext}$ is a scalar external potential operator (e.g., nuclei-electron), and $\hat{V}^{\lambda}_{{\rm H}xc}[n]$ is the Hartree-exchange-correlation potential operator keeping the one-electron density n constant for all values of the coupling constant $\lambda \geq 0$. Using the formalism of the multideterminant extension of the Kohn-Sham scheme (see, e.g., Refs. [25, 26]), for any λ, the *exact* energy can be expressed as the following minimization over multideterminant wave functions Ψ:

$$E \;=\; \min_{\Psi}\Big\{\langle\Psi|\hat{T} + \hat{V}_{\rm ext} + \lambda\hat{W}_{ee}|\Psi\rangle + \bar{E}^{\lambda}_{{\rm H}xc}[n_{\Psi}]\Big\}, \tag{4.3}$$

where n_{Ψ} is the density coming from Ψ and $\bar{E}^{\lambda}_{{\rm H}xc}[n] = E_{{\rm H}xc}[n] - E^{\lambda}_{{\rm H}xc}[n]$ is the *complement* λ-dependent Hartree-exchange-correlation density functional, i.e. the difference between the usual Kohn-Sham density functional $E_{{\rm H}xc}[n]$ and the λ-dependent density functional $E^{\lambda}_{{\rm H}xc}[n]$ corresponding to the Hamiltonian (6.2). This complement density functional generates the potential in Eq. (6.2) which keeps the density constant: $\hat{V}^{\lambda}_{{\rm H}xc}[n] = \int d\mathbf{r}\,\hat{n}(\mathbf{r})\,\delta\bar{E}^{\lambda}_{{\rm H}xc}[n]/\delta n(\mathbf{r})$, where $\hat{n}(\mathbf{r})$ is the density operator. Since the Hartree and exchange contributions are first order in the electron-electron interaction, their dependence on λ is just linear,

$$\bar{E}^{\lambda}_{\rm H}[n] = (1-\lambda)E_{\rm H}[n], \tag{4.4}$$

$$\bar{E}^{\lambda}_{x}[n] = (1-\lambda)E_{x}[n], \tag{4.5}$$

where $E_{\rm H}[n]$ and $E_x[n]$ are the usual Kohn-Sham Hartree and exchange density functionals. The correlation contribution is not linear in λ but can be obtained by uniform coordinate scaling of the density [27–31],

$$\bar{E}^{\lambda}_{c}[n] \;=\; E_c[n] - E^{\lambda}_c[n] = E_c[n] - \lambda^2 E_c[n_{1/\lambda}], \tag{4.6}$$

where $E_c[n]$ is the usual Kohn-Sham correlation functional, $E^{\lambda}_c[n]$ is the correlation functional corresponding to the Hamiltonian (6.2), and $n_{1/\lambda}(\mathbf{r}) = (1/\lambda)^3 n(\mathbf{r}/\lambda)$ is the scaled density.

To avoid possible confusions with previous work, we note that numerous exchange-correlation functional approximations have been constructed using the adiabatic-connection integral formula (see, e.g., Refs. [32–43]), $E_{xc}[n] = \int_0^1 U_{xc,\alpha}\,d\alpha$ where $U_{xc,\alpha}$ is the integrand (exchange + potential correlation energy) that needs to be approximated. In the same language, the complement exchange-correlation functional used in the present work would write $\bar{E}^{\lambda}_{xc}[n] = \int_{\lambda}^1 U_{xc,\alpha}\,d\alpha$. The confusion is possible because $U_{xc,\alpha}$ has sometimes been called $E_{xc,\alpha}$ in the literature. Although we do not use in practice this adiabatic-connection integral, it should help to clarify that in this work the coupling constant λ is fixed and the complement correlation functional $\bar{E}^{\lambda}_c[n]$ does include a kinetic correlation energy contribution.

We now define a *density-scaled one-parameter hybrid* (DS1H) approximation by restricting the minimization in Eq. (4.3) to single-determinant wave functions Φ:

$$E^{\rm DS1H,\lambda} \;=\; \min_{\Phi}\Big\{\langle\Phi|\hat{T} + \hat{V}_{\rm ext} + \lambda\hat{W}_{ee}|\Phi\rangle + \bar{E}^{\lambda}_{{\rm H}xc}[n_{\Phi}]\Big\}, \tag{4.7}$$

obtaining an energy which necessarily depends on λ. The minimizing single-determinant wave function Φ^λ is calculated by the self-consistent eigenvalue equation:

$$\left(\hat{T} + \hat{V}_{\text{ext}} + \lambda \hat{V}_{\text{H}x}^{\text{HF}}[\Phi^\lambda] + \hat{V}_{\text{H}xc}^{\lambda}[n_{\Phi^\lambda}]\right)|\Phi^\lambda\rangle = \mathcal{E}_0^\lambda |\Phi^\lambda\rangle, \tag{4.8}$$

where $\hat{V}_{\text{H}x}^{\text{HF}}[\Phi^\lambda]$ is the nonlocal HF potential operator evaluated with the DS1H wave function Φ^λ and $\hat{V}_{\text{H}xc}^{\lambda}[n_{\Phi^\lambda}]$ is the previously introduced local Hartree-exchange-correlation potential operator evaluated at the DS1H density n_{Φ^λ}. Evidently, in practice, Eq. (4.8) is decomposed into usual one-particle hybrid KS equations. For simplicity, we will now refer to this DS1H wave function and associated density as just Φ and n, respectively, the λ-dependence being implicit. The DS1H energy is thus finally written as

$$E^{\text{DS1H},\lambda} = \langle\Phi|\hat{T} + \hat{V}_{\text{ext}}|\Phi\rangle + E_{\text{H}}[n] + \lambda E_x^{\text{HF}}[\Phi] + (1-\lambda)E_x[n] + E_c[n] - \lambda^2 E_c[n_{1/\lambda}], \tag{4.9}$$

where the full Coulombic Hartree energy $E_{\text{H}}[n]$ has been recomposed, $E_x^{\text{HF}}[\Phi]$ is the HF exchange energy and in practice density-functional approximations must be used for $E_x[n]$ and $E_c[n]$. In the appendix, we give the explicit formulas for calculating the scaled functional $E_c[n_{1/\lambda}]$ and associated potential for LDA and GGA approximations. Neglecting the density scaling in the correlation functional, $E_c[n_{1/\lambda}] \approx E_c[n]$, in Eq. (4.9) gives an *one-parameter hybrid* (1H) approximation,

$$E^{\text{1H},\lambda} = \langle\Phi|\hat{T} + \hat{V}_{\text{ext}}|\Phi\rangle + E_{\text{H}}[n] + \lambda E_x^{\text{HF}}[\Phi] + (1-\lambda)E_x[n] + (1-\lambda^2)E_c[n], \tag{4.10}$$

which has a similar form than the standard one-parameter hybrid functionals such as B1LYP [44] or PBE1PBE (also known as PBE0) [45, 46], except that the correlation energy in Eq. (4.10) is weighted by $(1-\lambda^2)$ while in the standard one-parameter hybrid functionals it is weighted by a factor of 1.

All what is missing in Eq. (4.9) is the correlation energy associated with the scaled interaction $\lambda\hat{W}_{ee}$. It can be calculated by a nonlinear Rayleigh-Schrödinger perturbation theory [25, 47, 48] starting from the DS1H reference. Consider the following energy expression with the perturbation parameter α:

$$E^{\lambda,\alpha} = \min_{\Psi}\left\{\langle\Psi|\hat{T} + \hat{V}_{\text{ext}} + \lambda\hat{V}_{\text{H}x}^{\text{HF}}[\Phi] + \alpha\lambda\hat{W}|\Psi\rangle + \bar{E}_{\text{H}xc}^{\lambda}[n_\Psi]\right\}, \tag{4.11}$$

where $\lambda\hat{W} = \lambda\left(\hat{W}_{ee} - \hat{V}_{\text{H}x}^{\text{HF}}[\Phi]\right)$ is the scaled Møller-Plesset fluctuation perturbation operator. For $\alpha = 1$, Eq. (4.11) reduces to Eq. (4.3), so $E^{\lambda,\alpha=1}$ is the exact energy, independently of λ. The sum of the zeroth-order energy and first-order energy correction gives simply the DS1H energy, $E^{\text{DS1H},\lambda} = E^{\lambda,(0)} + E^{\lambda,(1)}$. Thanks to the existence of a Brillouin theorem just like in standard Møller-Plesset perturbation theory (see Refs. [25, 47, 48]), only double excitations contribute to the second-order energy correction which has a standard MP2 form,

$$E^{\lambda,(2)} = \lambda^2 \sum_{\substack{i<j \\ a<b}} \frac{|\langle ij||ab\rangle|^2}{\varepsilon_i + \varepsilon_j - \varepsilon_a - \varepsilon_b} = \lambda^2 E_c^{\text{MP2}}, \tag{4.12}$$

where i, j and a, b refer to occupied and virtual DS1H spin-orbitals, respectively, with associated orbital eigenvalues ε_k, and $\langle ij||ab\rangle$ are the antisymmetrized two-electron integrals. Note that the dependence on λ is not simply quadratic since the spin-orbitals and their eigenvalues implicitly depend on λ. Our final *density-scaled one-parameter double-hybrid* (DS1DH) approximation is then obtained by adding the second-order correction to the DS1H energy

$$E^{\mathrm{DS1DH},\lambda} = E^{\mathrm{DS1H},\lambda} + E^{\lambda,(2)}. \tag{4.13}$$

To summarize, the exchange-correlation energy in the DS1DH approximation is

$$E_{xc}^{\mathrm{DS1DH},\lambda} = \lambda E_x^{\mathrm{HF}} + (1-\lambda)E_x[n] + E_c[n] - \lambda^2 E_c[n_{1/\lambda}] + \lambda^2 E_c^{\mathrm{MP2}}. \tag{4.14}$$

To make connection with the standard double-hybrid approximations, we also define an *one-parameter double-hybrid* (1DH) approximation, obtained by neglecting the density scaling in the correlation functional, $E_c[n_{1/\lambda}] \approx E_c[n]$,

$$E_{xc}^{\mathrm{1DH},\lambda} = \lambda E_x^{\mathrm{HF}} + (1-\lambda)E_x[n] + (1-\lambda^2)E_c[n] + \lambda^2 E_c^{\mathrm{MP2}}, \tag{4.15}$$

which exactly corresponds to the double-hybrid approximation of Eq. (6.1) with parameters $a_x = \lambda$ and $a_c = \lambda^2$.

4.4 Computational details

Except for the B2-PLYP calculations which were carried out with GAUSSIAN 09 [49], all other calculations have been performed with a development version of the MOLPRO 2008 program [50], in which the DS1DH and 1DH approximations have been implemented. For $E_x[n]$ and $E_c[n]$, we use the LDA functional [51] and two GGA functionals, Perdew-Burke-Ernzerhof (PBE) [52] and BLYP [6, 7]. For DS1DH approximations, the corresponding density-scaled correlation energy is obtained from the formulas of the appendix. For a given value of the parameter λ, a self-consistent hybrid calculation is first performed and the MP2 correlation energy part calculated with the obtained orbitals is then added. The empirical parameter λ is optimized on the AE6 and BH6 test sets [53]. The AE6 set is a small representative benchmark set of six atomization energies consisting of SiH_4, S_2, SiO, C_3H_4 (propyne), $C_2H_2O_2$ (glyoxal), and C_4H_8 (cyclobutane). The BH6 set is a small representative benchmark set of forward and reverse hydrogen barrier heights of three reactions, OH + CH_4 → CH_3 + H_2O, H + OH → O + H_2, and H + H_2S → HS + H_2. We compute mean errors (MEs) and mean absolute errors (MAEs) as functions of the parameter λ. All the calculations for the AE6 and BH6 sets were performed at the optimized QCISD/MG3 [54, 55] geometries [56]. The best double-hybrid approximations are also compared on larger benchmark sets which consist of the set of 49 atomization energies of Ref. [57] (G2-1 test set [58, 59] except for the six molecules containing Li, Be, and Na) at MP2(full)/6-31G* geometries, and the DBH24/08 test set [15, 60] of 24 forward and reverse reaction barrier heights with QCISD/MG3 geometries. One practical advantage of these benchmark sets is that, as for the AE6 and BH6 sets, they come with reference values with zero-point energies removed and which can therefore be directly compared to the differences of electronic energies. We use the Dunning cc-pVTZ, cc-pVQZ, and aug-cc-pVQZ basis sets [61–64]. Diffuse basis functions are important for

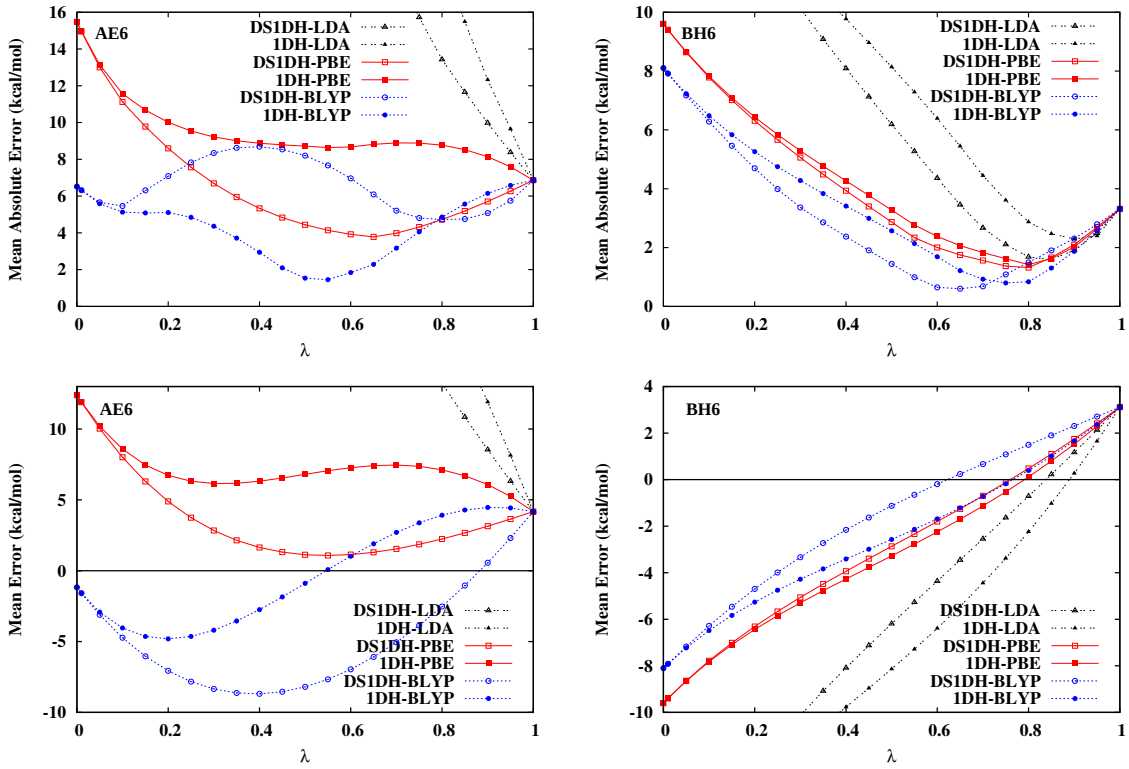

Figure 4.1: (Color online) MAEs and MEs for the AE6 (left) and BH6 (right) test sets as functions of the parameter λ for the 1DH and DS1DH approximations with LDA, PBE, and BLYP exchange-correlation density functionals. All calculations were carried out with the cc-pVQZ basis set.

describing the charged species in the DBH24/08 set. Core electrons are kept frozen in all our MP2 calculations. Spin-restricted calculations are performed for all the closed-shell systems, and spin-unrestricted calculations for all the open-shell systems.

4.5 Results and discussion

Figure 4.5 shows the MAEs and MEs for the AE6 and BH6 test sets as functions of the parameter λ for the DS1DH and 1DH approximations with the LDA, PBE, and BLYP exchange-correlation density functionals. For $\lambda = 0$, each double-hybrid approximation reduces to the corresponding standard Kohn-Sham density-functional approximation. For $\lambda = 1$, all our double-hybrid approximations reduce to MP2 with HF orbitals. The MAEs and MEs at the optimal values of λ which minimize the MAEs on the AE6 and BH6 sets are also reported in Table 4.1, and compared to those obtained with standard HF, LDA, PBE, BLYP, and MP2, as well as with other hybrid approximations.

Let us start by discussing the double-hybrid results for the AE6 atomization energies. Both DS1DH-LDA and 1DH-LDA have a larger MAE than MP2 for all $\lambda < 1$, which makes these double-hybrid approximations of little value. While 1DH-PBE also gives a larger MAE than MP2 for all $\lambda < 1$, DS1DH-PBE is much more accurate than both standard PBE and MP2 near the optimal parameter value of $\lambda = 0.65$. In contrast,

Table 4.1: MAEs and MEs (in kcal/mol) on the AE6 and BH6 test sets for several methods. For the single-hybrid DS1H, 1H, PBE1PBE, and B1LYP approximations and the double-hybrid DS1DH and 1DH approximations, the results are for the optimal values of λ which minimize the MAEs of the AE6 and BH6 sets, separately. For the range-separated hybrids, this is the range-separation parameter μ (in bohr^{-1}) which is optimized. All calculations were carried out with the cc-pVQZ basis set. The reference values [53] are given in the appendix (Table 4.5).

	AE6			BH6		
Method	λ or μ	MAE	ME	λ or μ	MAE	ME
HF		145.1	-145.1		12.2	12.2
LDA		76.9	76.9		18.0	-18.0
PBE		15.5	12.4		9.61	-9.61
BLYP		6.52	-1.18		8.10	-8.10
MP2		6.86	4.17		3.32	3.11
Single-hybrid approximations						
DS1H-LDA	$\lambda = 0.45$	5.90	-5.20	$\lambda = 0.50$	1.62	-1.62
1H-LDA	$\lambda = 0.45$	7.04	1.38	$\lambda = 0.60$	1.98	-0.59
DS1H-PBE	$\lambda = 0.20$	5.18	-3.85	$\lambda = 0.45$	1.00	0.35
1H-PBE	$\lambda = 0.20$	4.43	-2.00	$\lambda = 0.45$	0.97	-0.02
DS1H-BLYP	$\lambda = 0.05$	5.71	-3.72	$\lambda = 0.35$	1.70	-0.15
1H-BLYP	$\lambda = 0.05$	5.62	-3.53	$\lambda = 0.40$	1.80	-0.24
PBE1PBE	$\lambda = 0.30$	5.28	-2.06	$\lambda = 0.55$	1.22	-0.01
B1LYP	$\lambda = 0.05$	5.52	-3.25	$\lambda = 0.45$	1.94	-0.77
B3LYP		2.51	-1.95		4.95	-4.95
RSHX-PBE(GWS)	$\mu = 0.65$	7.78	1.08	$\mu = 0.55$	1.82	-0.33
RSHX-PBE(HSE) = LC-ωPBE	$\mu = 0.40$	4.57	-1.96	$\mu = 0.45$	1.09	-0.25
Double-hybrid approximations						
DS1DH-LDA	no minimum*			$\lambda = 0.85$	1.59	0.22
1DH-LDA	no minimum*			$\lambda = 0.90$	2.29	0.27
DS1DH-PBE	$\lambda = 0.65$	3.78	1.30	$\lambda = 0.80$	1.32	0.48
1DH-PBE	$\lambda = 0.55^{\dagger}$	8.64†	7.06†	$\lambda = 0.80$	1.42	0.12
DS1DH-BLYP	$\lambda = 0.80$	4.73	-2.52	$\lambda = 0.65$	0.60	0.24
1DH-BLYP	$\lambda = 0.55$	1.46	0.07	$\lambda = 0.75$	0.80	-0.18
B2-PLYP		1.39	-1.09		2.21	-2.21
RSH-PBE(GWS)+lrMP2	$\mu = 0.50$	3.48	-1.91	$\mu = 0.70$	1.55	0.73

* There is no minimum for $0 < \lambda < 1$. The global minimum is for $\lambda = 1.0$, i.e. MP2.

† This is a local minimum. The global minimum is for $\lambda = 1.0$, i.e. MP2.

DS1DH-BLYP appears to be less accurate than 1DH-BLYP. On the AE6 set, the latter leads to the smallest MAE among our one-parameter double-hybrid approximations with a minimal MAE of 1.46 kcal/mol for the optimal parameter $\lambda = 0.55$. The B2-PLYP double-hybrid gives a similar MAE of 1.39 kcal/mol (though with a ME farther away from zero). In fact, 1DH-BLYP is just an one-parameter version of the B2-PLYP double hybrid with optimal parameters $a_x = \lambda = 0.55$ and $a_c = \lambda^2 \simeq 0.30$ very close to the original B2-PLYP parameters $a_x = 0.53$ and $a_c = 0.27$.

The fact that neglecting the density scaling in the correlation functional, $E_c[n_{1/\lambda}] \approx E_c[n]$ (i.e., going from Eq. (6.3) to Eq. (6.4)), yields a greater accuracy on the AE6 set for the double-hybrid approximation based on the BLYP functional but worsen the double-hybrid approximation based on the PBE functional can be clarified by looking at the (signed) MEs. It appears that, in both cases, the 1DH approximation always gives a more positive ME in comparison to the DS1DH approximation, at the optimal values of λ, and in fact also for all λ (not shown). Since DS1DH-PBE gives a positive ME (1.30 kcal/mol) at the optimal λ, inherited from the large positive ME of standard PBE (12.4 kcal/mol), it follows that neglecting density scaling makes the ME even more positive (7.06 kcal/mol), thus deteriorating the accuracy of this double hybrid. On the contrary, since DS1DH-BLYP gives a negative ME (2.52 kcal/mol) at the optimal λ, inherited from the negative ME of standard BLYP (-1.18 kcal/mol), neglecting density scaling makes the ME vary in the right direction, reaching a ME of 0.07 kcal/mol and also improving the MAE.

Let us consider now the double-hybrid results for the BH6 barrier heights. The MAE curves of all the DS1DH and 1DH approximations now display a marked minimum at an intermediate value of λ, thus improving upon both the corresponding standard Kohn-Sham density-functional approximations and MP2. In comparison to AE6, the minimal MAEs for the BH6 set are obtained for larger values of λ, from 0.65 to 0.90, which is consistent with the commonplace experience that a larger fraction of HF exchange improves barrier heights (by decreasing the self-interaction error). For this BH6 set, the DS1DH approximations are found to give smaller MAEs than the 1DH approximations for all the three density-functional approximations tested here. The best double-hybrid approximation is DS1DH-BLYP with a minimal MAE of 0.60 kcal/mol at $\lambda = 0.65$. The B2-PLYP double-hybrid gives a larger MAE of 2.21 kcal/mol, but it has not been optimized for barrier heights.

For each of our three best one-parameter double-hybrid approximations, we have also determined a global optimal value of λ which minimizes the total MAE of the combined AE6+BH6 set, and which could be used in general applications: $\lambda = 0.65$ for DS1DH-PBE giving a total MAE of 2.77 kcal/mol, $\lambda = 0.70$ for DS1DH-BLYP giving a total MAE of 2.94 kcal/mol, and $\lambda = 0.65$ for 1DH-BLYP giving a total MAE of 1.75 kcal/mol. Note that the optimal fractions of HF exchange and MP2 correlation in 1DH-BLYP, $a_x = \lambda = 0.65$ and $a_c = \lambda^2 \approx 0.42$, roughly reproduce the two parameters of the B2GP-PLYP double hybrid, i.e. $a_x = 0.65$ and $a_c = 0.36$.

For comparison, we have also reported in Table 4.1 the MAEs and MEs obtained with the single-hybrid DS1H and 1H approximations, as well as the usual single-hybrid functionals PBE1PBE [45, 46] and B1LYP [44], both with reoptimization of the fraction of HF exchange λ, and the standard B3LYP functional [20, 65, 66] without reoptimization of the parameters. We have also considered range-separated single-hybrid functionals (also known as long-range corrected functionals [67]), here referred to as RSHX as in Ref. [68],

with two short-range exchange PBE functionals, the Goll-Werner-Stoll (GWS) one [69, 70] (which is a modified version of the one of Ref. [71]) and the Heyd-Scuseria-Ernzerhof (HSE) one [72]. For notational consistency, we refer to these two range-separated single-hybrid functionals as RSHX-PBE(GWS) and RSHX-PBE(HSE), respectively, although RSHX-PBE(HSE) is in fact known in the literature as LC-ωPBE [73]. In the case of range separation, this is the (nonlinear) inverse range parameter μ which plays the role of λ and which is optimized. The single hybrids DS1H-PBE and 1H-PBE give very similar results than PBE1PBE. The same is true for DS1H-BLYP and 1H-BLYP in comparison with B1LYP. It appears that PBE1PBE is less accurate than DS1DH-PBE on the AE6 set and about as accurate on the BH6 set. The single hybrids B1LYP and B3LYP are also found to be significantly less accurate than the best one-parameter double-hybrid approximation constructed with the BLYP functional, namely 1DH-BLYP, on both the AE6 and BH6 sets. RSHX-PBE(HSE) gives slightly smaller MAEs than PBE1PBE, but it is still less accurate than DS1DH-PBE on the AE6 set and only slightly more accurate on the BH6 set. Quite unexpectedly, RSHX-PBE(GWS) is much less accurate than PBE1PBE, which points to a weakness of the short-range exchange PBE functional of Ref. [70], at least when combined with the standard (full-range) correlation PBE functional. All these results globally confirm the greater potentiality of double hybrids over single hybrids.

Table 4.2: MAEs and MEs (in kcal/mol) on the AE6 and BH6 test sets for the DS1DH-PBE and RSH-PBE(GWS)+lrMP2 approximations with the cc-pVTZ and cc-pVQZ basis sets. The results are for the optimal values of λ or μ which minimize the MAEs of the AE6 and BH6 sets, separately.

		AE6			BH6		
Method	basis	λ or μ	MAE	ME	λ or μ	MAE	ME
DS1DH-PBE	cc-pVTZ	$\lambda = 0.60$	3.91	-3.71	$\lambda = 0.75$	1.15	0.02
	cc-pVQZ	$\lambda = 0.65$	3.78	1.30	$\lambda = 0.80$	1.32	0.48
RSH-PBE(GWS)+lrMP2	cc-pVTZ	$\mu = 0.50$	4.72	-3.84	$\mu = 0.70$	1.45	0.78
	cc-pVQZ	$\mu = 0.50$	3.48	-1.91	$\mu = 0.70$	1.55	0.73

We discuss now the results obtained with the range-separated double-hybrid approach of Ref. [25], using the short-range exchange-correlation PBE functional of Ref. [70], referred to as RSH-PBE(GWS)+lrMP2. For the AE6 set, we obtain an optimal value of $\mu = 0.50$ bohr^{-1}, corresponding to the value actually used in previous studies [25, 74–78], and a minimal MAE of 3.48 kcal/mol. This value is only marginally better than the MAE of the DS1DH-PBE double hybrid, 3.78 kcal/mol. For the BH6 set, the optimal value $\mu = 0.70$ corresponds to a larger range treated by HF exchange and MP2 correlation, and the minimal MAE of 1.55 kcal/mol is again very similar to the MAE of DS1DH-PBE, 1.32 kcal/mol. This suggests that standard double hybrids and range-separated double hybrids can be comparably accurate for atomization energies and barrier heights, provided that similar density-functional approximations are used. However, range-separated double hybrids have the advantage of having a much weaker basis dependence. This is shown in Table 4.2 which reports the MAEs and MEs on the AE6 and BH6 sets for the DS1DH-PBE and RSH-PBE(GWS)+lrMP2 approximations using the cc-pVTZ and cc-pVQZ basis sets. The basis dependence is clearly seen on the MEs. The absolute differences in MEs between the two basis sets for DS1DH-PBE, 5.01 kcal/mol and 0.46 kcal/mol for AE6 and BH6, respectively, are far greater than those of RSH-PBE(GWS)+lrMP2, 1.93 kcal/mol and 0.05 kcal/mol for AE6 and BH6, respectively. Notice that, for AE6, because the ME

of DS1DH-PBE changes sign when going from the cc-pVTZ to the cc-pVQZ basis, the variation of the corresponding MAE turns out to be fortuitously small, and so at first glance this hides the large basis dependence of DS1DH-PBE. Note also that the optimal value of the parameter λ is more dependent on the basis than the range-separation parameter μ. For RSH-PBE(GWS)+lrMP2, we have determined a global optimal value of $\mu = 0.58$ which minimizes the total MAE of the combined AE6+BH6 set, giving a total MAE of 2.63 kcal/mol. In the appendix, the MAEs and MEs at the optimal values of λ are recalculated using more recent reference energy values (Table 4.5) [79] and reported in Table 4.6. The small deviation between the reference values used in the Tables 4.1 and 4.6 does not affect the aforementioned conclusions.

Finally, we compare our best one-parameter double-hybrid approximation 1DH-BLYP (with the optimal parameter $\lambda = 0.65$), the standard double hybrid B2-PLYP and the range-separated double hybrid RSH-PBE(GWS)+lrMP2 (with the optimal parameter $\mu = 0.58$) on larger benchmark sets, the 49 atomization energies of the set of Ref. [57] (Table 4.3) and the DBH24/08 set of 24 reaction barrier heights (Table 4.4). For the set of atomization energies in Table 4.3, 1DH-BLYP is somewhat more accurate than B2-PLYP, with a slightly smaller MAE (1.4 vs. 1.6 kcal/mol) and a significantly smaller ME (0.3 vs. -1.0 kcal/mol). By contrast, the range-separated double hybrid RSH-PBE(GWS)+lrMP2 gives a MAE as large as 6.5 kcal/mol. This is most likely due to the fact that the short-range exchange-correlation functional used is based on PBE. Indeed, the previous results for the AE6 set (Table 4.1) show that PBE is a much less accurate functional than BLYP for atomization energies. Unfortunately, there is no short-range exchange-correlation functional based on BLYP available yet. In fact, it is a practical advantage of the double hybrids without range separation that do not require development of new density functional approximations. The range-separated coupled-cluster calculations on an extension of the G2/97 set of atomization energies by Goll *et al.* [70] show that a better accuracy can be reached by using a short-range exchange-correlation functional based on the TPSS functional [80]. For the reaction barrier heights of Table 4.4, 1DH-BLYP is on average more accurate than B2-PLYP, with a smaller MAE (1.4 vs. 2.0 kcal/mol) and an even smaller ME (-0.8 vs. -1.8 kcal/mol). The range-separated double hybrid RSH-PBE(GWS)+lrMP2 performs about equally well for the barrier heights, with a MAE of 2.1 kcal/mol and a ME of 1.1 kcal/mol.

4.6 Conclusions

We have rigorously derived a class of double-hybrid approximations, combining HF exchange and MP2 correlation with a semilocal exchange-correlation density functional. These double-hybrid approximations contain only one empirical parameter and uses a density-scaled correlation energy functional. Neglecting density scaling leads to an one-parameter version of the standard double-hybrid approximations. Calculations on the representative test set of atomization energies AE6 show that in practice neglecting density scaling in an approximate functional can either make the double-hybrid method less accurate (case of PBE) or more accurate (case of BLYP). Neglecting density scaling always leads to a less accurate double-hybrid method on the representative test set of reaction barrier heights BH6, for all the density-functional approximations tested here. Our best one-parameter double-hybrid approximation, 1DH-BLYP, roughly reproduces the two pa-

Table 4.3: Atomization energies (in kcal/mol) of the 49 molecules of the set of Ref. [57] (G2-1 test set except for the six molecules containing Li, Be, and Na). The calculated values were obtained using the double hybrids 1DH-BLYP and B2-PLYP, and the range-separated double hybrid RSH-PBE(GWS)+lrMP2 with the cc-pVQZ basis set and MP2(full)/6-31G* geometries. The results are for the optimal value of $\lambda = 0.65$ for 1DH-BLYP and the optimal value of $\mu = 0.58$ for RSH-PBE(GWS)+lrMP2 which minimize the total MAE of the combined AE6+BH6 set. The zero-point energies are removed in the reference values. For each method, the value with the largest error is indicated in boldface. The reference energy values were taken from Ref. [57]

Molecule	1DH-BLYP	B2-PLYP	RSH-PBE(GWS)+lrMP2	Reference
CH	83.12	83.70	78.38	84.00
CH_2 ($^3B_1$)	190.61	190.57	190.19	190.07
CH_2 ($^1A_1$)	178.51	178.84	170.26	181.51
CH_3	307.74	307.90	302.91	307.65
CH_4	419.70	419.19	410.84	420.11
NH	83.83	84.89	81.09	83.67
NH_2	183.02	183.94	177.12	181.90
NH_3	297.74	297.69	288.76	297.90
OH	106.64	106.43	104.49	106.60
OH_2	231.43	229.81	225.48	232.55
FH	140.47	139.00	137.20	141.05
SiH_2 ($^1A_1$)	151.11	151.77	143.21	151.79
SiH_2 ($^3B_1$)	131.56	131.78	133.05	131.05
SiH_3	226.10	226.67	220.05	227.37
SiH_4	321.41	321.95	311.89	322.40
PH_2	153.32	154.80	146.37	153.20
PH_3	239.45	240.73	229.18	242.55
SH_2	180.83	180.58	174.18	182.74
ClH	105.69	105.01	101.63	106.50
HCCH	406.96	404.45	399.05	405.39
H_2CCH_2	563.66	562.15	554.55	563.47
H_3CCH_3	711.68	710.22	701.94	712.80
CN	180.09	179.61	172.93	180.58
HCN	316.61	314.12	305.21	313.20
CO	261.67	258.28	254.60	259.31
HCO	282.86	280.62	277.00	278.39
H_2CO	376.06	373.56	367.85	373.73
H_3COH	512.96	510.38	505.00	512.90
N_2	231.77	229.24	218.09	228.46
H_2NNH_2	439.16	438.77	428.92	438.60
NO	156.75	155.04	151.17	155.22
O_2	125.03	122.71	119.73	119.99
HOOH	268.15	265.44	259.77	268.57
F_2	38.01	36.29	31.64	38.20
CO_2	**396.70**	391.23	390.46	389.14
Si_2	71.33	70.58	67.21	71.99
P_2	116.60	115.84	107.27	117.09
S_2	103.29	102.27	100.90	101.67
Cl_2	56.89	55.48	54.19	57.97
SiO	193.94	190.82	185.82	192.08
SC	171.31	168.86	163.07	171.31
SO	127.14	125.33	122.46	125.00
ClO	62.63	62.70	60.81	64.49
ClF	61.37	59.85	57.94	61.36
Si_2H_6	528.92	529.02	**517.07**	530.81
CH_3Cl	394.30	392.62	388.23	394.64
CH_3SH	472.15	470.71	463.90	473.84
HOCl	164.43	162.27	158.46	164.36
SO_2	257.24	**251.10**	244.46	257.86
MAE	1.4	1.6	6.5	
ME	0.3	-1.0	-6.4	

Table 4.4: Forward (F) and reverse (R) reaction barrier heights (in kcal/mol) that constitute the DBH24/08 test set. The calculated values were obtained using the double hybrids 1DH-BLYP and B2-PLYP, and the range-separated double hybrid RSH-PBE(GWS)+lrMP2 with the aug-cc-pVQZ basis set and QCISD/MG3 geometries. The results are for the optimal value of $\lambda = 0.65$ for 1DH-BLYP and the optimal value of $\mu = 0.58$ for RSH-PBE(GWS)+lrMP2 which minimize the total MAE of the combined AE6+BH6 set. The zero-point energies are removed in the reference values. For each method, the value with the largest error is indicated in boldface.

Reactions	1DH-BLYP	B2-PLYP	RSH-PBE(GWS)+lrMP2	Reference[a]
	F/R	F/R	F/R	F/R
Heavy-atom transfer				
$H+N_2O \rightarrow OH + N_2$	19.15/**77.74**	16.53/**77.02**	19.34/**77.14**	17.13/82.47
$H+ClH \rightarrow HCl + H$	17.26/17.26	15.94/15.94	19.77/19.77	18.00/18.00
$CH_3+FCl \rightarrow CH_3F + Cl$	5.29/58.78	3.02/56.24	8.22/64.21	6.75/60.00
Nucleophilic substitution				
$Cl^{-}\cdots CH_3Cl \rightarrow ClCH_3\cdots Cl^{-}$	11.55/11.55	10.76/10.76	15.4/15.4	13.41/13.41
$F^{-}\cdots CH_3Cl \rightarrow FCH_3\cdots Cl^{-}$	2.20/27.25	1.59/27.01	4.72/31.46	3.44/29.42
$OH^{-}+CH_3F \rightarrow HOCH_3 + F^{-}$	-3.51/16.04	-3.68/15.9	-1.59/21.58	-2.44/17.66
Unimolecular and association				
$H+N_2 \rightarrow HN_2$	14.63/10.33	12.29/10.5	14.04/13.1	14.36/10.61
$H+C_2H_4 \rightarrow CH_3CH_2$	2.96/43.04	1.77/42.53	2.701/45.76	1.72/41.75
$HCN \rightarrow HNC$	49.34/33.39	48.65/33.35	48.52/34.81	48.07/32.82
Hydrogen transfer				
$OH+ CH_4 \rightarrow CH_3 + H_2O$	4.68/18.54	4.26/17.1	6.03/19.75	6.70/19.60
$H + OH \rightarrow O + H_2$	9.96/10.8	8.06/9.72	13.44/10.03	10.10/13.10
$H+ H_2S \rightarrow H_2 + HS$	2.82/16.53	1.85/16.65	4.73/15.35	3.60/17.30
MAE	1.4	2.0	2.1	
ME	-0.8	-1.8	1.1	

[a]From Ref. [15].

rameters of the standard B2-PLYP or B2GP-PLYP double-hybrid approximations, which shows that these models are not only empirically close to an optimum for general chemical applications but are also theoretically supported. More intensive tests on larger benchmark sets of atomization energies and reaction barrier heights confirm that the double hybrid 1DH-BLYP with a fraction of HF exchange of $\lambda = 0.65$ can reach on average near-chemical accuracy for these properties.

The range-separation double hybrid RSH+lrMP2 using the short-range exchange-correlation PBE functional of Ref. [70] is competitive with the best global double hybrids for reaction barrier heights but gives larger errors for atomization energies. Nevertheless, the range-separated double hybrids have the advantage of a weaker basis dependence and a correct long-range behavior (important, e.g., for van der Waals interactions). One could try to improve the performance of the range-separated double hybrids for thermochemistry by either using better short-range exchange-correlation functionals (such as in Ref. [81]), or combining them with global double hybrids in a similar way as done for exchange in the CAM-B3LYP approximation [82].

Beside providing a rigorous derivation of the double-hybrid approximations, the formalism used in this work also paves the way toward other rigorous formulation of double-hybrid methods, replacing the MP2 part by some other approaches. For example, using the

random phase approximation would generate a hybrid method similar to the one proposed in Ref. [83], or using a configuration-interaction or multiconfiguration self-consistent-field approach would lead to a hybrid method capable of dealing with static electron correlation, in a similar but alternative way to the range-separated approaches [84–86].

Acknowledgments

K.S. would like to thank Prof. I. Othman (AEC) for his support. J.T. and A.S. acknowledge ANR (contract Wademecom 07-BLAN-0272). We also thank J. G. Ángyán for discussions.

4.7 Appendix

4.7.1 Density-scaled correlation energy and potential

In this appendix, we give explicit expressions for the density-scaled correlation energy functional which appears in Eq. (6.3)

$$E_c^\lambda[n] = \lambda^2 E_c[n_{1/\lambda}], \tag{4.16}$$

and its associated potential

$$v_c^\lambda[n](\mathbf{r}) = \frac{\delta E_c^\lambda[n]}{\delta n(\mathbf{r})}. \tag{4.17}$$

4.7.1.1 Density-scaled local-density approximations

For local-density approximations (LDA),

$$E_{c,\mathrm{LDA}}[n] = \int e_c(n(\mathbf{r}))d\mathbf{r}, \tag{4.18}$$

where e_c is the energy density, the density-scaled correlation energy is obtained as

$$\begin{aligned} E_{c,\mathrm{LDA}}^\lambda[n] &= \lambda^2 \int e_c\left(n_{1/\lambda}(\mathbf{r})\right) d\mathbf{r} \\ &= \lambda^2 \int e_c\left(n(\mathbf{r}/\lambda)/\lambda^3\right) d\mathbf{r} \\ &= \lambda^5 \int e_c\left(n(\mathbf{r})/\lambda^3\right) d\mathbf{r}, \end{aligned} \tag{4.19}$$

where the coordinate transformation $\mathbf{r} \to \lambda\mathbf{r}$ has been used. The associated potential is simply

$$v_{c,\mathrm{LDA}}^\lambda[n](\mathbf{r}) = \lambda^2 \frac{de_c}{dn}\left(n(\mathbf{r})/\lambda^3\right). \tag{4.20}$$

4.7.1.2 Density-scaled generalized-gradient approximations

For generalized-gradient approximations (GGA), usually written as a function of the density and the square of density gradient norm $|\nabla_{\mathbf{r}} n(\mathbf{r})|^2$,

$$E_{c,\mathrm{GGA}}[n] = \int e_c\left(n(\mathbf{r}), |\nabla_{\mathbf{r}} n(\mathbf{r})|^2\right) d\mathbf{r}, \tag{4.21}$$

the density-scaled correlation energy is

$$\begin{aligned} E^{\lambda}_{c,\mathrm{GGA}}[n] &= \lambda^2 \int e_c\left(n_{1/\lambda}(\mathbf{r}), \left|\nabla_{\mathbf{r}} n_{1/\lambda}(\mathbf{r})\right|^2\right) d\mathbf{r}, \\ &= \lambda^2 \int e_c\left(n(\mathbf{r}/\lambda)/\lambda^3, |\nabla_{\mathbf{r}} n(\mathbf{r}/\lambda)|^2/\lambda^6\right) d\mathbf{r}, \\ &= \lambda^5 \int e_c\left(n(\mathbf{r})/\lambda^3, |\nabla_{\mathbf{r}} n(\mathbf{r})|^2/\lambda^8\right) d\mathbf{r}, \end{aligned} \tag{4.22}$$

where the coordinate transformation $\mathbf{r} \to \lambda\mathbf{r}$, and consequently $\nabla_{\mathbf{r}} \to \nabla_{\lambda\mathbf{r}} = \nabla_{\mathbf{r}}/\lambda$, has been used. The associated potential is

$$v^{\lambda}_{c,\mathrm{GGA}}[n](\mathbf{r}) = \lambda^2 \frac{\partial e_c}{\partial n}\left(n(\mathbf{r})/\lambda^3, |\nabla_{\mathbf{r}} n(\mathbf{r})|^2/\lambda^8\right) - 2\nabla_{\mathbf{r}} \cdot \left[\frac{1}{\lambda^3}\frac{\partial e_c}{\partial |\nabla n|^2}\left(n(\mathbf{r})/\lambda^3, |\nabla_{\mathbf{r}} n(\mathbf{r})|^2/\lambda^8\right)\nabla_{\mathbf{r}} n(\mathbf{r})\right]. \tag{4.23}$$

The same scaling relations apply for spin-dependent functionals $E_c[n_\uparrow, n_\downarrow]$, i.e. the scaling of the spin densities $n_\uparrow$ and $n_\downarrow$ is the same as the scaling of the total density n, and the scaling of the spin-density gradients $|\nabla n_\uparrow|^2$, $|\nabla n_\downarrow|^2$, and $\nabla n_\uparrow \cdot \nabla n_\downarrow$ is the same as the scaling of total density gradient $|\nabla n|^2$.

4.7.2 Theoretical reference values for the AE6 and BH6 test sets

Table 4.5: Theoretical reference values for the test sets AE6 and BH6 in kcal/mol

	Lynch-Truhlar[a]	Haunschild-Klopper[b]
AE6		
SiH_4	322.40	324.59 ±0.30
SiO	192.08	192.35 ±0.53
S_2	101.67	103.22 ±0.37
C_3H_4 (propyne)	704.79	701.44 ±0.39
$C_2H_2O_2$ (glyoxal)	633.35	632.44 ±0.67
C_4H_8 (cyclobutane)	1149.01	1145.36 ±0.74
BH6		
$OH + CH_4 \rightarrow CH_3 + H_2O$	6.7	6.36 ±0.09
$CH_3 + H_2O \rightarrow OH + CH_4$	20.2	19.43 ±0.16
$H + OH \rightarrow O + H_2$	10.1	10.71 ±0.14
$O + H_2 \rightarrow H + OH$	13.1	13.12 ±0.12
$H + H_2S \rightarrow HS + H_2$	3.6	3.8 ±0.05
$HS + H_2 \rightarrow H + H_2S$	17.4	17.28 ±0.09

[a]From Ref. [53].
[b]From Ref. [79].

Table 4.6: MAEs and MEs (in kcal/mol) on the AE6 and BH6 test sets for several methods. For the single-hybrid DS1H, 1H, PBE1PBE, and B1LYP approximations and the double-hybrid DS1DH and 1DH approximations, the results are for the optimal values of λ which minimize the MAEs of the AE6 and BH6 sets, separately. For the range-separated hybrids, this is the range-separation parameter μ (in bohr^{-1}) which is optimized. All calculations were carried out with the cc-pVQZ basis set. The reference values were taken from Ref. [79].

	AE6			BH6		
Method	λ or μ	MAE	ME	λ or μ	MAE	ME
HF		144.4	-144.4		12.3	12.3
LDA		77.6	77.6		17.9	-17.9
PBE		16.9	13.0		9.54	-9.54
BLYP		5.94	-0.53		8.04	-8.04
MP2		8.24	4.82		3.34	3.18
Single-hybrid approximations						
DS1H-LDA	$\lambda = 0.45$	6.47	-4.55	$\lambda = 0.50$	1.67	-1.55
1H-LDA	$\lambda = 0.45$	8.00	2.03	$\lambda = 0.65$	2.10	-1.00
DS1H-PBE	$\lambda = 0.20$	4.67	-3.20	$\lambda = 0.45$	0.92	0.42
1H-PBE	$\lambda = 0.20$	5.90	-1.36	$\lambda = 0.45$	0.94	0.05
DS1H-BLYP	$\lambda = 0.05$	4.84	-3.07	$\lambda = 0.35$	1.78	-0.09
1H-BLYP	$\lambda = 0.05$	4.73	-2.90	$\lambda = 0.40$	1.88	-0.18
PBE1PBE	$\lambda = 0.30$	6.44	-1.41	$\lambda = 0.55$	1.20	0.05
B1LYP	$\lambda = 0.05$	4.61	-2.60	$\lambda = 0.45$	2.03	-0.71
B3LYP		1.97	-1.30		4.88	-4.88
RSHX-PBE(GWS)	$\mu = 0.65$	9.73	1.73	$\mu = 0.55$	1.85	-0.26
RSHX-PBE(HSE) = LC-ωPBE	$\mu = 0.45$	5.91	-3.42	$\mu = 0.45$	0.91	-0.14
Double-hybrid approximations						
DS1DH-LDA	no minimum*			$\lambda = 0.85$	1.51	0.29
1DH-LDA	no minimum*			$\lambda = 0.90$	2.21	0.34
DS1DH-PBE	$\lambda = 0.65$	5.25	1.95	$\lambda = 0.75$	1.14	-0.05
1DH-PBE	$\lambda = 0.55^{\dagger}$	10.1†	7.71†	$\lambda = 0.80$	1.34	0.18
DS1DH-BLYP	$\lambda = 0.75$	4.37	-3.21	$\lambda = 0.65$	0.36	0.31
1DH-BLYP	$\lambda = 0.55$	1.77	0.72	$\lambda = 0.75$	0.51	-0.11
B2-PLYP		1.72	-0.44		2.14	-2.14
RSH-PBE(GWS)+lrMP2	$\mu = 0.58$	3.38	-2.79	$\mu = 0.58$	1.42	-0.2

* There is no minimum for $0 < \lambda < 1$. The global minimum is for $\lambda = 1.0$, i.e. MP2.

† This is a local minimum. The global minimum is for $\lambda = 1.0$, i.e. MP2.

Bibliography

[1] P. Hohenberg and W. Kohn, Phys. Rev. **136**, B 864 (1964).

[2] W. Kohn and L. J. Sham, Phys. Rev. **140**, A1133 (1965).

[3] W. Kohn, Rev. Mod. Phys. **71**, 1253 (1999).

[4] S. Kümmel and L. Kronik, Rev. Mod. Phys. **80**, 3 (2008).

[5] S. Grimme, J. Chem. Phys. **124**, 034108 (2006).

[6] A. D. Becke, Phys. Rev. A **38**, 3098 (1988).

[7] C. Lee, W. Yang and R. G. Parr, Phys. Rev. B **37**, 785 (1988).

[8] T. Schwabe and S. Grimme, Phys. Chem. Chem. Phys. **8**, 4398 (2006).

[9] C. Adamo and V. Barone, J. Chem. Phys. **108**, 664 (1998).

[10] D. C. Graham, A. S. Menon, L. Goerigk, S. Grimme and L. Radom, J. Phys. Chem. A **113**, 9861 (2009).

[11] A. Tarnopolsky, A. Karton, R. Sertchook, D. Vuzman and J. M. L. Martin, J. Phys. Chem. A **112**, 3 (2008).

[12] A. Karton, A. Tarnopolsky, J.-F. Lamére, G. C. Schatz and J. M. L. Martin, J. Phys. Chem. A **112**, 12868 (2008).

[13] Y. Zhao, B. J. Lynch and D. G. Truhlar, J. Phys. Chem. A **108**, 4786 (2004).

[14] Y. Zhao, B. J. Lynch and D. G. Truhlar, Phys. Chem. Chem. Phys. **7**, 43 (2005).

[15] J. Zheng, Y. Zhao and D. G. Truhlar, J. Chem. Theory Comput. **5**, 808 (2009).

[16] J. C. Sancho-García and A. J. Pérez-Jiménez, J. Chem. Phys. **131**, 084108 (2009).

[17] Y. Zhang, X. Xu and W. A. Goddard III, Proc. Natl. Acad. Sci. U.S.A. **106**, 4963 (2009).

[18] I. Y. Zhang, Y. Luo and X. Xu, J. Chem. Phys. **132**, 194105 (2010).

[19] I. Y. Zhang, Y. Luo and X. Xu, J. Chem. Phys. **133**, 104105 (2010).

[20] A. D. Becke, J. Chem. Phys. **98**, 5648 (1993).

[21] T. Schwabe and S. Grimme, Phys. Chem. Chem. Phys. **9**, 3397 (2007).

[22] T. Benighaus, R. A. DiStasio Jr., R. C. Lochan, J.-D. Chai and M. Head-Gordon, J. Phys. Chem. A **112**, 2702 (2008).

[23] J. Harris, Phys. Rev. A **29**, 1648 (1984).

[24] A. Görling and M. Levy, Phys. Rev. B **47**, 13105 (1993).

[25] J. G. Ángyán, I. C. Gerber, A. Savin and J. Toulouse, Phys. Rev. A **72**, 012510 (2005).

[26] J. Toulouse, F. Colonna and A. Savin, Phys. Rev. A **70**, 062505 (2004).

[27] M. Levy and J. P. Perdew, Phys. Rev. A **32**, 2010 (1985).

[28] M. Levy, W. Yang and R. G. Parr, J. Chem. Phys. **83**, 2334 (1985).

[29] M. Levy, Phys. Rev. A **43**, 4637 (1991).

[30] M. Levy, *The Single-Particle Density in Physics and Chemistry, eds. N.H. March and B.M. Deb* (Academic Press, London, 1987).

[31] M. Levy and J. P. Perdew, Phys. Rev. B **48**, 11638 (1993).

[32] A. D. Becke, J. Chem. Phys. **98**, 1372 (1993).

[33] M. Levy, N. H. March and N. C. Handy, J. Chem. Phys. **104**, 1989 (1996).

[34] M. Ernzerhof, Chem. Phys. Lett. **263**, 499 (1996).

[35] O. V. Gritsenko, R. van Leeuwen, and E. J. Baerends, Int. J. Quantum Chem.: Quantum Chem. Symp. **30**, 1375 (1996).

[36] K. Burke, M. Ernzerhof and J. P. Perdew, Chem. Phys. Lett. **265**, 115 (1997).

[37] M. Ernzerhof, J. P. Perdew and K. Burke, Int. J. Quantum Chem. **64**, 285 (1997).

[38] M. Seidl, J. P. Perdew and M. Levy, Phys. Rev. A **59**, 51 (1999).

[39] A. Seidl, J. P. Perdew and S. Kurth, Phys. Rev. A **62**, 012502 (2000).

[40] M. Siedl, J. P. Perdew and S. Kurth, Phys. Rev. Lett. **84**, 5070 (2000).

[41] P. Mori-Sánchez, A. J. Cohen and W. Yang, J. Chem. Phys. **124**, 091102 (2006).

[42] A. J. Cohen, P. Mori-Sánchez and W. Yang, J. Chem. Phys. **126**, 191109 (2007).

[43] A. J. Cohen, P. Mori-Sánchez and W. Yang, J. Chem. Phys. **127**, 034101 (2007).

[44] C. Adamo and V. Barone, Chem. Phys. Lett. **274**, 242 (1997).

[45] M. Ernzerhof and G. E. Scuseria, J. Chem. Phys. **110**, 5029 (1999).

[46] C. Adamo and V. Barone, J. Chem. Phys. **101**, 6158 (1999).

[47] E. Fromager and H. J. A. Jensen, Phys. Rev. A **78**, 022504 (2008).

[48] J. G. Ángyán, Phys. Rev. A **78**, 022510 (2008).

[49] M. J. Frisch, G. W. Trucks, H. B. Schlegel, G. E. Scuseria, M. A. Robb, J. R. Cheeseman, G. Scalmani, V. Barone, B. Mennucci, G. A. Petersson, H. Nakatsuji, M. Caricato, X. Li, H. P. Hratchian, A. F. Izmaylov, J. Bloino, G. Zheng, J. L. Sonnenberg, M. Hada, M. Ehara, K. Toyota, R. Fukuda, J. Hasegawa, M. Ishida, T. Nakajima, Y. Honda, O. Kitao, H. Nakai, T. Vreven, J. A. Montgomery, Jr., J. E. Peralta, F. Ogliaro, M. Bearpark, J. J. Heyd, E. Brothers, K. N. Kudin, V. N. Staroverov, R. Kobayashi, J. Normand, K. Raghavachari, A. Rendell, J. C. Burant, S. S. Iyengar, J. Tomasi, M. Cossi, N. Rega, J. M. Millam, M. Klene, J. E. Knox, J. B. Cross, V. Bakken, C. Adamo, J. Jaramillo, R. Gomperts, R. E. Stratmann, O. Yazyev, A. J. Austin, R. Cammi, C. Pomelli, J. W. Ochterski, R. L. Martin, K. Morokuma, V. G. Zakrzewski, G. A. Voth, P. Salvador, J. J. Dannenberg, S. Dapprich, A. D. Daniels, Ã. Farkas, J. B. Foresman, J. V. Ortiz, J. Cioslowski and D. J. Fox, Gaussian 09 Revision A.1, Gaussian Inc. Wallingford CT 2009.

[50] H.-J. Werner, P. J. Knowles, R. Lindh, F. R. Manby, M. Schütz et al., MOLPRO, version 2008.2, a package of ab initio programs (2008), see www.molpro.net.

[51] S. J. Vosko, L. Wilk and M. Nusair, Can. J. Phys. **58**, 1200 (1980).

[52] J. P. Perdew, K. Burke and M. Ernzerhof, Phys. Rev. Lett. **77**, 3865 (1996).

[53] B. J. Lynch and D. G. Truhlar, J. Phys. Chem. A **107**, 8996 (2003).

[54] P. L. Fast, M. L. Sanchez and D. G. Truhlar, Chem. Phys. Lett. **306**, 407 (1999).

[55] L. A. Curtiss, P. C. Redfern, K. Raghavachari, V. Rassolov and J. A. Pople, J. Chem. Phys. **110**, 4703 (1999).

[56] B. Lynch, Y. Zhao and D. Truhlar, http://comp.chem.umn.edu/database.

[57] P. L. Fast, J. Corchado, M. L. Sanchez and D. G. Truhlar, J. Phys. Chem. A **103**, 3139 (1999).

[58] L. A. Curtiss, K. Raghavachari, G. W. Trucks and J. A. Pople, J. Chem. Phys. **94**, 7221 (1991).

[59] L. A. Curtiss, K. Raghavachari, P. C. Redfern and J. A. Pople, J. Chem. Phys. **106**, 1063 (1997).

[60] J. Zheng, Y. Zhao and D. G. Truhlar, J. Chem. Theory Comput. **3**, 569 (2007).

[61] T. H. Dunning, J. Chem. Phys. **90**, 1007 (1989).

[62] R. A. Kendall, T. H. Dunning and R. J. Harrison, J. Chem. Phys. **96**, 6796 (1992).

[63] D. Woon and T. Dunning, J. Chem. Phys. **98**, 1358 (1993).

[64] D. Woon and T. Dunning, J. Chem. Phys. **100**, 2975 (1994).

[65] V. Barone and C. Adamo, Chem. Phys. Lett. **224**, 432 (1994).

[66] P. J. Stephens, F. J. Devlin, C. F. Chabalowski and M. J. Frisch, J. Phys. Chem. **98**, 11623 (1994).

[67] H. Iikura, T. Tsuneda, T. Yanai and K. Hirao, J. Chem. Phys. **115**, 3540 (2001).

[68] I. C. Gerber and J. G. Ángyán, Chem. Phys. Lett. **415**, 100 (2005).

[69] E. Goll, H.-J. Werner and H. Stoll, Phys. Chem. Chem. Phys. **7**, 3917 (2005).

[70] E. Goll, H.-J. Werner, H. Stoll, T. Leininger, P. Gori-Giorgi and A. Savin, Chem. Phys. **329**, 276 (2006).

[71] J. Toulouse, F. Colonna and A. Savin, J. Chem. Phys. **122**, 014110 (2005).

[72] J. Heyd, G. E. Scuseria and M. Ernzerhof, J. Chem. Phys. **118**, 8207 (2003).

[73] O. A. Vydrov and G. E. Scuseria, J. Chem. Phys. **125**, 234109 (2006).

[74] I. C. Gerber and J. G. Ángyán, Chem. Phys. Lett. **416**, 370 (2005).

[75] I. C. Gerber and J. G. Ángyán, J. Chem. Phys. **126**, 044103 (2007).

[76] E. Goll, T. Leininger, F. R. Manby, A. Mitrushchenkov, H.-J. Werner and H. Stoll, Phys. Chem. Chem. Phys. **10**, 3353 (2008).

[77] W. Zhu, J. Toulouse, A. Savin and J. G. Ángyán, J. Chem. Phys. **132**, 244108 (2010).

[78] J. Toulouse, W. Zhu, J. G. Ángyán and A. Savin, Phys. Rev. A **82**, 032502 (2010).

[79] R. Haunschild and W. Klopper, Theor. Chem. Acc. **131**, 1112 (2012).

[80] J. Tao, J. P. Perdew, V. N. Staroverov and G. E. Scuseria, Phys. Rev. Lett. **91**, 146401 (2003).

[81] E. Goll, M. Ernst, F. Moegle-Hofacker and H. Stoll, J. Chem. Phys. **130**, 234112 (2009).

[82] T. Yanai, D. P.Tew and N. C. Handy, Chem. Phys. Lett. **393**, 51 (2004).

[83] A. Ruzsinszky, J. P. Perdew and G. I. Csonka, J. Chem. Theory Comput. **6**, 127 (2010).

[84] T. Leininger, H. Stoll, H.-J. Werner and A. Savin, Chem. Phys. Lett. **275**, 151 (1997).

[85] R. Pollet, A. Savin, T. Leininger and H. Stoll, J. Chem. Phys. **116**, 1250 (2002).

[86] E. Fromager, J. Toulouse and H. J. A. Jensen, J. Chem. Phys. **126**, 074111 (2007).

Chapter 5

Rationale for a new class of double-hybrid approximations in density-functional theory

This chapter, written in collaboration with J. Toulouse, Eric Brémond and Carlo Adamo, has been published in Journal of Chemical Physics [J. Chem. Phys. **135**, 101102 (2011)].

5.1 Abstract

We provide a rationale for a new class of double-hybrid approximations introduced by Brémond and Adamo [J. Chem. Phys. **135**, 024106 (2011)] which combine an exchange-correlation density functional with Hartree-Fock exchange weighted by λ and second-order Møller-Plesset (MP2) correlation weighted by λ^3. We show that this double-hybrid model can be understood in the context of the density-scaled double-hybrid model proposed by Sharkas *et al.* [J. Chem. Phys. **134**, 064113 (2011)], as approximating the density-scaled correlation functional $E_c[n_{1/\lambda}]$ by a linear function of λ, interpolating between MP2 at $\lambda = 0$ and a density-functional approximation at $\lambda = 1$. Numerical results obtained with the Perdew-Burke-Ernzerhof density functional confirms the relevance of this double-hybrid model.

5.2 Introduction

The double-hybrid (DH) approximations introduced by Grimme [1], after some related earlier work [2, 3], are increasingly popular for electronic-structure calculations within density-functional theory. They consist in mixing Hartree-Fock (HF) exchange with a semilocal exchange density functional and second-order Møller-Plesset (MP2) correlation with a semilocal correlation density functional:

$$E_{xc}^{\mathrm{DH}} = a_x E_x^{\mathrm{HF}} + (1 - a_x) E_x[n] + (1 - a_c) E_c[n] + a_c E_c^{\mathrm{MP2}}, \tag{5.1}$$

where the first three terms are calculated in a usual self-consistent hybrid Kohn-Sham (KS) calculation, and the last perturbative term is evaluated with the previously obtained

orbitals and added *a posteriori*. The two empirical parameters a_x and a_c can be determined by fitting to a thermochemistry database. For example, the B2-PLYP double-hybrid approximation [1] is obtained by choosing the Becke 88 (B) exchange functional [4] for $E_x[n]$ and the Lee-Yang-Parr (LYP) correlation functional [5] for $E_c[n]$, and the empirical parameters $a_x = 0.53$ and $a_c = 0.27$ are optimized for the G2/97 subset of heats of formation. Another approach has been proposed in which the perturbative contribution is evaluated with normal B3LYP orbitals rather than orbitals obtained with the weighted correlation density functional $(1 - a_c)E_c[n]$ [6, 7].

Recently, Sharkas, Toulouse, and Savin [8] have provided a rigorous reformulation of the double-hybrid approximations based on the adiabatic-connection formalism, leading to the *density-scaled one-parameter double-hybrid* (DS1DH) approximation

$$E_{xc}^{\mathrm{DS1DH},\lambda} = \lambda E_x^{\mathrm{HF}} + (1-\lambda)E_x[n] + E_c[n] - \lambda^2 E_c[n_{1/\lambda}] + \lambda^2 E_c^{\mathrm{MP2}}, \tag{5.2}$$

where $E_c[n_{1/\lambda}]$ is the usual correlation energy functional evaluated at the scaled density $n_{1/\lambda}(\mathbf{r}) = (1/\lambda)^3 n(\mathbf{r}/\lambda)$. This reformulation shows that only one independent empirical parameter λ is needed instead of the two parameters a_x and a_c. The connection with the original double-hybrid approximations can be made by neglecting the density scaling

$$E_c[n_{1/\lambda}] \approx E_c[n], \tag{5.3}$$

which leads to the *one-parameter double-hybrid* (1DH) approximation [8]

$$E_{xc}^{\mathrm{1DH},\lambda} = \lambda E_x^{\mathrm{HF}} + (1-\lambda)E_x[n] + (1-\lambda^2)E_c[n] + \lambda^2 E_c^{\mathrm{MP2}}. \tag{5.4}$$

Equation (6.4) exactly corresponds to the double-hybrid approximation of Eq. (6.1) with parameters $a_x = \lambda$ and $a_c = \lambda^2$.

5.3 Theory

Very recently, Brémond and Adamo [9] have proposed a new class of double-hybrid approximations where the correlation functional is weighted by $(1 - \lambda^3)$ and the MP2 correlation energy is weighted by λ^3, instead of $(1 - \lambda^2)$ and λ^2, respectively. Applying this formula with the Perdew-Burke-Ernzerhof (PBE) [10] exchange-correlation density functional, they have constructed the PBE0-DH double-hybrid approximation which performs reasonably well. In this work, we give a rationale for this class of double-hybrid approximations. For this, we start by recalling that the density-scaled correlation functional $E_c[n_{1/\lambda}]$ tends to the second-order Görling-Levy (GL2) [11] correlation energy when the density is squeezed up to the high-density limit (or weak-interaction limit)

$$\lim_{\lambda \to 0} E_c[n_{1/\lambda}] = E_c^{\mathrm{GL2}}, \tag{5.5}$$

which is finite for nondegenerate KS systems. The GL2 correlation energy can be decomposed as (see, e.g., Ref. [12])

$$E_c^{\mathrm{GL2}} = E_c^{\mathrm{MP2}} + E_c^{\Delta\mathrm{HF}}, \tag{5.6}$$

where E_c^{MP2} is the usual MP2 correlation energy expression

$$E_c^{\mathrm{MP2}} = -\frac{1}{4} \sum_{ij} \sum_{ab} \frac{|\langle \phi_i \phi_j || \phi_a \phi_b \rangle|^2}{\varepsilon_a + \varepsilon_b - \varepsilon_i - \varepsilon_j}, \tag{5.7}$$

with the antisymmetrized two-electron integrals $\langle\phi_i\phi_j||\phi_a\phi_b\rangle$, and $E_c^{\Delta\mathrm{HF}}$ is an additional contribution involving the difference between the local multiplicative KS exchange potential $\hat{v}_x^{\mathrm{KS}}$ and the nonlocal nonmultiplicative HF exchange potential $\hat{v}_x^{\mathrm{HF}}$

$$E_c^{\Delta\mathrm{HF}} = -\sum_i \sum_a \frac{\left|\langle\phi_i|\hat{v}_x^{\mathrm{KS}} - \hat{v}_x^{\mathrm{HF}}|\phi_a\rangle\right|^2}{\varepsilon_a - \varepsilon_i}. \tag{5.8}$$

In both Eqs. (5.7) and (5.8), ϕ_k are the KS orbitals and ε_k are their associated energies, and the indices i,j and a,b stand for occupied and virtual orbitals, respectively. The single-excitation contribution $E_c^{\Delta\mathrm{HF}}$ vanishes for two-electron systems, and in most other cases is negligible [12], so that the GL2 correlation energy is well approximated by just the MP2 contribution (evaluated with KS orbitals), $E_c^{\mathrm{GL2}} \approx E_c^{\mathrm{MP2}}$. This leads us to propose an approximation for $E_c[n_{1/\lambda}]$ based on a linear interpolation formula

$$E_c[n_{1/\lambda}] \approx (1-\lambda)E_c^{\mathrm{MP2}} + \lambda E_c[n]. \tag{5.9}$$

Plugging Eq. (5.9) into Eq. (6.3), we directly arrive at what we call the *linearly scaled one-parameter double-hybrid* (LS1DH) approximation

$$E_{xc}^{\mathrm{LS1DH},\lambda} = \lambda E_x^{\mathrm{HF}} + (1-\lambda)E_x[n] + (1-\lambda^3)E_c[n] + \lambda^3 E_c^{\mathrm{MP2}}, \tag{5.10}$$

with the weights $(1-\lambda^3)$ and λ^3, thus giving a stronger rationale to the expression that Brémond and Adamo have proposed on the basis of different considerations. Further insight into this approximation can be gained by rewriting Eq. (5.9) in the alternative form

$$E_c[n_{1/\lambda}] \approx E_c^{\mathrm{MP2}} + \lambda\left(E_c[n] - E_c^{\mathrm{MP2}}\right), \tag{5.11}$$

which can then be interpreted as a first-order expansion in λ around $\lambda = 0$ with $E_c[n] - E_c^{\mathrm{MP2}}$ approximating the third-order correlation energy correction $E_c^{(3)}[n]$ in Görling-Levy perturbation theory. In comparison, the zeroth-order approximation $E_c[n_{1/\lambda}] \approx E_c^{\mathrm{MP2}}$ plugged in Eq. (6.3) just gives the usual one-parameter hybrid (1H) approximation with the full correlation density functional [13, 14]

$$E_{xc}^{\mathrm{1H},\lambda} = \lambda E_x^{\mathrm{HF}} + (1-\lambda)E_x[n] + E_c[n]. \tag{5.12}$$

In this sense, the LS1DH approximation of Eq. (5.10) can be considered as a next-order approximation in λ beyond the usual hybrid approximation.

5.4 Results

Figure 5.1 illustrates the different approximations to the density-scaled correlation energy $E_c[n_{1/\lambda}]$ as a function of λ for the He and Be atoms. The accurate reference curve is from the parametrization of Ref. [15]. For $\lambda = 1$, it reduces to the exact correlation energy, while for $\lambda = 0$ it is the GL2 correlation energy which tends to overestimate the correlation energy. In between these two limits, it is nearly linear with λ. The PBE correlation energy without density scaling [Eq. (5.3)] is the crudest approximation to $E_c[n_{1/\lambda}]$. The PBE correlation energy with density scaling (taken from the parametrization of Ref. [15])

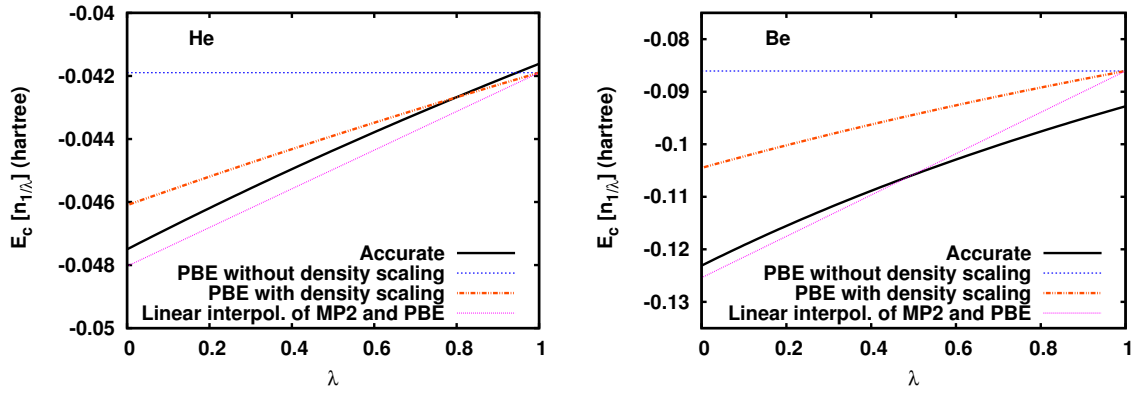

Figure 5.1: (Color online) Density-scaled correlation energy $E_c[n_{1/\lambda}]$ for the He (left) and Be (right) atoms as a function of λ. Accurate calculations (from the parametrizations of Ref. [15]) are compared with different approximations: PBE without density scaling [Eq. (5.3)], PBE with density scaling (from the parametrizations of Ref. [15]), and linear interpolation between MP2 (with PBE orbitals) and PBE [Eq. (5.9)]. The MP2 calculations for He and Be (including core excitations) have been performed with the cc-pV5Z and cc-pCV5Z basis sets [16, 17], respectively.

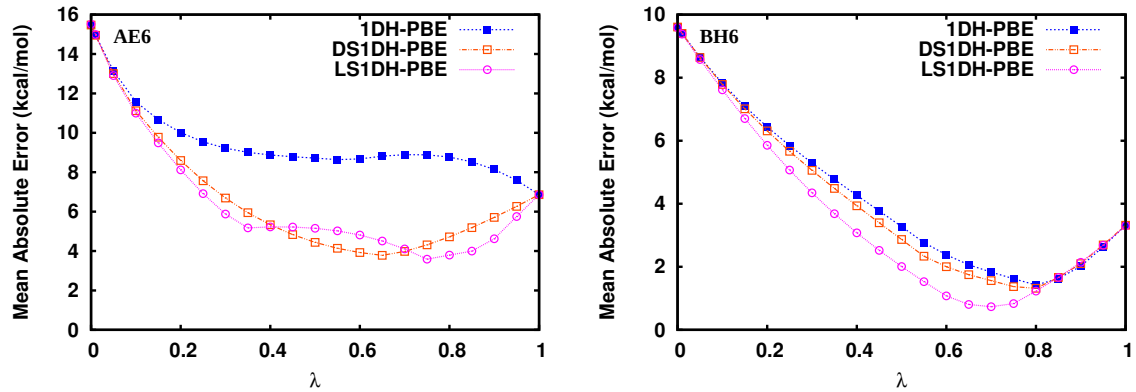

Figure 5.2: (Color online) Mean absolute errors for the AE6 (left) and BH6 (right) test sets as functions of the parameter λ for the 1DH, and DS1DH, and LS1DH approximations with the PBE exchange-correlation density functional. All calculations were carried out with the cc-pVQZ basis set.

gives a nearly linear curve. It is a fairly good approximation for He, but a less good approximation for Be where it underestimates the correlation energy for all λ, especially at $\lambda = 0$. This is due to the presence of static correlation in this system that is not described by the PBE functional. Finally, the linear interpolation of Eq. (5.9) between MP2 (evaluated with PBE orbitals) and PBE appears as a good approximation for both He and Be. In fact, the linear interpolation is clearly the best approximation for Be, at least with the PBE functional.

For a more comprehensive comparison of the different approximations, we have performed calculations on the AE6 and BH6 test sets [18] with the 1DH, DS1DH, and LS1DH double hybrids for the PBE functional, using a development version of the MOLPRO 2010 program [19]. The AE6 set is a small representative benchmark set of six atomization energies consisting of SiH_4, S_2, SiO, C_3H_4 (propyne), $C_2H_2O_2$ (glyoxal), and C_4H_8 (cyclobutane). The BH6 set is a small representative benchmark set of forward and reverse barrier heights of three reactions, $OH + CH_4 \rightarrow CH_3 + H_2O$, $H + OH \rightarrow O + H_2$, and $H + H_2S \rightarrow HS + H_2$. All the calculations are performed at the optimized QCISD/MG3 geometries [20]. We use the Dunning cc-pVQZ basis set [21, 22]. Core electrons are kept frozen in all our MP2 calculations. Spin-restricted calculations are performed for all the closed-shell systems, and spin-unrestricted calculations for all the open-shell systems. In Fig. 5.2, we plot the mean absolute errors (MAE) for the two sets as a function of λ. For the AE6 set, the MAEs of the DS1DH and LS1DH approximations are quite similar, and are both much smaller that the MAE of the 1DH approximation for a wide range of λ. For the BH6 set, the LS1DH approximation gives a MAE which is significantly smaller than those of both DS1DH and 1DH for intermediate values of λ.

As regards the choice of the parameter λ, the present data on the AH6 set gives an optimal value of $\lambda = 0.75$ for the LS1DH double hybrid, with a minimal MAE of 3.59 kcal/mol, and for the BH6 set the optimal value is $\lambda = 0.70$ giving a minimal MAE of 0.73 kcal/mol. However, the MAE is not very sensitive to the value of λ around the optimal value, and Brémond and Adamo [9] have argued for using $\lambda = 0.5$ in defining the PBE0-DH approximation, using a similar argument as the one used by Becke for his "half-and-half" hybrid [23].

5.5 Conclusions

In summary, we have shown that the new class of double-hybrid approximations named here LS1DH [Eq. (5.10)] can be understood as approximating the density-scaled correlation functional $E_c[n_{1/\lambda}]$ by a linear function of λ, interpolating between MP2 at $\lambda = 0$ and a density-functional approximation at $\lambda = 1$. Numerical results obtained with the PBE density functional confirms that the LS1DH approximation is a relevant double-hybrid model, and in fact tends to be more accurate than the DS1DH double-hybrid model [Eq. (6.3)] in which density scaling is applied to the PBE correlation functional. More generally, it can be expected that the LS1DH double-hybrid model will be more accurate than the DS1DH double-hybrid model when applied with a density-functional approximation that is inaccurate in the high-density limit. We hope that this work will help constructing other theoretically justified double-hybrid approximations.

Acknowledgments

We thank A. Savin for discussions. This work was partly supported by Agence Nationale de la Recherche (ANR) via contract numbers 07-BLAN-0272 (Wademecom) and 10-BLANC-0425 (DinfDFT). Sanofi-Aventis is also acknowledged for financial support.

Bibliography

[1] S. Grimme, J. Chem. Phys. **124**, 034108 (2006).

[2] Y. Zhao, B. J. Lynch and D. G. Truhlar, J. Phys. Chem. A **108**, 4786 (2004).

[3] Y. Zhao, B. J. Lynch and D. G. Truhlar, Phys. Chem. Chem. Phys. **7**, 43 (2005).

[4] A. D. Becke, Phys. Rev. A **38**, 3098 (1988).

[5] C. Lee, W. Yang and R. G. Parr, Phys. Rev. B **37**, 785 (1988).

[6] Y. Zhang, X. Xu and W. A. Goddard III, Proc. Natl. Acad. Sci. U.S.A. **106**, 4963 (2009).

[7] I. Y. Zhang and X. Xu, Int. Rev. Phys. Chem **30**, 115 (2011).

[8] K. Sharkas, J. Toulouse and A. Savin, J. Chem. Phys. **134**, 064113 (2011).

[9] E. Brémond and C. Adamo, J. Chem. Phys. **135**, 024106 (2011).

[10] J. P. Perdew, K. Burke and M. Ernzerhof, Phys. Rev. Lett. **77**, 3865 (1996).

[11] A. Görling and M. Levy, Phys. Rev. B **47**, 13105 (1993).

[12] E. Engel, in *A Primer in Density Functional Theory*, edited by C. Fiolhais, F. Nogueira and M. A. L. Marques (Springer, Berlin, 2003), Vol. 620 of Lecture Notes in Physics, pp. 56–122.

[13] A. D. Becke, The Journal of Chemical Physics **104** (1996).

[14] M. Ernzerhof, J. P. Perdew and K. Burke, in *Density Functional Theory*, edited by R. Nalewajski (Springer-Verlag, Berlin, 1996).

[15] F. Colonna and A. Savin, J. Chem. Phys. **110**, 2828 (1999).

[16] D. Woon and T. Dunning, J. Chem. Phys. **100**, 2975 (1994).

[17] B. P. Prascher, D. E. Woon, T. H. D. J. K. A. Peterson and A. K. Wilson, Theor. Chem. Acc. **128**, 69 (2011).

[18] B. J. Lynch and D. G. Truhlar, J. Phys. Chem. A **107**, 8996 (2003).

[19] H.-J. Werner, P. J. Knowles, G. Knizia, F. R. Manby, M. Schütz, and others, MOLPRO, version 2010.1, a package of ab initio programs, Cardiff, UK, 2010, see http://www.molpro.net.

[20] B. Lynch, Y. Zhao and D. Truhlar, http://comp.chem.umn.edu/database.

[21] T. H. Dunning, J. Chem. Phys. **90**, 1007 (1989).

[22] D. Woon and T. Dunning, J. Chem. Phys. **98**, 1358 (1993).

[23] A. D. Becke, J. Chem. Phys. **98**, 1372 (1993).

Chapter 6

Double-hybrid density-functional theory applied to molecular crystals

The chapter corresponds to a paper in preparation.

6.1 Abstract

We test the performance of a number of two- and one-parameter double-hybrid approximations, combining semilocal exchange-correlation density functionals with periodic local second-order Møller-Plesset (LMP2) perturbation theory, for calculating lattice energies of a set of molecular crystals: urea, formamide, formic acid, ammonia, and carbon dioxide. All double-hybrid methods perform better than the corresponding Kohn-Sham calculations with the same functionals, but not better than standard LMP2. The one-parameter double-hybrid approximations based on the PBEsol density functional gives lattice energies per molecule with an accuracy of about 5 kJ/mol, which is similar to the accuracy of LMP2. The fact that these double-hybrid approximations underestimate the lattice energy of the carbon dioxide crystal suggests that these approximations miss a part of dispersion interactions.

6.2 Introduction

The reliable computational prediction of the lattice energies of molecular crystals is important in materials science [1–4]. It requires an accurate treatment of different types of intermolecular interactions, including electrostatics [5], induction [6, 7], and dispersion interactions [8]. Kohn-Sham density-functional theory (DFT) [9, 10] using standard (semi)local density functionals can account for electrostatic and induction interactions in molecular crystals [11–13]. However, these usual semilocal functionals fail to adequately model the dispersion interactions [14–17] which are an important source of attraction even in the hydrogen-bonded crystals [18]. One possibility for improving the prediction of crystal lattice energies is to use empirical [19–28] or non-empirical [29–31] dispersion-corrected density functionals.

Another possibility for theoretical prediction of molecular crystal lattice energies is to use wave-function type correlation methods such as second-order Møller-Plesset perturbation theory (MP2), coupled-cluster singles doubles with perturbative triples [CCSD(T)],

or symmetry-adapted perturbation theory (SAPT) on finite clusters [32–35]. However, the accurate simulation of a periodic system by a finite cluster is difficult and the results may depend very much on the size of the clusters. More satisfying is the use of fully periodic wave-function correlation methods such as MP2 [36–42], the random-phase approximation [41, 43, 44], or quantum Monte Carlo [16]. In particular, the periodic local MP2 (LMP2) method as implemented in the CRYSCOR program [42, 45, 46] is well suited for weakly bound systems such as rare-gas solids [47–49] and molecular crystals [50–52].

In the present work, we investigate the performance of a number of double-hybrid (DH) approximations combining semilocal density functionals with periodic LMP2 for prediction of the lattice energies of a set of molecular crystals. The DH approximations have been introduced a few years ago [53] and have proven capable to reach near chemical accuracy for atomic and molecular properties such as atomization energies, reaction barrier heights, ionization potentials, and electron affinities. To the best of our knowledge, only DH approximations using two empirical parameters constructed with the Becke 88 (B) exchange functional [54] and the Lee-Yang-Parr (LYP) correlation functional [55] have recently been applied to molecular crystals and no improvement over MP2 was found [40]. Here, we test the Perdew-Burke-Ernzerhof (PBE) [56] and the modified PBEsol [57] exchange-correlation functionals in the one-parameter DH scheme recently proposed by some of us [58].

The paper is organized as follows. In Section 6.3, we review the one-parameter DH approximations and the main equations of the periodic LMP2 method, and we indicate the modifications made for the present implementation. After giving computational details on the calculations in Section 6.4, we present and discuss the results obtained with various DH approximations on five molecular crystals: urea, formamide, formic acid, ammonia, and carbon dioxide. Section 6.6 summarizes our conclusions.

6.3 Theory

6.3.1 One-parameter double-hybrid approximations

After some related earlier work [59, 60], Grimme [53] introduced the procedure which is now commonly used in DH approximations. First, a normal self-consistent DFT calculation is carried out using a fraction a_x of Hartree-Fock (HF) exchange E_x^{HF}, a fraction $(1 - a_x)$ of a semilocal exchange density functional $E_x[n]$, and a fraction $(1 - a_c)$ of a semilocal correlation density functional $E_c[n]$. Subsequently, the MP2 correlation energy E_c^{MP2} calculated using the previously generated orbitals is added with the fraction a_c. The resulting exchange-correlation energy can thus be written as

$$E_{xc}^{\mathrm{DH}} = a_x E_x^{\mathrm{HF}} + (1 - a_x)E_x[n] + (1 - a_c)E_c[n] + a_c E_c^{\mathrm{MP2}}. \tag{6.1}$$

Many DH approximations relying on this procedure have been developed [53, 61–64]. For example, the B2-PLYP approximation [53] is obtained by choosing the B exchange functional for $E_x[n]$ and the LYP correlation functional for $E_c[n]$, and the two empirical parameters $a_x = 0.53$ and $a_c = 0.27$ as optimized for the G2/97 [65] subset of heats of formation.

Recently, a rigorous reformulation of the DH approximations was provided [58] by applying the multideterminant extension of the Kohn-Sham scheme [66, 67] to the adiabatic-

connection Hamiltonian

$$\hat{H}^{\lambda} = \hat{T} + \hat{V}_{\rm ext} + \lambda \hat{W}_{ee} + \hat{V}^{\lambda}_{{\rm H}xc}[n], \tag{6.2}$$

which links the non-interacting Kohn-Sham Hamiltonian ($\lambda = 0$) to the exact Hamiltonian ($\lambda = 1$). In this expression, $\hat{T}$ is the kinetic energy operator, $\hat{V}_{\rm ext}$ is a scalar external potential operator (e.g., nuclei-electron), and $\hat{V}^{\lambda}_{{\rm H}xc}[n]$ is the Hartree-exchange-correlation potential operator keeping the one-electron density n constant for all values of the coupling constant λ. This leads to the density-scaled one-parameter double-hybrid (DS1DH) approximation

$$E_{xc}^{{\rm DS1DH},\lambda} = \lambda E_x^{\rm HF} + (1-\lambda)E_x[n] + E_c[n] - \lambda^2 E_c[n_{1/\lambda}] + \lambda^2 E_c^{\rm MP2}, \tag{6.3}$$

where $E_c[n_{1/\lambda}]$ is the correlation energy functional evaluated at the scaled density $n_{1/\lambda}(\mathbf{r}) = (1/\lambda)^3 n(\mathbf{r}/\lambda)$. Neglecting the density scaling in the correlation functional, $E_c[n_{1/\lambda}] \approx E_c[n]$, leads to one-parameter double-hybrid (1DH) approximation

$$E_{xc}^{{\rm 1DH},\lambda} = \lambda E_x^{\rm HF} + (1-\lambda)E_x[n] + (1-\lambda^2)E_c[n] + \lambda^2 E_c^{\rm MP2}. \tag{6.4}$$

In comparison to the original DH approximations, only one empirical parameter needs to be determined. DS1DH and 1DH approximations using the BLYP and PBE exchange-correlation functionals have been constructed and the optimal parameter was found to be about $\lambda \approx 0.65$ or 0.70 for atomization energies and reaction barrier heights of molecular systems [58].

6.3.2 Periodic local MP2

We now briefly review the main equations of the periodic local MP2 method that we use and indicate the required modifications for implementing the one-parameter DH approximations. The implementation of two-parameter DH approximations require obvious similar modifications.

The first-order perturbative correction to the HF wave function is written as

$$|\Psi^{(1)}\rangle = \frac{1}{2} \sum_{(\mathbf{ij})\in P} \sum_{(\mathbf{ab})\in[\mathbf{ij}]} T^{\mathbf{ij}}_{\mathbf{ab}} |\Phi^{\mathbf{ab}}_{\mathbf{ij}}\rangle, \tag{6.5}$$

where $\Phi^{\mathbf{ab}}_{\mathbf{ij}}$ are doubly excited determinants and $T^{\mathbf{ij}}_{\mathbf{ab}}$ are the corresponding amplitudes. In this expression, the labels (**i**,**j**) refer to pairs of occupied Wannier functions (WFs) taken from a truncated list P, in which the first WF **i** is located in the reference unit cell and the second WF **j** is restricted within a given distance to the first WF **i**. The labels (**a**, **b**) refer to pairs of mutually non-orthogonal virtual projected atomic orbitals (PAOs) and the sum is restricted to the pair-domain [**ij**] of PAOs which are spatially close to at least one of the WF **i** or **j**. This truncation of the virtual space makes the LMP2 method scales linearly with the supercell size.

The double excitation amplitudes $T^{\mathbf{ij}}_{\mathbf{ab}}$ are obtained by solving the following system of linear equations [42, 68, 69]

$$K^{\mathbf{ij}}_{\mathbf{ab}} + \sum_{\mathbf{cd}} \left\{ F_{\mathbf{ac}} T^{\mathbf{ij}}_{\mathbf{cd}} S_{\mathbf{db}} + S_{\mathbf{ac}} T^{\mathbf{ij}}_{\mathbf{cd}} F_{\mathbf{db}} - S_{\mathbf{ac}} \Big[\sum_{\mathbf{k}} (F_{\mathbf{ik}} T^{\mathbf{kj}}_{\mathbf{cd}} + T^{\mathbf{ik}}_{\mathbf{cd}} F_{\mathbf{kj}}) \Big] S_{\mathbf{db}} \right\} = 0, \tag{6.6}$$

where $K^{\mathbf{ij}}_{\mathbf{ab}} = (\mathbf{ia}|\mathbf{jb})$ are the two-electron exchange integrals, $S_{\mathbf{db}}$ is the overlap between PAOs, and $F_{\mathbf{ik}}$ and $F_{\mathbf{db}}$ are elements of the Fock matrix in WF and PAO basis, which is obtained by transformation of the Fock matrix in the atomic orbital (AO) basis

$$F_{\mu\nu} = h_{\mu\nu} + J_{\mu\nu} + K_{\mu\nu}, \tag{6.7}$$

where $h_{\mu\nu}$, $J_{\mu\nu}$, and $K_{\mu\nu}$ are the one-electron Hamiltonian, Coulomb, and exchange matrices, respectively. For closed-shell systems, $J_{\mu\nu} = \sum_{\rho\sigma} P_{\rho\sigma}(\mu\nu|\sigma\rho)$ and $K_{\mu\nu} = (-1/2)\sum_{\rho\sigma} P_{\rho\sigma}(\mu\rho|\sigma\nu)$ where $P_{\rho\sigma}$ is the density matrix and $(\mu\nu|\sigma\rho)$ are the two-electron integrals. In the local basis, the occupied-occupied and virtual-virtual blocks of the Fock matrix are not diagonal, which means that Eq. (6.6) has to be solved iteratively for the amplitudes $T^{\mathbf{ij}}_{\mathbf{ab}}$. When the convergence is reached, the LMP2 correlation energy per unit cell is given as

$$E_c^{\mathrm{LMP2}} = \sum_{\mathbf{ij}\in P} \sum_{(\mathbf{ab})\in[\mathbf{ij}]} K^{\mathbf{ij}}_{\mathbf{ab}}(2T^{\mathbf{ij}}_{\mathbf{ab}} - T^{\mathbf{ij}}_{\mathbf{ba}}). \tag{6.8}$$

For the one-parameter DH approximations, the Fock matrix of Eq. (6.7) is replaced by

$$F_{\mu\nu}^{\mathrm{hybrid}} = h_{\mu\nu} + J_{\mu\nu} + \lambda K_{\mu\nu} + V^{\lambda}_{xc,\mu\nu}, \tag{6.9}$$

with the scaled exchange matrix $\lambda K_{\mu\nu}$ and the exchange-correlation potential matrix $V^{\lambda}_{xc,\mu\nu}$ corresponding to the density functional used. Note that, because of self consistency, the density matrix $P_{\rho\sigma}$ in $J_{\mu\nu}$ and $K_{\mu\nu}$ also depends on λ. This is essentially the only non-trivial modification to be made in the program. Indeed, one can see that using the scaled interaction $\lambda\hat{W}_{ee}$ of Eq. (6.2) corresponds to scaling the two-electron exchange integrals, $K^{\mathbf{ij}}_{\mathbf{ab}} \to \lambda K^{\mathbf{ij}}_{\mathbf{ab}}$, in Eq. (6.6), implying the scaling of the amplitudes $T^{\mathbf{ij}}_{\mathbf{ab}} \to \lambda T^{\mathbf{ij}}_{\mathbf{ab}}$. Using Eq. (6.8), it means that we just need to scale the LMP2 correlation energy by λ^2

$$E_c^{\mathrm{LMP2}} \to \lambda^2 E_c^{\mathrm{LMP2}}, \tag{6.10}$$

as it was already indicated in Eqs. (6.3) and (6.4).

There is an additional point to consider when using the dual-basis set scheme [70, 71]. The reliable description of the correlated wave functions needs the use of rather large basis sets and especially with diffuse functions when treating weakly bound systems. However, such basis sets may lead to linear-dependency problems in the periodic self-consistent-field calculation (SCF) that precedes the LMP2 step. The dual-basis set scheme helps overcome these difficulties by using a smaller basis for the SCF calculation and additional basis functions for the LMP2 calculation. In this scheme, Brillouin's theorem does not apply in the LMP2 calculation and hence single excitations contribute to the LMP2 correlation energy

$$E_{c,\mathrm{singles}}^{\mathrm{LMP2}} = \sum_{\mathbf{ia}} F_{\mathbf{ia}} T^{\mathbf{i}}_{\mathbf{a}}, \tag{6.11}$$

where the single excitation amplitudes $T^{\mathbf{i}}_{\mathbf{a}}$ are determined from

$$F_{\mathbf{ia}} + \sum_{\mathbf{b}} F_{\mathbf{ab}} T^{\mathbf{i}}_{\mathbf{b}} - \sum_{\mathbf{bj}} F_{\mathbf{ij}} T^{\mathbf{i}}_{\mathbf{b}} S_{\mathbf{ba}} = 0, \tag{6.12}$$

where the Fock matrix in these formulas are defined in the large basis set but built from density matrices in the small one (*i.e.*, the indices μ and ν in $F_{\mu\nu}$ run over the large basis set while the indices ρ and σ in $P_{\rho\sigma}$ belong to the small one) [72]. For the case of the one-parameter DH approximations, since the two-electron integrals do not explicit appear in Eqs. (6.11) and (6.12), the evaluation of the single excitation contribution do not require other modifications than simply using the dual-basis version of the Fock matrix of Eq. (6.9) in Eqs. (6.11) and (6.12). We note, however, that because the one-parameter DH approximations are based on a nonlinear Rayleigh-Schrödinger perturbation theory [67, 73, 74], when Brillouin's theorem does not apply, there is in principle an additional single-excitation contribution to the second-order correlation energy coming from the second-order functional derivative of the Hartree-exchange-correlation energy, but we neglect this additional contribution in this work.

6.4 Computational details

The one-parameter DS1DH and 1DH approximations using the BLYP, PBE, and PBEsol functionals, as well as the two-parameter DH approximations, B2-PLYP ($a_x = 0.53$, $a_c = 0.27$) [53], B2GP-PLYP ($a_x = 0.65$, $a_c = 0.36$) [63], and mPW2-PLYP ($a_x = 0.55$, $a_c = 0.25$) [61], have been implemented in a development version of the CRYSTAL09 [75] and CRYSCOR09 [45, 46] suite of programs. For the DS1DH approximations, the expressions of the density-scaled correlation energy $E_c[n_{1/\lambda}]$ and the corresponding potential are given in the appendix of Ref. [58].

We study five molecular crystals: urea $CO(NH_2)_2$, formamide $HCONH_2$, formic acid HCOOH, ammonia NH_3 and carbon dioxide CO_2. The experimental crystal structures were used [76–79]. The truncation tolerances of lattice sums for one- and two-electron integrals were set to 7 7 7 12 40 (TOLINTEG parameters [75]). A grid consisting of 75 radial points and up to 974 angular points was used in evaluating the exchange-correlation functional. The shrinking factors were set to 4 for the **k** points grid to sample the irreducible Brillouin zone. Each calculation is done in two steps: a periodic SCF hybrid calculation is first performed using CRYSTAL09, and then the periodic LMP2 correlation energy is calculated using CRYSCOR09 and added to the SCF energy after multiplication by the proper scaling factor. For urea, formamide, and formic acid, we employ the polarized split-valence double-zeta Gaussian basis set 6-31G(d,p) [80] in the SCF calculations [81]. This basis is then augmented by polarization functions with small exponents (d functions for C, N and O atoms, p functions for H atoms, taken from the aug-cc-pVDZ basis set [82]), and the resulting basis set is denoted by p-aug-6-31G(d,p) [52]. The virtual space of the extended basis set is employed in the subsequent LMP2 calculation. When we use this dual-basis set technique, the contribution of single excitations to the LMP2 correlation energy is evaluated and added. This contribution does not exceed 2% of the calculated lattice energy. In practice, the dual-basis matrices are obtained through a non-self-consistent SCF (GUESDUAL [75]) which uses the density matrix from a previous SCF run to allocate the additional basis functions. For ammonia and carbon dioxide, we use the p-aug-6-31G(d,p) basis set for both the SCF and LMP2 calculations. Core electrons are kept frozen in all LMP2 calculations. The occupied valence orbital space is spanned by the localized [83] symmetry-adapted [84] mutually orthogonal Wannier functions (WFs) supplied by the PROPERTIES module of CRYSTAL. The virtual orbital space is spanned

by mutually nonorthogonal PAOs, which are constructed by projecting the individual AO basis functions on the virtual space [68]. The explicit computations cover WF pairs up to distance $d_{\mathbf{ij}} = 12$ Å, where the two-electron repulsion integrals were evaluated via the density fitting periodic (DFP) scheme [85] for $d_{\mathbf{ij}} \leq 8$ Å and via the multipolar approximation for $8 < d_{\mathbf{ij}} \leq 12$ Å. The contribution of the WF pairs with $d_{\mathbf{ij}} > 12$ Å to the correlation energy was estimated through the Lennard-Jones extrapolation technique. Excitation PAO domains have been restricted to the molecular units.

Single-point, static (*i.e.* at 0 K) energies are computed to evaluate the counterpoise-corrected lattice energy $E_{\mathrm{LE}}^{\mathrm{CP}}(V)$ per molecule at a given volume V of the unit cell

$$E_{\mathrm{LE}}^{\mathrm{CP}}(V) \;=\; E_{\mathrm{bulk}}/Z - E_{\mathrm{mol+ghosts}}^{[\mathrm{bulk}]}, \tag{6.13}$$

where Z is the number of the molecular units in the unit cell, and E_{bulk} and $E_{\mathrm{mol+ghosts}}^{[\mathrm{bulk}]}$ are total energies of the bulk system (per cell) and of the molecule in the crystalline bulk geometry with ghost functions, respectively, at a given cell volume. At least 50 ghost atoms surrounding the central molecule were used. The ghost functions, in the standard Boys-Bernardi counterpoise scheme [86], are supposed to eliminate the inconsistency between the finite basis sets used in the molecular and bulk calculations to obtain basis set superposition error (BSSE) free lattice energies. The structural deformation of the molecule induced by the crystal packing is not included, *i.e.*, the difference between the energies of the isolated molecules in the bulk and in the gas phase conformations is neglected, $E_{\mathrm{mol}}^{[\mathrm{bulk}]} = E_{\mathrm{mol}}^{[\mathrm{gas}]}$.

6.5 Results and discussion

The calculated lattice energies of crystalline urea, formamide, ammonia and carbon dioxide are compared to the experimental sublimation enthalpies after corrections for thermal and zero-point effects [28], while the lattice energy of formic acid is directly compared to the experimental one [52]. Although this set of five molecular crystals is statistically small, it includes systems ranging from a purely dispersion bound crystal (carbon dioxide) to structures with hydrogen bonds of varying strengths (urea, formamide, formic acid, ammonia).

To have a first global view of the performance of the different one-parameter DH approximations and the dependence on the parameter λ, we show in Fig. 6.1 mean absolute errors (MAEs) on the five lattice energies as a function of λ for the DS1DH and 1DH methods using the BLYP, PBE, and PBEsol density functionals. For $\lambda = 0$, each method reduces to a standard periodic Kohn-Sham calculation with the corresponding density functional. For $\lambda = 1$, all methods reduce to a standard periodic LMP2 calculation. Kohn-Sham BLYP and PBE calculations at $\lambda = 0$ give much larger MAEs (about 32 kJ/mol and 16 kJ/mol, respectively) than LMP2 (about 5 kJ/mol).

The DS1DH and 1DH approximations using the BLYP and PBE functionals inherit the bad performance of these functionals and always give larger MAEs than standard LMP2 for all $\lambda < 1$. In contrast, the PBEsol functional (which is a modified version of the PBE functional to improve the description of solids) gives a MAE at $\lambda = 0$ (about 8 kJ/mol) that is comparable to LMP2. Consequently, the DS1DH-PBEsol and 1DH-PBEsol approximations give almost constant MAEs as a function of λ, with a slight

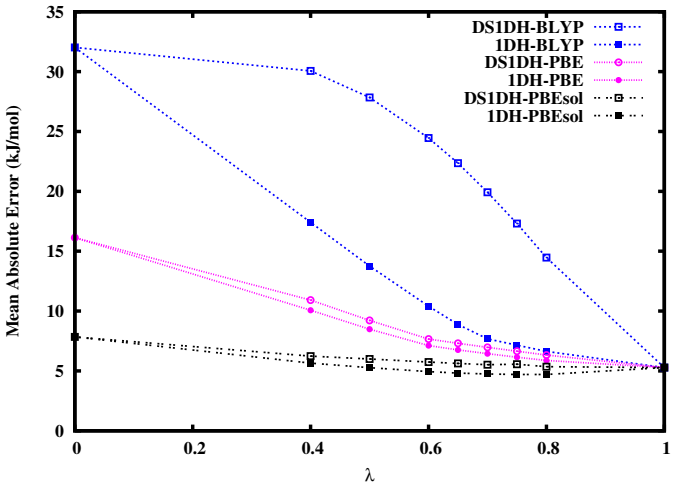

Figure 6.1: MAEs on the counterpoise-corrected lattice energies per molecule (in kJ/mol) of the urea, formamide, formic acid, ammonia, and carbon dioxide crystals, as functions of the parameter λ for the DS1DH and 1DH approximations with the BLYP, PBE, and PBEsol exchange-correlation density functionals.

minimum for 1DH-PBEsol reached at around $\lambda = 0.70$. Note that neglecting density scaling in the LYP correlation functional, *i.e.* going from DS1DH-BLYP to 1DH-BLYP, significantly reduces the MAEs, which is similar to what was observed for atomization energies of molecular systems [58]. However, neglecting density scaling in the PBE and PBEsol density functionals only marginally decreases the MAEs on the lattice energies of the molecular crystals considered here, whereas it was found that molecular atomization energies were significantly deteriorated when neglecting density scaling in PBE [58]. The understanding of the effects of density scaling with different functionals for calculating diverse properties requires further study.

Table 6.1 reports the lattice energies of the five studied molecular crystals calculated by HF, LMP2, Kohn-Sham, and various double-hybrid methods. For DS1DH-BLYP, 1DH-BLYP, DS1DH-PBE, and 1DH-PBE, we use the values of λ previously optimized on a set of atomization energies and reaction barrier heights of molecular systems [58] ($\lambda = 0.65$ or 0.70 depending on the double-hybrid method considered). For DS1DH-PBEsol and 1DH-PBEsol, we use $\lambda = 0.70$ (corresponding to a LMP2 fraction of $\lambda^2 = 0.49$) which according to Fig. 6.1 yields a similar or slightly lower MAE than LMP2. We also report results obtained with the two-parameter double-hybrid approximations B2-PLYP, B2GP-PLYP, and mPW2-PLYP, which have smaller fractions of LMP2 ($a_c = 0.27$, 0.36, and 0.25, respectively). Among the non-double-hybrid methods, HF, BLYP and PBE strongly underestimate the lattice energies of the five crystals. PBEsol gives good lattice energies for urea and ammonia, but still underestimated lattice energies for carbon dioxide, and, to a less extent, for formamide and formic acid. This is most likely due to dispersion interactions that are not properly accounted for. A more uniform accuracy on the lattice energies is obtained with LMP2. All the double-hybrid methods give smaller MAEs that the corresponding Kohn-Sham calculations with the same functionals. However, B2-PLYP, B2GP-PLYP, mPW2-PLYP, DS1DH-BLYP, 1DH-BLYP, DS1DH-PBE, and 1DH-PBE still tend to significantly underestimate the lattice energies. The DS1DH-PBEsol and 1DH-PBEsol approximations give overall reasonably good lattice energies, with a

Table 6.1: Counterpoise-corrected lattice energies per molecule (in kJ/mol) of the urea, formamide, formic acid, ammonia and carbon dioxide crystals, calculated by several methods. For the DS1DH-BLYP, 1DH-BLYP, DS1DH-PBE, and 1DH-PBE double-hybrid approximations, we use the values of λ which were previously optimized in Ref. [58]. For the DS1DH-PBEsol and 1DH-PBEsol double-hybrid approximations, we use a value of $\lambda = 0.70$ which roughly minimizes the MAE of 1DH-PBEsol for this set of molecular crystals. All calculations were carried out with experimental geometries. For each method, the value with the largest error is indicated in boldface.

Method	Parameter λ	$CO(NH_2)_2$[a]	$HCONH_2$[a]	HCOOH[a]	NH_3[b]	CO_2[b]	MAE
HF		75.40	48.11	**38.36**	8.45	5.03	27.24
BLYP		70.00	41.00	**30.25**	13.74	-3.53	32.02
PBE		89.53	58.82	**47.15**	27.91	7.48	16.13
PBEsol		102.96	70.25	58.32	37.27	**10.59**	7.84
LMP2		**109.88**	76.44	61.60	32.35	25.76	5.28
B2-PLYP		92.66	63.30	**51.16**	25.58	14.12	12.94
B2GP-PLYP		98.37	68.07	**56.39**	27.93	17.78	8.60
mPW2-PLYP		100.86	70.40	**59.37**	30.15	20.57	6.61
DS1DH-BLYP	$\lambda = 0.70$	85.17	55.11	**43.56**	19.64	8.45	19.92
1DH-BLYP	$\lambda = 0.65$	98.01	67.95	**55.49**	27.94	17.74	8.88
DS1DH-PBE	$\lambda = 0.65$	101.05	70.84	**57.91**	30.54	17.92	7.31
1DH-PBE	$\lambda = 0.65$	102.74	72.30	59.32	31.69	**18.32**	6.76
DS1DH-PBEsol	$\lambda = 0.70$	106.74	75.50	62.33	33.65	**20.33**	5.52
1DH-PBEsol	$\lambda = 0.70$	**109.07**	77.50	64.29	35.22	21.00	4.75
Best estimate		99.43[c]	78.74[c]	68.00[d]	37.57[c]	27.80[c]	

[a]With dual-basis set technique: 6-31G(d,p) basis for SCF and p-aug-6-31G(d,p) basis for LMP2.
[b]With p-aug-6-31G(d,p) basis for both SCF and LMP2 calculations.
[c]From Ref. [28], [d]From Ref. [52].

similar averaged accuracy than LMP2. One should note however that DS1DH-PBEsol and 1DH-PBEsol give a lattice energy of the carbon dioxide crystal that is significantly more underestimated than in LMP2, suggesting that these double-hybrid approximations miss a part of the dispersion interactions.

We now investigate the dependence of the results on the basis set. Table 6.2 shows the LMP2 lattice energies calculated using the 6-31G(d,p), p-aug-6-31G(d,p), and p-aug-6-311G(d,p) basis sets. The latter triple-zeta basis set has been tailored according to the same technique (outlined in the Computational Details section) used for p-aug-6-31G(d,p). For urea, the LMP2 calculation could not be converged with the p-aug-6-311G(d,p) basis set. The large difference between the values calculated with the 6-31G(d,p) basis set and those calculated with the p-aug-6-31G(d,p) basis set shows that the augmentation of the 6-31G(d,p) basis set with low-exponent polarization functions, which act as diffuse functions, is mandatory for a correct description of the lattice energies. The largest difference in the values of the LMP2 lattice energies calculated with the p-aug-6-311G(d,p) and the p-aug-6-31G(d,p) basis sets is 2.68 kJ/mol for the formic acid crystal. This system is composed of infinite hydrogen-bonded chains with pure dispersion inter-chain interactions [51], and the sensitivity to the basis set might be due to these inter-chain interactions.

In Figure 6.2, we show the lattice energy of the formic acid crystal calculated with the 1DH-PBEsol double-hybrid approximation as a function of λ for the two basis sets p-aug-6-31G(d,p) and p-aug-6-311G(d,p). As expected, the dependence on the basis set

Table 6.2: Counterpoise-corrected lattice energies per molecule of the molecular crystal test set with the LMP2 method with three different basis sets.

Basis set	$CO(NH_2)_2$	$HCONH_2$	HCOOH	NH_3	CO_2
6-31G(d,p)	95.04	63.51	50.00	26.82	16.16
p-aug-6-31G(d,p)	109.88[a]	76.44[a]	61.60[a]	32.35	25.76
p-aug-6-311G(d,p)	-	77.26[a]	64.27[a]	31.78	25.26

[a]With dual-basis set technique: 6-31G(d,p) basis for SCF.

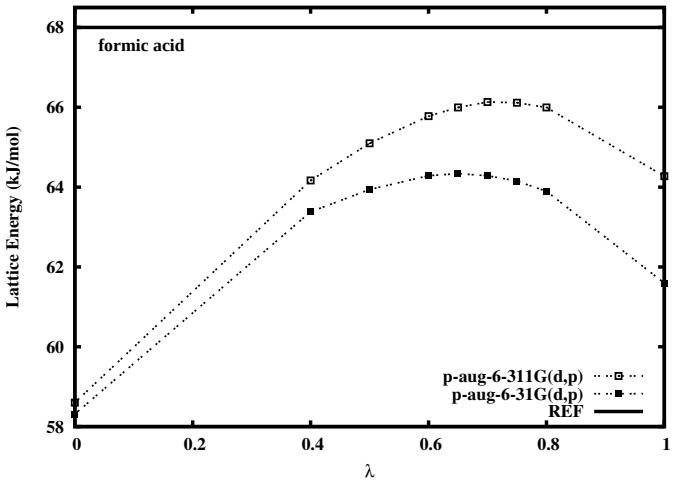

Figure 6.2: Counterpoise-corrected lattice energy per molecule of the formic acid molecular crystal as a function of the parameter λ for the 1DH-PBEsol double-hybrid approximation with p-aug-6-31G(d,p) and p-aug-6-311G(d,p) basis sets. The reference value is from Ref. [52].

decreases as λ is reduced from $\lambda = 1$ (corresponding to LMP2) to $\lambda = 0$ (corresponding to Kohn-Sham PBEsol which has a very small basis set dependence). However, at the value of the parameter used, $\lambda = 0.70$, the dependence on the basis set of 1DH-PBEsol is not significantly smaller than that of LMP2. This is a disadvantage of the DH approximations based on a linear decomposition of the electron-electron interaction, in comparison to DH schemes based on a range separation of the interaction which have a faster basis convergence [67, 87, 88].

6.6 Conclusions

We have implemented a number of double-hybrid approximations in the CRYSTAL09 and CRYSCOR09 suite of programs, and tested them for calculating lattice energies of five molecular crystals: urea, formamide, formic acid, ammonia, and carbon dioxide. The one-parameter double-hybrid approximations based on the PBEsol density functional, DS1DH-PBEsol and 1DH-PBEsol, with a fraction of HF exchange of $\lambda = 0.70$ and a fraction of LMP2 correlation of $\lambda^2 = 0.49$, gives lattice energies per molecule with an accuracy of about 5 kJ/mol, which is similar to the accuracy of LMP2. The results on the purely dispersion bound carbon dioxide crystal suggest that the DS1DH-PBEsol and 1DH-PBEsol double-hybrid approximations miss a part of dispersion interactions. This could be improved by either adding semi-empirical dispersion corrections [21] or using

range-separated double-hybrid methods [67].

Acknowledgments

We thank Peter Reinhardt (UPMC, Paris) for helpful discussions and technical assistance.

Bibliography

[1] C. B. Aakerøy and K. R. Seddon, Chem. Soc. Rev. **22**, 397 (1993).

[2] P. G. Karamertzanis, P. R. Anandamanoharan, P. Fernandes, P. W. Cains, M. Vickers, D. A. Tocher, A. J. Florence and S. L. Price, J. Phys. Chem. B **111**, 5326 (2007).

[3] M. D. Gourlay, J. Kendrick and F. J. J. Leusen, Crystal Growth & Design **7**, 56 (2007).

[4] O.-P. Kwon, B. Ruiz, A. Choubey, L. Mutter, A. Schneider, M. Jazbinsek, V. Gramlich and P. Günter, Chem. Mater. **18**, 4049 (2006).

[5] D. S. Coombes, S. L. Price, D. J. Willock and M. Leslie, J. Phys. Chem. **100**, 7352 (1996).

[6] G. G. Ferenczy, G. I. Csonka, G. Náray-szabó and J. G. Ángyán, J. Comput. Chem. **19**, 38 (1998).

[7] G. W. A. Welch, P. G. Karamertzanis, A. J. Misquitta, A. J. Stone and S. L. Price, J. Chem. Theory Comput. **4**, 522 (2008).

[8] A. J. Stone and S. Tsuzuki, J. Phys. Chem. B **101**, 10178 (1997).

[9] P. Hohenberg and W. Kohn, Phys. Rev. **136**, B 864 (1964).

[10] W. Kohn and L. J. Sham, Phys. Rev. **140**, A1133 (1965).

[11] C. A. Morrison and M. M. Siddick, Chem.âEur. J. **9**, 628 (2003).

[12] A. D. Fortes, J. P. Brodholt, I. G. Wood and L. Vocadlo, J. Chem. Phys. **118**, 5987 (2003).

[13] X.-H. Ju, H.-M. Xiao and L.-T. Chen, Int. J. Quantum Chem. **102**, 224 (2005).

[14] S. Kristyan and P. Pulay, Chem. Phys. Lett. **229**, 175 (1994).

[15] P. Hobza, J. Sponer and T. Reschel, J. Comput. Chem. **16**, 1315 (1995).

[16] K. Hongo, M. A. Watson, R. S. Sánchez-Carrera, T. Iitaka and A. Aspuru-Guzik, J. Phys. Chem. Lett. **1**, 1789 (2010).

[17] Y. Zhao and D. G. Truhlar, J. Chem. Theory Comput. **3**, 289 (2007).

[18] S. Tsuzuki, H. Orita, K. Honda and M. Mikami, J. Phys. Chem. B **114**, 6799 (2010).

[19] M. A. Neumann and M.-A. Perrin, J. Phys. Chem. B **109**, 15531 (2005).

[20] T. Li and S. Feng, Pharm. Res. **23**, 2326 (2006).

[21] B. Civalleri, C. Zicovich-Wilson, L. Valenzano and P. Ugliengo, Cryst. Eng. Comm **10**, 405 (2008).

[22] P. G. Karamertzanis, G. M. Day, G. W. A. Welch, J. Kendrick, F. J. J. Leusen, M. A. Neumann and S. L. Price, J. Phys. Chem. **128**, 244708 (2008).

[23] P. Ugliengo, C. Zicovich-Wilson, S. Tosoni and B. Civalleri, J. Mater. Chem. **19**, 2564 (2009).

[24] C. M. Zicovich-Wilson, B. Kirtman, B. Civalleri and A. Ramírez-Solís, Phys. Chem. Chem. Phys. **12**, 3289 (2010).

[25] D. C. Sorescu and B. M. Rice, J. Phys. Chem. C **114**, 6734 (2010).

[26] R. Balu, E. F. C. Byrd and B. M. Rice, J. Phys. Chem. B **115**, 803 (2011).

[27] W. Reckien, F. Janetzko, M. F. Peintinger and T. Bredow, J. Comput. Chem. **33**, 2023 (2012).

[28] A. O. de-la Roza and E. R. Johnson, J. Chem. Phys. **137**, 054103 (2012).

[29] M. Dion, H. Rydberg, E. Schröder, D. C. Langreth and B. I. Lundqvist, Phys. Rev. Lett. **92**, 246401 (2004).

[30] T. Thonhauser, V. R. Cooper, S. Li, A. Puzder, P. Hyldgaard and D. C. Langreth, Phys. Rev. B. **76**, 125112 (2007).

[31] F. Shimojo, Z. Wu, A. Nakano, R. K. Kalia and P. Vashishta, J. Chem. Phys. **132**, 094106 (2010).

[32] M. Alfredsson, L. Ojamae and K. G. Hermansson, Int. J. Qunatum Chem. **60**, 767 (1996).

[33] T. Ikeda, K. Nagayoshi and K. Kitaura, Chem. Phys. Lett. **370**, 218 (2003).

[34] A. L. Ringer and C. D. Sherrill, Chem.âEur. **14**, 2542 (2008).

[35] R. Podeszwa, B. M. Rice and K. Szalewicz, Phys. Rev. Lett. **101**, 115503 (2008).

[36] J.-Q. Sun and R. J. Bartlett, J. Chem. Phys. **104**, 8553 (1996).

[37] P. Y. Ayala, K. N. Kudin and G. E. Scuseria, J. Chem. Phys. **115**, 9698 (2001).

[38] M. Marsman, A. Grüneis, J. Paier and G. Kresse, J. Chem. Phys. **130**, 184103 (2009).

[39] A. Grüneis, M. Marsman and G. Kresse, J. Chem. Phys. **133**, 074107 (2010).

[40] M. D. Ben, J. Hutter and J. VandeVondele, J. Chem. Theory Comput. **8**, 4177 (2012).

[41] M. D. Ben, J. Hutter and J. VandeVondele, J. Chem. Theory Comput. , DOI: 10.1021/ct4002202 (2013).

[42] C. Pisani, M. Busso, G. Capecchi, S. Casassa, R. Dovesi, L. Maschio, C. Zicovich-Wilson and M. Schütz, J. Phys. Chem. **122**, 094113 (2005).

[43] D. Lu, Y. Li, D. Rocca and G. Galli, Phys. Rev. Lett. **102**, 206411 (2009).

[44] Y. Li, D. Lu, H.-V. Nguyen and G. Galli, J. Phys. Chem. A **114**, 1944 (2010).

[45] L. Maschio, J. Chem. Theory Comput. **7**, 2818 (2011).

[46] C. Pisani, M. Schütz, S. Casassa, D. Usvyat, L. Maschio, M. Lorenz and A. Erba, Phys. Chem. Chem. Phys. **14**, 7615 (2012).

[47] S. Casassa, M. Halo and L. Maschio, J. Phys.: Conf. Ser **117**, 012007 (2008).

[48] M. Halo, S. Casassa, L. Maschio and C. Pisani, Chem. Phys. Lette **467**, 294 (2009).

[49] M. Halo, S. Casassa, L. Maschio and C. Pisani, Phys. Chem. Chem. Phys. **11**, 586 (2009).

[50] L. Maschio, D. Usvyat, M. Schütz and B. Civalleri, J. Chem. Phys. **132**, 134706 (2010).

[51] L. Maschio, D. Usvyat and B. Civalleri, CrystEngComm **12**, 2429 (2010).

[52] L. Maschio, B. Civalleri, P. Ugliengo and A. Gavezzotti, J. Phys. Chem. **115**, 11179 (2011).

[53] S. Grimme, J. Chem. Phys. **124**, 034108 (2006).

[54] A. D. Becke, Phys. Rev. A **38**, 3098 (1988).

[55] C. Lee, W. Yang and R. G. Parr, Phys. Rev. B **37**, 785 (1988).

[56] J. P. Perdew, K. Burke and M. Ernzerhof, Phys. Rev. Lett. **77**, 3865 (1996).

[57] J. P. Perdew, A. Ruzsinszky, G. I. Csonka, O. A. Vydrov, G. E. Scuseria, L. A. Constantin, X. L. Zhou and K. Burke, Phys. Rev. Lett. **100**, 136406 (2008).

[58] K. Sharkas, J. Toulouse and A. Savin, J. Chem. Phys. **134**, 064113 (2011).

[59] Y. Zhao, B. J. Lynch and D. G. Truhlar, J. Phys. Chem. A **108**, 4786 (2004).

[60] Y. Zhao, B. J. Lynch and D. G. Truhlar, Phys. Chem. Chem. Phys. **7**, 43 (2005).

[61] T. Schwabe and S. Grimme, Phys. Chem. Chem. Phys. **8**, 4398 (2006).

[62] A. Tarnopolsky, A. Karton, R. Sertchook, D. Vuzman and J. M. L. Martin, J. Phys. Chem. A **112**, 3 (2008).

[63] A. Karton, A. Tarnopolsky, J.-F. Lamére, G. C. Schatz and J. M. L. Martin, J. Phys. Chem. A **112**, 12868 (2008).

[64] J. C. Sancho-García and A. J. Pérez-Jiménez, J. Chem. Phys. **131**, 084108 (2009).

[65] L. A. Curtiss, K. Raghavachari, P. C. Redfern and J. A. Pople, J. Chem. Phys. **106**, 1063 (1997).

[66] J. Toulouse, F. Colonna and A. Savin, Phys. Rev. A **70**, 062505 (2004).

[67] J. G. Ángyán, I. C. Gerber, A. Savin and J. Toulouse, Phys. Rev. A **72**, 012510 (2005).

[68] P. Pulay and S. Saebø, Theor. Chim. Acta **69**, 357 (1986).

[69] C. Pisani, L. Maschio, S. Casassa, M. Halo, M. Schütz and D. Usvyat, J. Comput. Chem. **29**, 2113 (2008).

[70] R. P. Steele and R. A. DiStasio and Y. Shao and J. Kong and M. Head-Gordon, J. Chem. Phys. **125**, 074108 (2006).

[71] R. A. DiStasio and R. P. Steele and M. Head-Gordon, Mol. Phys. **105**, 2731 (2007).

[72] K. Wolinski and P. Pulay, J. Chem. Phys. **118**, 9497 (2003).

[73] J. G. Ángyán, Phys. Rev. A **78**, 022510 (2008).

[74] E. Fromager and H. J. A. Jensen, Phys. Rev. A **78**, 022504 (2008).

[75] R. Dovesi, V. R. Saunders, C. Roetti, R. Orlando, C. M. Zicovich-Wilson, F. Pascale, B. Civalleri, K. Doll, N. M. Harrison, I. J. Bush, P. D′Arco and M. Llunell., CRYSTAL, Release CRYSTAL09 (2009), see http://www.crystal.unito.it.

[76] F. H. Allen, Acta Cryst. **B58**, 380 (2002).

[77] A. Simon and K. Peters, Acta Cryst. **B36**, 2750 (1980).

[78] H. Kiefte, R. Penney, S. W. Breckon and M. J. Clouter, J. Chem. Phys. **86**, 662 (1987).

[79] E. I. Voitovich, A. M. Tolkachev and V. G. Manzhelii, J. Low Temp. Phys. **5**, 435 (1971).

[80] P. Hariharan and J. Pople, Theoret. Chim. Acta **1973**, 213 (28).

[81] W. F. Perger, R. Pandey, M. A. Blanco and J. Zhao, Chem. Phys. Lett. **388**, 175 (2004).

[82] T. H. Dunning, J. Chem. Phys. **90**, 1007 (1989).

[83] C. Zicovich-Wilson, R. Dovesi and V. R. Saunders, J. Chem. Phys. **115**, 9708 (2001).

[84] S. Casassa, C. Zicovich-Wilson and C. Pisani, Theor. Chem. Acc. **116**, 726 (2006).

[85] L. Maschio and D. Usvyat, Phys. Rev. B **78**, 073102 (2008).

[86] S. F. Boys and F. Bernardi, Mol. Phys. **19**, 553 (1970).

[87] J. Toulouse, I. C. Gerber, G. Jansen, A. Savin and J. G. Ángyán, Phys. Rev. Lett. **102**, 096404 (2009).

[88] J. Toulouse, W. Zhu, J. G. Ángyán and A. Savin, Phys. Rev. A **82**, 032502 (2010).

Chapter 7

Conclusion générale et perspectives

L'essence des méthodes développées dans ce travail de thèse réside dans l'extension multidéterminantale de la méthode de Kohn-Sham basée sur une décomposition linéaire de l'opérateur d'interaction biélectronique en deux fragments complémentaires $\lambda\hat{W}_{ee}$ et $(1-\lambda)\hat{W}_{ee}$, dont les proportions dépendent d'un paramètre λ à fixer. Cette formulation rigoureuse met en jeu un calcul de type fonction d'onde pour la contribution $\lambda\hat{W}_{ee}$ à l'énergie complété par une fonctionnelle de la densité pour la contribution $(1-\lambda)\hat{W}_{ee}$. Cette approche est en principe exacte. En pratique, il faut bien sûr utiliser des approximations pour la fonction d'onde et les fonctionnelles d'échange et de corrélation.

En utilisant cette procédure, nous avons développé les hybrides multiconfigurationnels à un paramètre avec transformation d'échelle (*scaling*) de la densité, MCDS1H, ou sans *scaling* de la densité, MC1H. Ces hybrides combinent la DFT avec la méthode MCSCF pour traiter les effets de corrélation statique des systèmes moléculaires en théorie de la fonctionnelle de la densité. Cette approche peut être vue comme une généralisation directe des hybrides habituelles. En effet, la valeur moyenne de $\lambda\hat{W}_{ee}$ sur la fonction d'onde MCSCF introduit essentiellement une fraction λ d'énergie de corrélation statique, en plus d'une fraction λ d'énergie d'échange exacte. Il a été montré qu'une bonne valeur du paramètre est $\lambda = 0.25$, c'est-à-dire correspondant à la même fraction d'échange exacte habituellement utilisée pour les hybrides globales. Quelques exemples sur des courbes d'énergie potentielle des molécules diatomiques montrent qu'autour de la distance d'équilibre, les hybrides multiconfigurationnels donnent des énergies très proches de celles obtenues par les calculs Kohn-Sham standard avec des hybrides globales comme PBE0 ou B3LYP. Aux grandes distances internucléaires R, les hybrides globales donnent des courbes d'énergie qui ont une dépendance incorrecte en $1/R$ ce qui est le signe d'une mauvaise description de la corrélation statique. Les hybrides multiconfigurationnels corrigent ce comportement en introduisant un fraction de corrélation statique et donnent des courbes d'énergie qui saturent correctement à grande distance comme la courbe MCSCF. Ceci confirme que les hybrides multiconfigurationnels peuvent apporter une amélioration au traitement des effets de corrélation de (quasi-)dégénérescence en comparaison aux méthodes Kohn-Sham standard avec des hybrides globales. Dans la présente implémentation, il reste néanmoins une erreur significative sur l'énergie à la dissociation due aux fonctionnelles d'échange-corrélation approchées utilisées qui ne dépendent que la densité totale. Un perfectionnement de la méthode pourrait être obtenu en construisant des fonctionnelles d'échange-corrélation dépendantes, en plus de la densité électronique, de la densité de spin ou d'une autre quantité comme la densité de paires à la coalescence

(*on-top pair density*) afin d'améliorer l'énergie de la molécule dissociée qui a un caractère de couches ouvertes.

La même procédure nous a permis de mieux comprendre les approximations doubles hybrides (DH) et de les justifier théoriquement. Cette approche consiste à traiter l'interaction $\lambda\hat{W}_{ee}$ au niveau Hartree-Fock et ajouter la corrélation manquante associée à cette interaction selon une théorie de perturbation Møller-Plesset du deuxième ordre (MP2). Cela conduit à deux nouvelles formes d'approximations doubles hybrides à un seul paramètre empirique λ : DS1DH avec *scaling* de la densité et 1DH sans *scaling* de la densité. Les approximations DS1DH-PBE et 1DH-BLYP avec les valeurs optimisées de λ apportent une amélioration pour les propriétés thermochimiques en comparaison aux méthodes non hybrides correspondantes. Pour les énergies d'atomisation, l'approximation double hybride à un paramètre 1DH-BLYP avec la valeur optimisée sur l'ensemble AE6 de λ=0.55 donne des résultats très proches de ceux de l'approximation double hybride à deux paramètres B2-PLYP. De plus, le seul paramètre λ de 1DH-BLYP donne des fractions d'échange exact et de corrélation MP2, $a_x=\lambda=0.55$ et $a_c=\lambda^2 \approx 0.3$, très proches de celles optimisées séparément pour B2-PLYP, a_x=0.53 et a_c=0.27. Pour les propriétés thermochimiques et cinétiques, l'approximation double hybride 1DH-BLYP avec la valeur optimisée sur l'ensemble AE6+BH6 de λ=0.65 peut atteindre en moyenne une précision proche de la précision chimique. Nous avons vérifié que ces conclusions restaient valables sur des ensembles de tests plus grands. L'approximation double hybride à un paramètre avec *scaling* linéaire LS1DH est obtenue du modèle DS1DH en approchant la fonctionnelle de la corrélation avec *scaling*, $E_c[n_{1/\lambda}]$, par une interpolation linéaire entre l'énergie de corrélation MP2, E_c^{MP2}, et l'énergie de corrélation de Kohn-Sham habituelle, $E_c[n]$. L'approximation LS1DH-PBE avec la valeur de λ=0.50 reproduit exactement l'approximation PBE0-DH. Ceci donne donc une base théorique plus solide pour cette approximation. Plus généralement, on s'attend à ce que cette approximation LS1DH soit plus précise que l'approximation DS1DH pour des fonctionnelles de corrélation qui sont imprécises dans la limite des hautes densités.

En effectuant des calculs sur cinq cristaux moléculaires, nous avons testé les capacités des diverses approximations doubles hybrides à décrire les interactions faibles dans les solides. Toutes les approximations doubles hybrides sont plus performantes que les méthodes DFT correspondantes. La sous-estimation de l'énergie réticulaire du cristal d'oxyde de carbone calculée par l'approximation 1DH-PBEsol est due à une partie d'interaction de dispersion manquante. L'ajout des corrections de dispersion semi-empiriques ou l'utilisation des approximations doubles hybrides à séparation de portée peuvent être proposés pour remédier à cette difficulté.

Pour finir, mentionnons que cette approche basée sur la séparation linéaire de l'interaction électronique présente deux avantages pratiques sur l'approche de la décomposition longue portée/courte portée de l'énergie en théorie de la fonctionnelle de la densité : (a) Il suffit d'une seule liste d'intégrales biélectroniques coulombiennes multipliées par λ pour le calcul de type fonction d'onde et par (1-λ) pour l'énergie de Hartree complémentaire, alors que pour la décomposition longue portée/courte portée il faut une liste d'intégrales calculées avec l'interaction de longue portée pour le calcul de type fonction d'onde, et une liste d'intégrales calculées avec l'interaction de courte portée pour l'énergie de Hartree courte portée; (b) Les fonctionnelles d'échange-corrélation complémentaires sont obtenues des fonctionnelles habituelles par des relations de transformation d'échelle, alors que pour la

décomposition longue portée/courte portée il faut développer des nouvelles fonctionnelles d'échange-corrélation de courte portée. Quant à la performance, les deux méthodes sont souvent proches. Les approximations MCDS1H-PBE (λ=0.25) et MC-srPBE (μ=0.40) donnent des courbes d'énergie potentielle très similaires pour les molécules diatomiques considérées dans cette thèse. L'approximation double hybride à séparation de portée RSH+lrMP2 donne des barrières de réaction comparables à celles obtenues avec la double hybride globale 1DH-BLYP, mais les énergies d'atomisation calculées par l'approximation RSH+lrMP2 sont moins bonnes que celles données par l'approximation 1DH-BLYP. Notons qu'une amélioration de la fonctionnelle de courte portée pourrait changer ces conclusions. Cependant, la dépendance vis-à-vis de la taille de la base est plus faible pour les méthodes basées sur la décomposition longue portée/courte portée que pour celles basées sur la décomposition linéaire. En plus, la décomposition longue portée/courte portée permet de traiter explicitement les effets de corrélation de longue portée telles que les interactions de dispersion de van der Waals. Il serait intéressant de poursuivre l'idée de la combinaison d'une approximation double hybride à séparation de portée avec une approximation double hybride globale à la manière de ce qui a été fait pour la fonctionnelle CAM-B3LYP pour les hybrides simples. Ceci nous permettrait de coupler les approximations doubles hybrides globales avec des méthodes connues pour leur efficacité à traiter les interactions de longue portée comme l'approximation des phases aléatoires.